I. DEPOLYMERIZATION-MACROCYCLIZATION OF (*o*-PHENYLENE-ETHYNYLENE)-*ALT*-(ARYLENE-ETHYNYLENE) COPOLYMERS
II. IMPROVING EXISTING WATER FILTRATION MEMBRANES VIA COVALENT MODIFICATION

BY

JAMES HAROLD HERBISON

DISSERTATION

Submitted in partial fulfillment of the requirements for
the degree of Doctor of Philosophy in Chemistry
in the Graduate College of the
University of Illinois at Urbana-Champaign, 2014

Urbana, Illinois

Doctoral Committee:

Professor Jeffrey S. Moore, Chair
Professor Wilfred A. van der Donk
Professor Steven C. Zimmerman
Professor Jianjun Cheng

Abstract

I. Depolymerization-Macrocyclization of (*o*-Phenylene-Ethynylene)-*alt*-(Arylene-Ethynylene) Copolymers

The synthesis of shape-persistent arylene-ethynylene macrocycles via alkyne metathesis remains an open area of investigation due to gaps in understanding about how monomer structure affects product distribution. In our efforts to close this gap, we studied how monomers with two different geometries would mix under metathesis conditions to form distributions of macrocycles using a depolymerization-macrocyclization method. Instead, we found that starting with (*o*-phenylene-ethynylene)-*alt*-(arylene-ethynylene) copolymers resulted in selective formation of the alternating macrocycles even with a diverse set of co-monomers. Through testing various theories, we propose that this selectivity is due to a regioselective interaction of the molybdenum catalyst with the asymmetric alkyne so that the reaction cannot reach the thermodynamic product distribution.

II. Improving Existing Water Filtration Membranes via Covalent Modification

Over a billion people in the world already have limited access to safe drinking water, and the problem is steadily growing worse due to contamination of our water supply. Therefore, we need an efficient, sustainable method for the purification of water that can remove the wide array of toxic solutes in water. Reverse osmosis is an attractive technique for water purification because of how versatile it is, with a range of membrane materials that can potentially be optimized to exhibit certain properties, such as selective rejection of certain solutes and permeation of others. Our collaboration has previously demonstrated the use of polyaramide dendrimers to improve commercial filtration membranes, though the coating was found to be unstable and the beneficial effects were lost over time. Thus, we have now developed a method for covalently attaching the dendrimer to the active layer of the membrane. The covalently modified membranes have improved filtration properties relative to the original membrane and have been shown to be more stable than the analogous dendrimer coating.

To my family and to Anastasia – my wonderful partner through it all

Acknowledgements

I must first express my deepest gratitude to Jeff, for being the best advisor I could have ever imagined. From giving me the opportunity to work with him in the beginning through his continued support to the end, it has been a true pleasure to be a member of his group. His advice, patience, ideas, amazing attitude, and genuine care for his students have had a considerable impact on me and were some of the factors that got me through the many difficult parts of graduate school. I also deeply appreciated his management style, which allowed me to work independently and have my own achievements and failures while he was still always there when I needed advice. I feel that I am much more prepared for a career as a scientist for having been a part of this group and having worked with Jeff.

I must also say thank you to all of the Moore Group members through the years, as it has been an honor to work alongside all of you. There is an astounding level of talent within the group and I have learned a huge amount from the people I have worked with. Everyone has made the group a friendly and supportive work environment that made the rigors of graduate school easier to deal with. In particular, I would like to thank Dustin Gross and Aaron Finke for guiding me through the beginning of my graduate school career and for their advice on chemistry and how to proceed in my project. I would also like to thank Scott Sisco for our discussions about reactions and for often acting as a sounding board as I worked through problems in my research. Josh Ritchey, Mike Evans, and Preston May deserve special thanks for making me feel welcome in the group when I first started and also for being great friends in the time we were all here. In the same way, I would like to thank Josh Kaitz for his friendship through the latter portion of my time here. I would also like to particularly thank Olivia Lee for the tremendous amount of help that she has provided in this last year, and especially her help with my dissertation, and for always being willing to volunteer to do something for the good of the group. I also need to express my gratitude for the wonderful undergraduate students that I had the privilege of mentoring: Faisal Masood, Will Schaeffer, Carlos de los Reyes. Their help with synthesizing compounds, allowing me to talk through obstacles in my research with them, and all in all being a pleasure to work with was invaluable to me. I also want to express my gratitude to everyone in RAL whom I worked with on a day to day basis: Masashi Arai, Kevin Cheng, Pinnan Cheng, Mani Chikannagari, Yuan Gao, Nag Gavvalapalli, Bora Inci, Phil Janowicz, Sye He Kim, Yi

Ren, Nina Sekerak, Brian Wall, Anna Yang, and Lijuan Zhu. Even though I did not see them much, I would also like to thank the group members in Beckman for their help over the years through group meeting and practice talks: Mary Caruso, Doug Davis, Charles Diesendruck, Hefei Dong, Liz Glogowski, Koushik Ghosh, Josh Grolman, Matt Kryger, Aaron Esser-Kahn, Andy Li, Susan Odom, Catherine Possanza, Ian Robertson, Yang Song, Shijia Tang, Windy Santa Cruz, and Ke Yang.

I would also like to acknowledge my doctoral committee for their advice during my time here and the great ideas they have given me about my research and about being a scientist in general: Professor Wilfred A. van der Donk, Professor Steven C. Zimmerman, and Professor Jianjun Cheng. I want to extend special thanks to Professor Kami L. Hull for filling in on my committee for my Original Research Proposal.

The staff in the Organic office has been fantastic during my time here, and I need to thank them for everything they have done to help with any questions or problems that I have had. I would especially like to thank Becky Duffield for being so kind and helpful at all times, and for always providing a good chat when it was needed or a good venting session when that became necessary too.

I need to give a heartfelt thank you to my family for supporting me through graduate school. Their willingness to patiently let me complain about problems that I was having and their well-placed words of encouragement helped me beyond words. I hope that you know how much you all mean to me and how much your support has helped me through everything.

Lastly, but certainly not least, I would like to thank my fantastic girlfriend Anastasia for everything that she has done and for being there for me throughout everything. I cannot even begin to express how much you mean to me and how much your being there has allowed me to get to where I am.

Table of Contents

Chapter 1

Arylene-Ethynylene Macrocycles and Their Syntheses

1.1: Arylene-Ethynylene Macrocycles

Arylene-ethynylene macrocycles (AEMs) are a class of shape-persistent macrocycles, often cyclic oligomers, composed of rigid aromatic units connected by an alkyne linker (Figure 1.1). These compounds share a number of structural traits, including a rigid, carbon-rich skeleton with large π-system surface and a relatively large internal cavity. This cavity and the periphery of the macrocycle can also be selectively functionalized with relative ease based on the aryl units built into the backbone of the macrocycle.

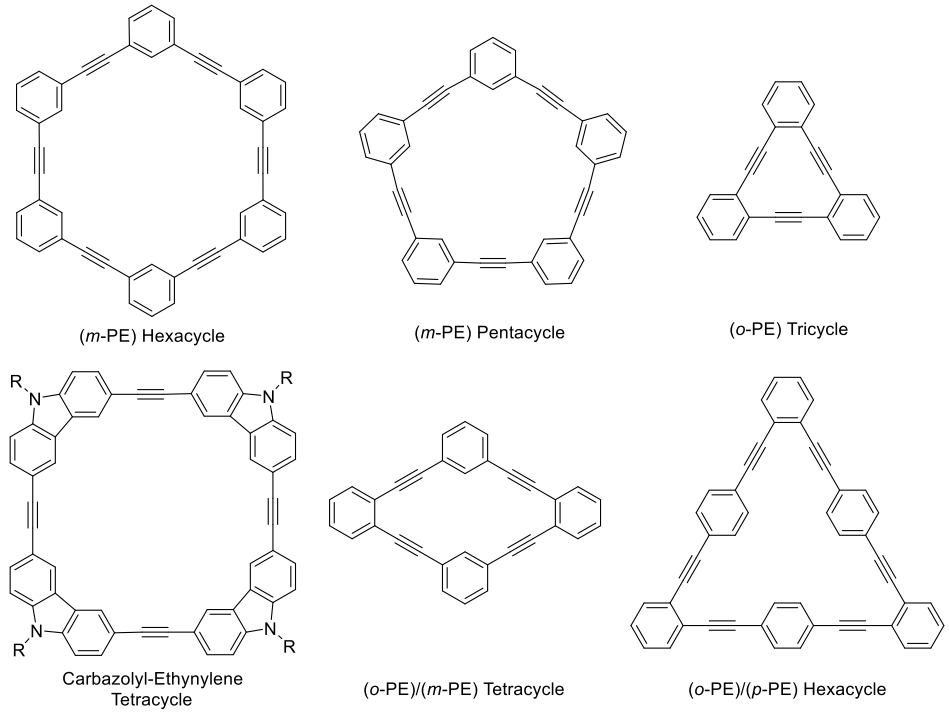

Figure 1.1: Examples of arylene-ethynylene macrocycles containing *m*-phenylene-ethynylene (*m*-PE), *o*-phenylene-ethynylene (*o*-PE), carbazoylyl-ethynylene (CE), or *p*-phenylene-ethynylene (*p*-PE) monomer units with functional sites abbreviated or removed for clarity.

The structural characteristics of arylene-ethynylene macrocycles have attracted a significant amount of interest to this class of compounds for their potential physical properties and supramolecular chemistry. Due to the high amount of surface area in the π-system and the rigidity of the typically planar backbone, various studies have been performed on their aggregation in both solution phase and solid state, and for their ability to form functional

materials, such as liquid-crystals.[1-7] Using a carbazolyl-ethynylene macrocycle, Moore and coworkers found that the compound self-assembled into fluorescent fibrils, which could be used to detect various explosive compounds via fluorescence quenching.[8] The interest in AEMs also stems from their physical properties and electronic structure where there can be either full conjugation or cross-conjugation across the entire macrocycle, depending on the structure of the aryl units. For example, Hartley and co-workers synthesized "push-pull" macrocycles to study the communication between electron-rich and electron-deficient units on opposite sides of a molecule through cross-conjugated *m*-phenylene or conjugated thiophene linkers (Figure 1.2).[9]

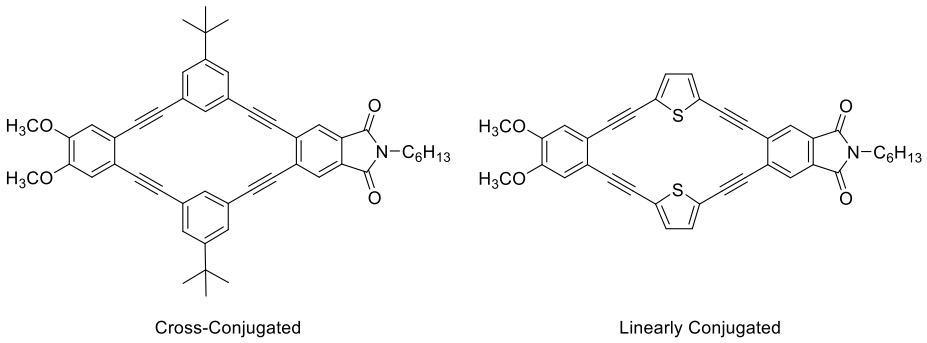

Figure 1.2: "Push-pull" macrocycles synthesized to study the electronic properties of AEMs.

The cavity of the macrocycle has also attracted interest for its potential applications, including porous materials, host-guest applications, and other potential applications.[1-2,5,10-11] Tobe *et al.* demonstrated various AEMs can each form a self-assembled monolayer, many of which are nanoporous,[12-14] while others were applied in the study of host guest interactions.[10] In another example that incorporates pyridine units in the backbone with nitrogen facing the interior, Yamaguchi and Yoshida demonstrated the formation of a complex between the macrocycle and antimony pentachloride.[11]

The exterior of the macrocycle typically features various sites for the simple installation of functional groups to impart the molecule with different properties. Since the arylene-ethynylene backbones often exhibit limited solubility, these sites are usually used for the attachment of solubilizing chains. Even a minor change in these solubilizing chains can significantly impact the properties of the macrocycle, such as packing involved in supramolecular chemistry. Tobe and coworkers have shown that the solubilizing chains play a large role in how various macrocycles form self-assembled monolayers, where the side chains intercalate with each other which aligns the macrocycles in an ordered fashion over the extended system.[10,12-16]Small differences in the structure of the side chains, such as the number of carbon

atoms or even whether it is an odd or even number of carbon atoms, change the morphology of the monolayer and how the macrocycles align with each other, which in turn affects the properties of the monolayer like its porosity. More recently, Moore *et al.* have shown that changing the lengths of the solubilizing chains causes drastic changes in molecular packing that lead to variations in crystal morphology.[17]

1.2: Synthesis via Kinetic Methods

The synthesis of arylene-ethynylene macrocycles often relies heavily on kinetically controlled methods, typically cross-coupling reactions. Cross-coupling and similar reactions are powerful tools for the construction of carbon-carbon bonds and the incorporation of alkyne moieties because they are simple to implement without the need for complex catalytic systems or rigorously controlled environments. Most cross-coupling reactions can be performed with standard Schlenk-line techniques for an air free environment, rather than requiring a glove box, and with readily available palladium-based catalysts and common co-catalysts. Analogous alkyne homocoupling reactions are also used to afford similar products with butadiyne spacers rather than ethynyl groups.

There are three common strategies for the synthesis of arylene-ethynylene macrocycles via cross-coupling methodology: (1) one-pot oligomerization and cyclization; (2) cyclization of a presynthesized linear precursor; and (3) coupling of two separate fragments (Figure 1.3). The strategies often share common intermediates, and each varies according to the preparation prior to cyclization and the conditions of the cyclization reaction. Despite the aforementioned advantages, the irreversibility of cross-coupling reactions often leads to a broad product distribution and low yield of the desired AEM. If the oligomer has grown beyond the desired length, or if the cyclization reaction occurs before it is the proper length, the resulting compound becomes an undesired byproduct that detracts from the overall yield of the macrocycle (Figure 1.3). Since the reaction is irreversible, these flaws cannot be corrected, resulting in wasted materials.

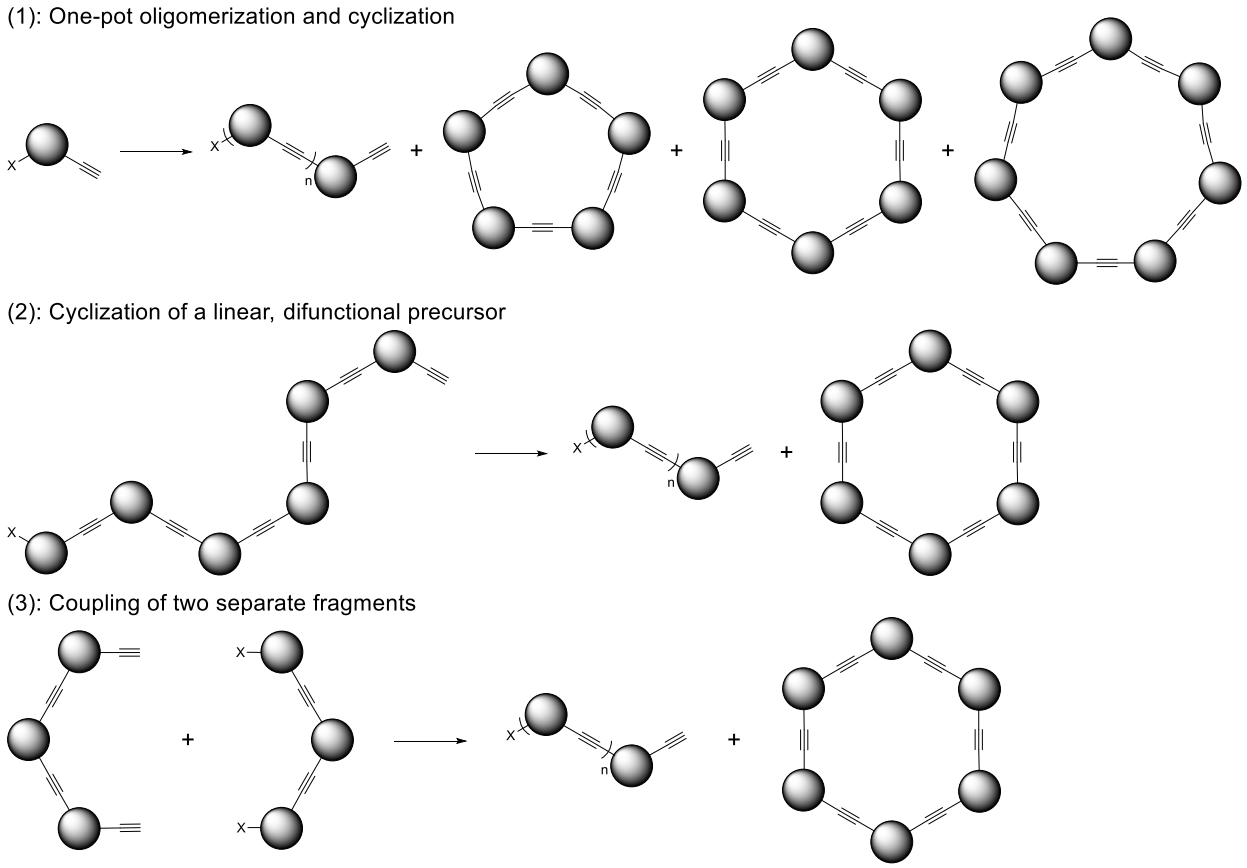

Figure 1.3: Representation of the common strategies for synthesis of AEMs via cross-coupling and the potential byproducts from each strategy.

1.2.1: One-Pot Oligomerization and Cyclization

In the first reported synthesis of an arylene-ethynylene macrocycle, the *o*-phenylene-ethynylene (*o*-PE) tricycle was prepared by Campbell and coworkers using a Stephens-Castro coupling to synthsize the *o*-PE oligomer and cyclize it to form the macrocycle in the same reaction mixture.[18] The tricycle was isolated in only 26% yield, likely due to the formation of various byproducts as demonstrated by the isolation of a second product which the authors identified as the *o*-phenylene-ethynylene tetracycle. The first synthesis of a *m*-phenylene-ethynylene (*m*-PE) hexacycle was reported by Staab and Neunhoeffer, who also used a one-pot Stephens-Castro coupling reaction (Scheme 1.1).[19] The yield of the hexacycle was even lower (4.6%) than reported for the *o*-PE tricycle, which is consistent with the hypothesis that the yields are decreased by the formation of byproducts. Because the *o*-PE system has less degree of freedom in the linear precursor, the cyclization step may be more facile.

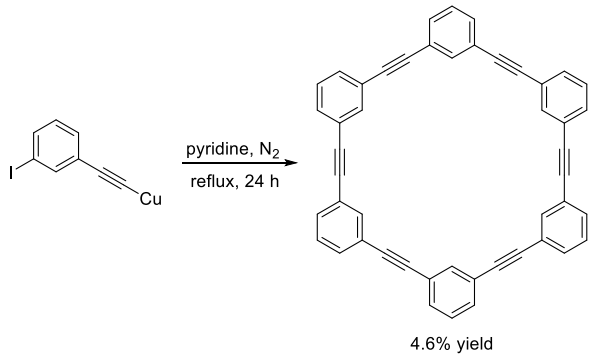

Scheme 1.1: The first synthesis of a *m*-phenylene-ethynylene hexacycle using a one-pot oligomerization and cyclization method.

Various new strategies have been developed for one-pot oligomerization and cyclization of AEMs to improve the overall product yields. Some involve adaptations of the original syntheses with optimized reaction conditions to increase the yields, such as using an ionic liquid as the solvent to promote cyclization as demonstrated by Pan and coworkers.[20] Iyoda *et al.* developed another strategy focused on simplifying the starting material of the oligmerization-cyclization reaction to the symmetrical *o*-diiodophenylene monomer and acetylene (Scheme 1.2).[21] Both of these reports resulted in similar yields of the *o*-PE tricycle but demonstrated the ability to improve the overall yield of macrocycle formation by simple changes to the reaction conditions.

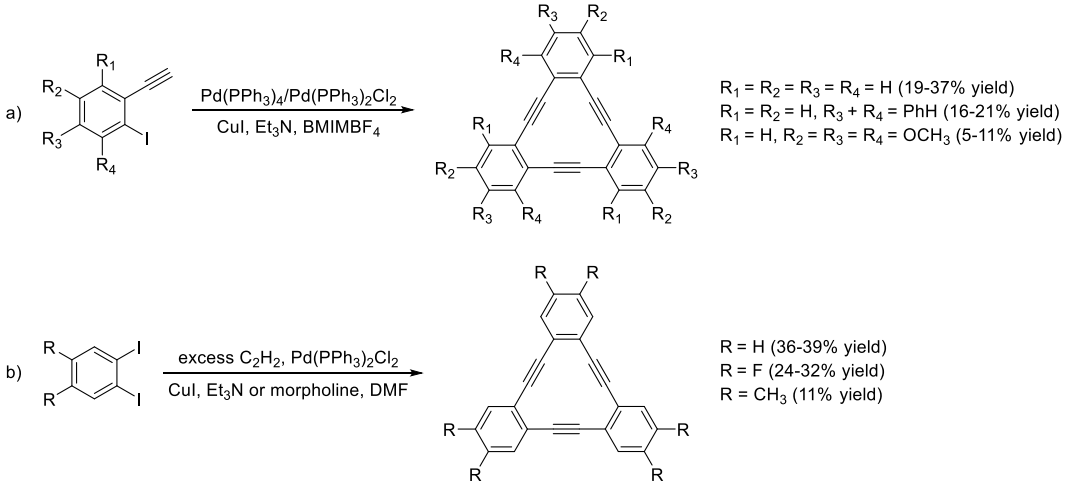

Scheme 1.2: Strategies showing the optimization of the oligomerization-cyclization reaction by modifying the reaction conditions (a) or by simplifying the starting material (b).

Preorganization of monomers via a template is another approach to favor cyclization over intermolecular reactions that increase the oligomer size. Non-covalent interactions were first used, such as the work of Sanders and Anderson to synthesize porphyrin-butadiyne macrocycles

using bipyridyl or terpyridyl templates to coordinate with a porphyrins.[22] Covalently attaching templates requires more extensive monomer synthesis due to template attachment than other one-pot strategies. However, by changing the reaction pathway to a series of intramolecular couplings rather than oligomer growth via intermolecular reactions followed by the intramolecular cyclization, the yield of macrocycle is significantly improved. This approach is exemplified by the synthesis of an extended *m*-phenylene-butadiynylene/*p*-phenylene-ethynylene (*p*-PE) macrocycle by Höger and coworkers where the cyclization step proceeded in 94% yield (Scheme 1.3)[23]. In a control system where the monomers are not attached, the reaction results in a mixture of higher oligomers with the macrocycle present in only 20-25% yield, demonstrating the effect of the template.

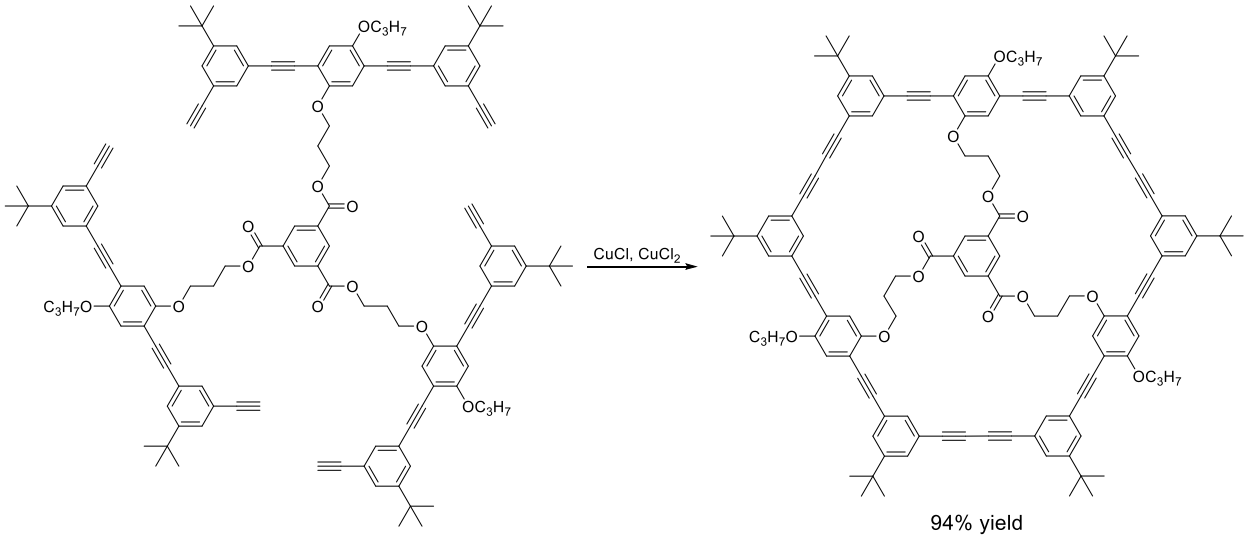

Scheme 1.3: Use of a covalently attached template to increase the yield of the macrocyclization step.

The major advantage to using a one-pot oligomerization and cyclization strategy is its simplicity. The starting materials are readily available allowing for efficient preparation of the materials for the cyclization reaction to make the macrocycle. However, the formation of several byproducts not only reduces the overall yield of the desired macrocycle but also leads to complications with purification due to the structural similarities of all oligomers. This method also allows for the least amount of control over the product structure when multiple distinct aryl units are used because the reaction will result in a statistical mixture of coupling products. Although the use of templates does allow for improved control of the product structure and can drastically increase yields, it further complicates the synthesis of starting materials and limits monomer scope.

1.2.2: Cyclization of a Presynthesized Linear Precursor

Moore and Zhang demonstrated a different method to prepare arylene-ethynylene macrocycles in their preparation of a *m*-phenylene-ethynylene macrocycle.[24] Instead of performing the oligomerization and cyclization in the same reaction, they first synthesized the linear hexamer in a stepwise fashion and subjected it to the cyclization reaction under pseudohigh-dilution conditions to favor the intramolecular cyclization (Scheme 1.4). This strategy allowed for a high yield in the cyclization reaction (75%) and was successful in synthesizing a larger alternating *m*-PE/*p*-PE macrocycle in comparable yield (70%). Biasing the reaction conditions toward intramolecular coupling affords greater product yields by minimizing the side reactions present in the one-pot strategy, which is dependent on both intra- and intermolecular coupling.

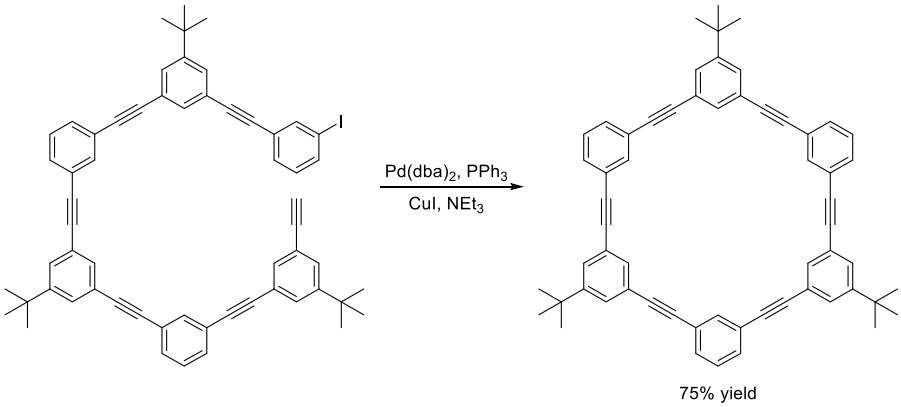

Scheme 1.4: The synthesis of a *m*-PE hexacycle demonstrating the cyclizing of a presynthesized linear oligomer

This first example also highlights the incredible degree of control over the product structure. Moore and coworkers further emphasized this advantage when they demonstrated the versatility of the strategy through the synthesis of macrocycles with multiple ring sizes and specifically designed substitution patterns (Figure 1.4).[25] This degree of control is unfeasible via the one-pot method where the oligomer growth reaction would result in a statistical mixture of possible coupling products prior to cyclization.

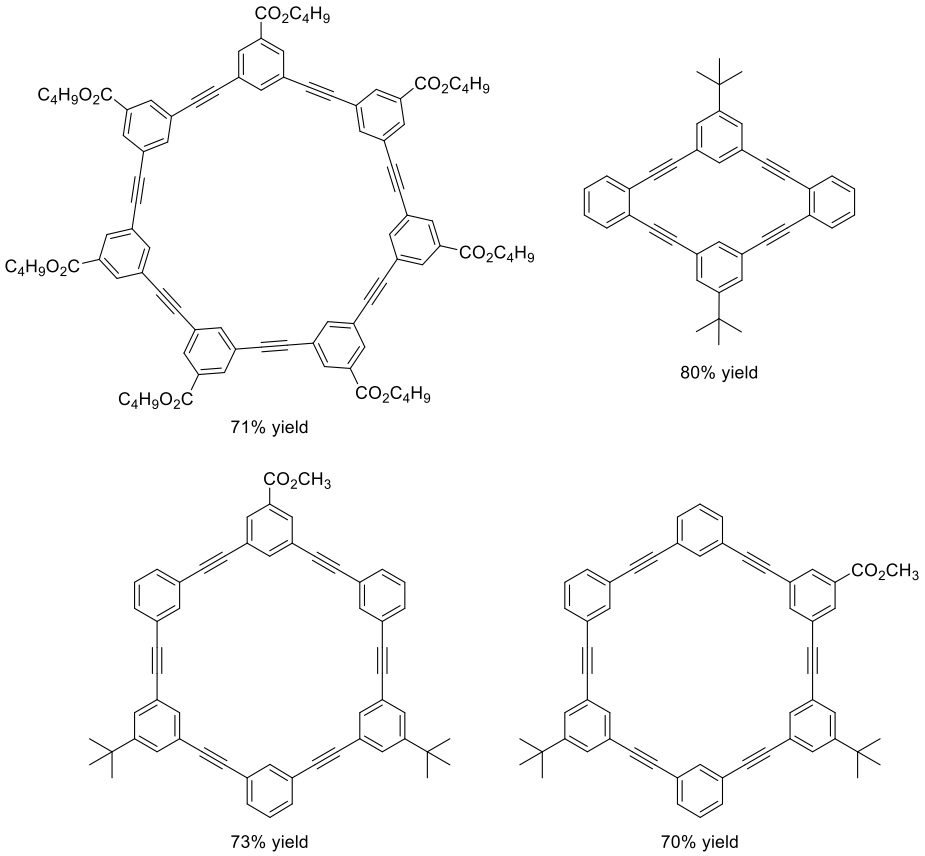

Figure 1.4: Example macrocycles demonstrating the significant control over product structure with the cyclization of a presynthesized linear precursor.

The major limitation of this strategy is the extensive synthesis of the linear precursor. Even by shortening the synthesis with a convergent approach, controlling the oligomer growth still necessitates a large number of iterative coupling and deprotection steps. In general, each synthetic intermediate requires purification in order to minimize subsequent side reactions and to allow for monitoring at each step. Inherent to this issue, larger macrocycles need more synthetic steps to prepare, while the one-pot method only uses the synthesis of the monomer regardless of the size of the product macrocycle.

1.2.3: Coupling of Two Separate Fragments

The third strategy for synthesizing arylene-ethynylene macrocycles is a hybrid of the first two strategies where two oligomer fragments of the macrocycle are first synthesized and then coupled together. As an early example of this method, Höger and Enkelmann synthesized a linear arylene-ethynylene backbone with two terminal alkynes on the ends prior to coupling together by an Eglington-Glaser reaction to create butadiynyl-linkages (Scheme 1.5).[26]

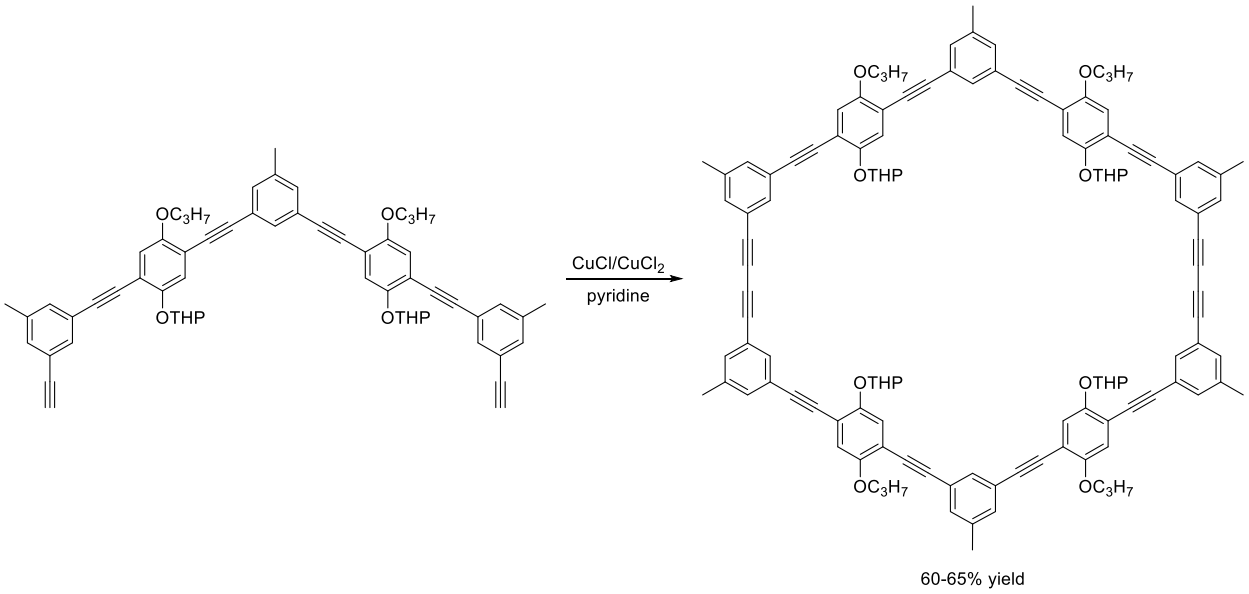

Scheme 1.5: One-step macrocyclization by coupling two fragments together.

With this strategy, there is still a large degree of control over the structure of the product macrocycle, but it requires fewer synthetic steps than preparing a single linear precursor. However, it still requires a lengthier synthetic route than the one-pot method and needs both inter- and intramolecular coupling steps, limiting the opportunity to bias the reaction conditions toward cyclization. Even though this strategy has some of the inherent disadvantages of the other two, it is still widely employed for the synthesis of arylene-ethynylene macrocycles, as demonstrated by its use by Zhao and coworkers for the synthesis of alternating AEMs (Scheme 1.6).[7]

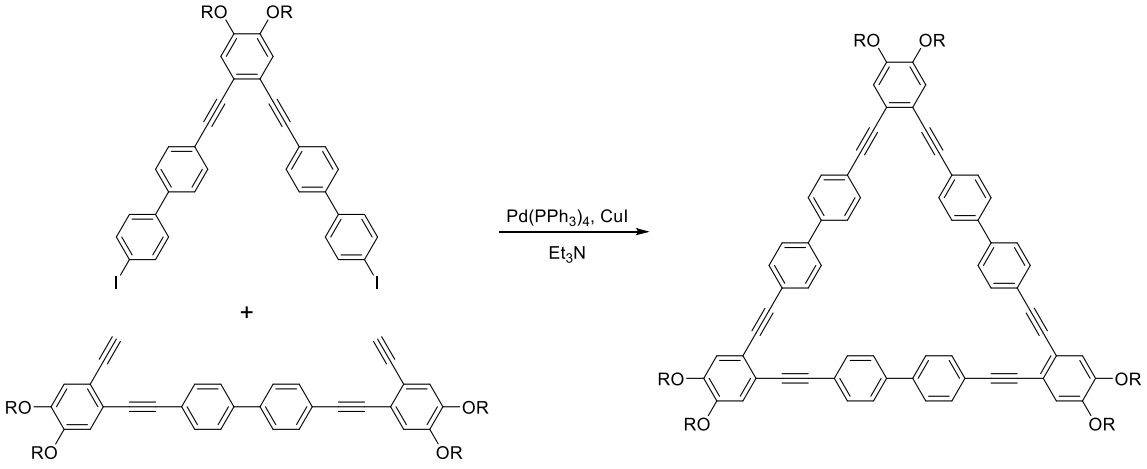

Scheme 1.6: Synthesis of an exemplary alternating *o*-PE/biphenylene-ethynylene AEM via the coupling of two fragments.

1.3: Synthesis via Alkyne Metathesis

Under kinetic control, the cross-coupling macrocyclizations are irreversible, so any byproducts formed by an undesired coupling reaction cannot be incorporated into the desired product, thereby decreasing the yield of the target macrocycle. Thus, the way to avoid this flaw is to perform these reactions under thermodynamic control which would allow the system to self-correct and form the most thermodynamically stable product distribution under the principals of dynamic covalent chemistry (DCC). This approach has been successfully used to synthesize macrocycles similar to AEMs that incorporate imine linkages using imine metathesis.[27-29] The analogous alkyne metathesis reaction offers an unprecedented opportunity toward the synthesis of arylene-ethynylene macrocycles.

The first use of alkyne metathesis toward the synthesis of AEMs was reported by Bunz and coworkers on the synthesis of *m*-phenylene-ethynylene hexacycles with the [$Mo(CO)_6$] catalytic system (Scheme 1.7).[30] The isolated yield of the macrocycles was low (0.5-6%), which may have been caused by the low reactivity of the poorly defined, *in situ* catalytic system or by the tedious purification of the macrocycles from the polymeric byproducts formed simultaneously. This catalytic system is not ideal because of the very high temperature required for the reaction to occur. For example, the reactions used to synthesize the *m*-PE hexacycles by Bunz *et al.* were performed at 150 °C.

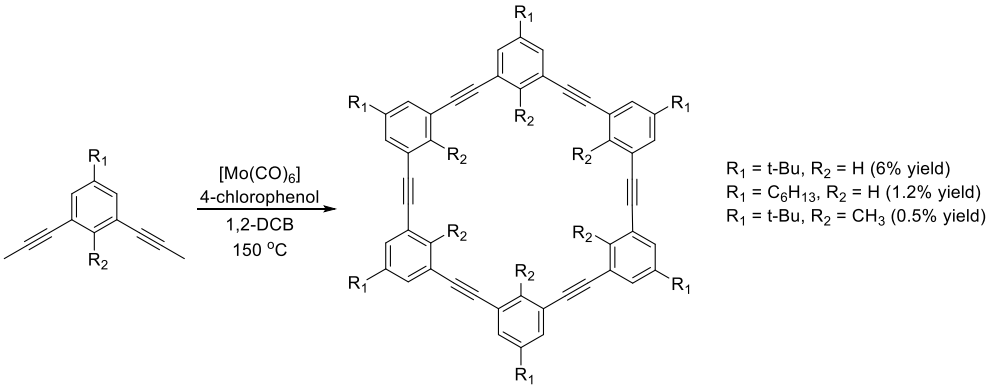

Scheme 1.7: The first example of the synthesis of *m*-PE hexacycles via alkyne metathesis.

Vollhardt and coworkers demonstrated the use of the Schrock tungsten-based alkyne metathesis catalyst in their synthesis of *o*-phenylene-ethynylene tricycles (Scheme 1.8).[31] The macrocyclic products were isolated in significantly higher yields than those synthesized by Bunz. This was also the first example of using alkyne metathesis in a system with monomers of two different geometries to synthesize an *o*-PE/*m*-PE alternating tetracycle in 19% yield (Scheme

1.8). The low yield for the tetracycle is most likely due to the formation of a statistical mixture of various unisolated macrocycles, including the *ortho*-tricycle and the *meta*-hexacycle. Despite the promising results, the authors noted that the reaction failed when the monomer was functionalized with substituents *ortho* to the alkynes. The still relatively high reaction temperature (80 °C) and long reaction times (8-140 hours) suggested that the Schrock catalyst was still not sufficiently reactive for widespread use of alkyne metathesis to synthesize AEMs.

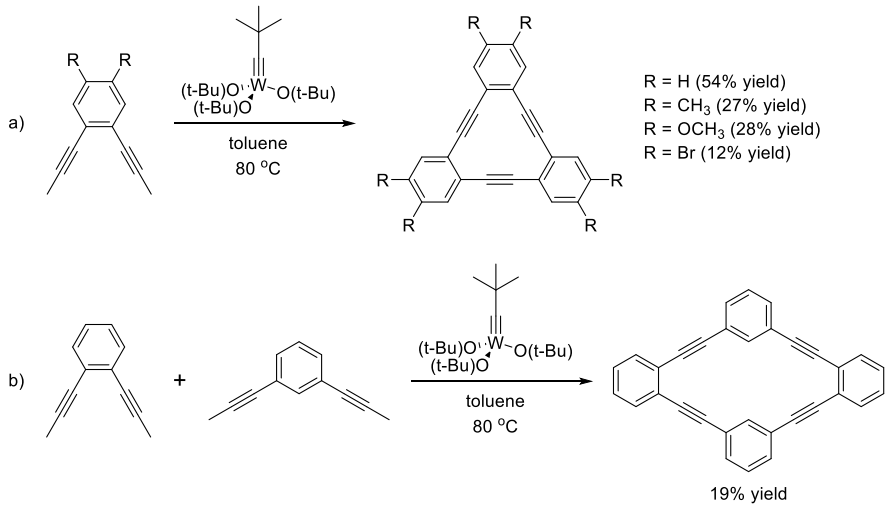

Scheme 1.8: Synthesis of (a) *o*-PE tricycles and (b) an *o*-PE/*m*-PE alternating macrocycle with a well-defined alkyne metathesis catalyst

Aware of the need for a catalyst with enhanced reactivity that is synthetically accessible, Moore and Zhang built on the work of Fürstner[32] by developing a synthesis for a trisamidomolybdenum(VI) propylidyne precatalyst (EtC≡Mo[N(Mes)t-Bu]$_3$) that produces an active catalyst system when mixed with a phenol or silanol ligand.[33-34] The synthesis was accomplished via a reductive recycle strategy where the stoichiometric byproduct formed during carbyne formation reacts with magnesium turnings to be converted back into the starting material to produce more of the target complex (Scheme 1.9). This strategy allows for the synthesis of the molybdenum alkylidyne complex in moderate yield (54%) on a multigram scale, making it reasonably accessible. Isolating the precatalyst from the chloromolybdenum byproduct also increased the reactivity of the catalyst system relative to other analogous catalyst systems where the molybdenum mixture was used without separating the byproduct.

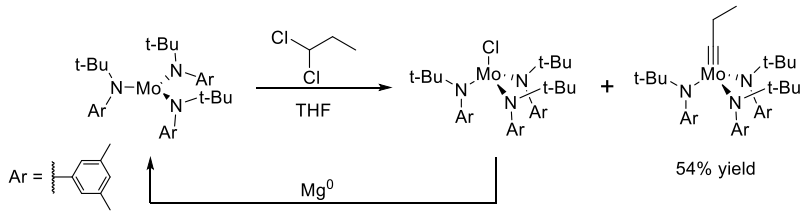

Scheme 1.9: The reductive-recycle strategy allowing for access to the trisamidomolybdenum(VI) propylidyne precatalyst in moderate yield.

With the EtC≡Mo[N(Mes)t-Bu]$_3$ catalytic system, initial syntheses of AEMs were successful with propynyl- and butynyl-functionalized monomers in high yields.[35] However, these yields were only achievable in small scales with constant removal of the volatile byproducts. When gram-scale reactions were attempted, the small byproduct could not be removed quickly enough to prevent its polymerization by the metathesis catalyst, yielding undesired products. To circumvent this flaw, the monomer was functionalized with a bulky benzoylbiphenyl substituent that would produce an insoluble byproduct after cross-metathesis (Scheme 1.10). This precipitation serves to drive the reaction equilibrium toward the desired thermodynamic products while preventing side reaction with the catalyst.

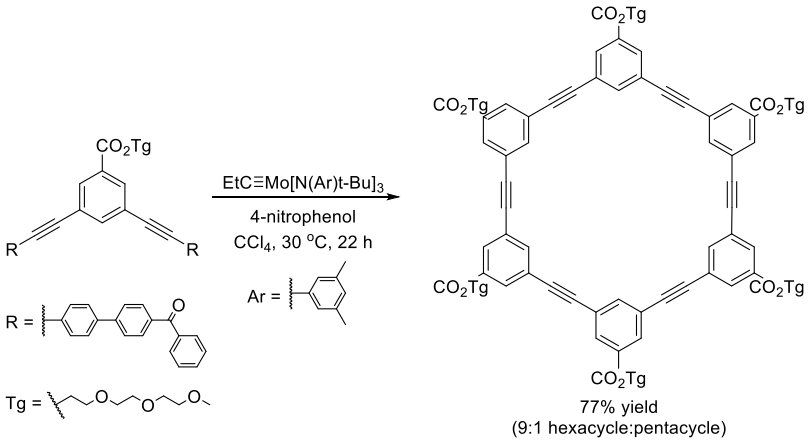

Scheme 1.10: Synthesis of a *m*-PE hexacycle by precipitation-driven metathesis conditions.

This precipitation-driven method has since been used to synthesize various AEMs in moderate to high yields, demonstrating one design principle for predicting the product structure from rigid monomers with C_2-symmetry (Figure 1.5).[35-36] At a basic level, the product structure is dictated by the effective angle between the alkynes and follows simple geometry by the angles found in polygons. From a thermodynamic perspective, this observation can be explained by the minimization of ring strain which results in a lower-energy product. When there is a small difference in the angle of two polygons, such as between a pentagon and a hexagon, both

products may be formed due to the reaction's being at equilibrium. In the case of *m*-phenylene-ethynylene macrocycles, both the pentacycle and hexacycle are formed with the hexacycle as the major product, reflecting the small ΔG value between the two compounds.

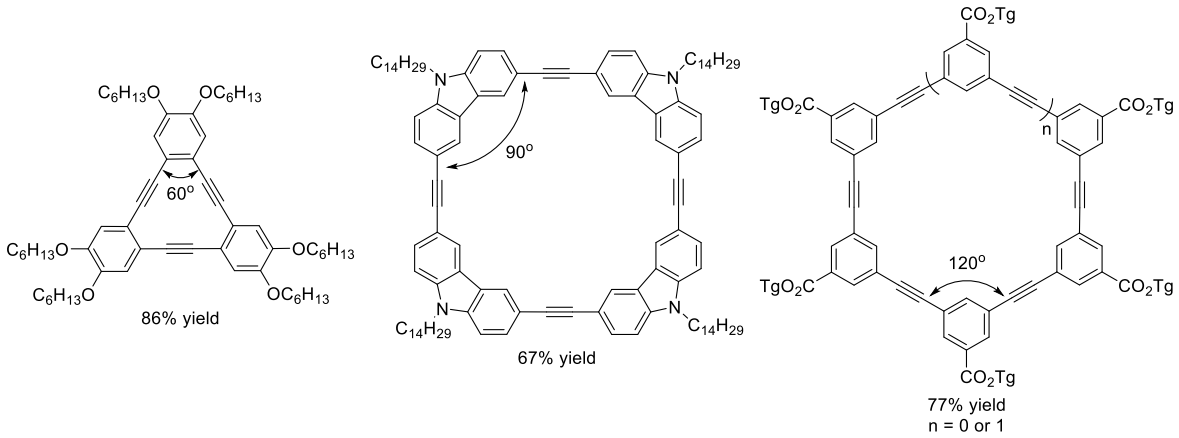

Figure 1.5: AEMs synthesized by precipitation-driven metathesis conditions demonstrating the significance of monomer geometry.

When studying the reaction progress of the precipitation-driven reactions, it was noted that oligomers longer than the desired length first formed under the metathesis condition and then they self-corrected to form the macrocycle.[37] This result is in agreement with the dynamic nature of the reaction since the product distribution is dictated by the thermodynamics of the system and should not be influenced by the starting material. Building on this result, Moore and Gross developed the strategy further by demonstrating the synthesis of carbazolyl-ethynylene macrocycles via depolymerization of the corresponding homopolymers synthesized by Sonogashira polycondesation (Scheme 1.11).[38] This new method has several advantages compared to the monomer-based methods: (1) the solubility of the starting material is improved by the lack of bulky benzoylbiphenyl groups, providing access to previously unusable monomers; (2) the atom economy of the reaction is significantly improved since a stoichiometric amount of byproduct is not produced; and (3) the synthesis is shortened because the monomers required for polymerization are intermediates toward the precipitation-based monomer, and the polymer requires no further purification beyond precipitation from methanol.

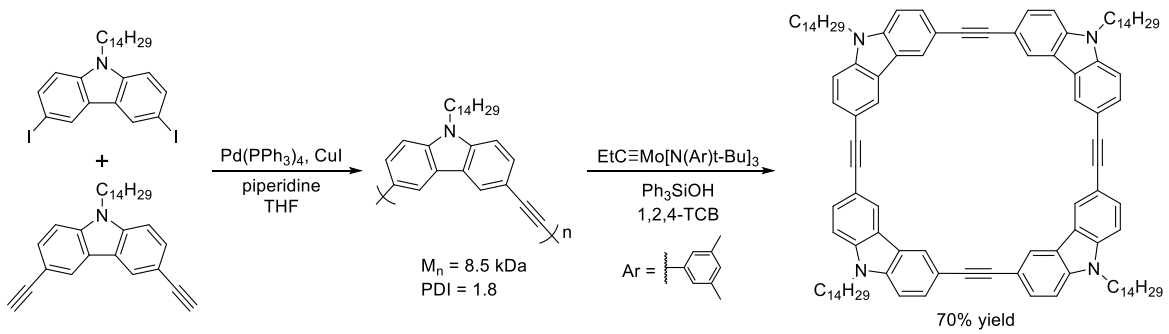

Scheme 1.11: Synthesis of a carbazolyl-ethynylene macrocycle via depolymerization-macrocyclization.

The modularity of the depolymerization-macrocyclization method was attractive the study of systems containing multiple distinct monomers. The basis for this idea was tested using an alternating carbazolyl-ethynylene copolymer where the alternating units contained different solubilizing chains. Upon depolymerization, a statistical mixture of macrocycles was formed with each combination of how the solubilizing chains could be placed on the macrocycle. This result demonstrated the potential for how this method could be used to synthesize libraries of novel AEMs in a facile manner. Expanding to alternating copolymers containing carbazole/*para*-phenyl or carbazole/*meta*- phenyl monomer combinations further showed this capability of the method.[39] Chapter 2 details the syntheses and mechanistic studies of alternating copolymers containing *ortho*-substituted monomers, which displayed a surprising reactivity.

1.4: References

1) Venkataraman, D.; Lee, S.; Zhang, J.; Moore, J.S. *Nature*, **1994**, *371*, 591-593.

2) Moore, J.S. *Acc. Chem. Res.* **1997**, *30*, 402-413.

3) Mindyuk, O.Y.; Stetzer, M.R.; Heiney, P.A.; Nelson, J.C.; Moore, J.S. *Adv. Mater.* **1998**, *10*, 1363-1366.

4) Bunz, U.H.F.; Rubin, Y.; Tobe, Y. *Chem. Soc. Rev.* **1999**, *28*, 107-119.

5) Grave, C.; Schlüter, A.D. *Eur. J. Org. Chem.* **2002**, 3075-3098.

6) Höger, S. *Chem. Eur. J.* **2004**, *10*, 1320-1329.

7) Li, T.; Yue, K.; Yan, Q.; Huang, H.; Wu, H.; Zhu, N.; Zhao, D. *Soft Matter* **2012**, *8*, 2405-2415.

8) Naddo, T.; Che, Y.; Zhang, W.; Balakrishnan, K.; Yang, X.; Yen, M.; Zhao, J.; Moore, J.S.; Zang, L. *J. Am. Chem. Soc.* **2007**, *129*, 6978-6979.

9) Leu, W.C.W.; Fritz, A.E.; Digianantonio, K.M.; Hartley, C.S. *J. Org. Chem.* **2012**, *77*, 2285-2298.

10) Tahara, K.; Lei, S.; Mamdouh, W.; Yamaguchi, Y.; Ichikawa, T.; Uji-i, H.; Sonoda, M.; Hirose, K.; De Schryver, F.C.; De Feyter, S.; Tobe, Y. *J. Am. Chem. Soc.* **2008**, *130*, 6666-6667.

11) Yamaguchi, Y.; Yoshida, Z. *Chem. Eur. J.* **2003**, *9*, 5430-5440.

12) Adisoejoso, J.; Tahara, K.; Lei, S.; Szabelski, P.; Rżysko, W.; Inukai, K.; Blunt, M.O.; Tobe, Y.; De Feyter, S. *ACS Nano* **2012**, *6*, 897-903.

13) Ghijsens, E.; Ivasenko, O.; Tahara, K.; Yamaga, H.; Itano, S.; Balandina, T.; Tobe, Y.; De Feyter, S. *ACS Nano* **2013**, *7*, 8031-8042.

14) Li, B.; Tahara, K.; Adisoejoso, J.; Vanderlinden, W.; Mali, K.S.; De Gendt, S.; Tobe, Y.; De Feyter, S. *ACS Nano* **2013**, *7*, 10764-10772.

15) Tahara, K.; Furukawa, S.; Uji-i, H.; Uchino, T.; Ichikawa, T.; Zhang, J.; Mamdouh, W.; Sonoda, M.; De Schryver, F.C.; De Feyter, S.; Tobe, Y. *J. Am. Chem. Soc.* **2006**, *128*, 16613-16625.

16) Kim, J.; Tahara, K.; Jung, J.; De Feyter, S.; Tobe, Y.; Kim, Y.; Kawai, M. *J. Phys. Chem. C* **2012**, *116*, 17082-17088.

17) Finke, A.D.; Gross, D.E.; Han, A.; Moore, J.S. *J. Am. Chem. Soc.* **2011**, *133*, 14063-14070.

18) Campbell, I.D.; Eglinton, G.; Henderson, W.; Raphael, R.A. *Chem. Commun.* **1966**, 87-89.

19) Staab, H.A.; Neunhoeffer, K. *Synthesis* **1974**, 424-425.

20) Li, Y.; Zhang, J.; Wang, W.; Miao, Q.; She, X.; Pan, X. *J. Org. Chem.* **2005**, *70*, 3285-3287.

21) Iyoda, M.; Vorasingha, A.; Kuwatani, Y.; Yoshida, M. *Tetrahedron Lett.* **1998**, *39*, 4701-4704.

22) Anderson, H.L.; Sanders, J.K.M. *Angew. Chem. Int. Ed. Engl.* **1990**, *29*, 1400-1403.

23) Höger, S. J. *Polym. Sci. Part A: Polym. Chem.* **1999**, *37*, 2685-2698.

24) Moore, J.S.; Zhang, J. *Angew. Chem. Int. Ed. Engl.* **1992**, *31*, 922-924.

25) Zhang, J.; Pesak, D.J.; Ludwick, J.L.; Moore, J.S. *J. Am. Chem. Soc.* **1994**, *116*, 4227-4239.

26) Höger, S.; Enkelmann, V. *Angew. Chem. Int. Ed. Engl.* **1995**, *34*, 2713-2716.

27) Zhao, D.; Moore, J.S. *J. Org. Chem.* **2002**, *67*, 3548-3554.

28) MacLachlan, M.J. *Pure Appl. Chem.* **2006**, *4*, 873-888.

29) Hartley, C.S.; Moore, J.S. *J. Am. Chem. Soc.* **2007**, *129*, 11682-11683.

30) Ge, P.; Fu, W.; Herrmann, W.A.; Herdtweck, E.; Campana, C.; Adams, R.D.; Bunz, U.H.F. *Angew. Chem. Int. Ed.* **2000**, *39*, 3607-3610.

31) Miljanić, O.Š.; Vollhardt, K.P.C.; Whitener, G.D. *Synlett* **2003**, 29-34.

32) Fürstner, A.; Mathes, C.; Lehmann, C.W. *J. Am. Chem. Soc.* **1999**, *121*, 9453-9454.

33) Zhang, W.; Kraft, S.; Moore, J.S. *J. Am. Chem. Soc.* **2004**, *126*, 329-335.

34) Zhang, W.; Lu, Y.; Moore, J.S. *Org. Synth.* **2007**, *84*, 163-176.

35) Zhang, W.; Moore, J.S. *J. Am. Chem. Soc.* **2004**, *126*, 12796.

36) Zhang, W.; Brombosz, S.M.; Mendoza, J.L.; Moore, J.S. *J. Org. Chem.* **2005**, *70*, 10198-10201.

37) Zhang, W.; Moore, J.S. *J. Am. Chem. Soc.* **2005**, *127*, 11862-11870.

38) Gross, D.E.; Moore, J.S. *Macromolecules* **2011**, *44*, 3685-3687.

39) Gross, D.E.; Discekici, E.; Moore, J.S. *Chem. Commun.* **2012**, *48*, 4426-4428.

Chapter 2

Depolymerization-Macrocyclization of (*o*-Phenylene-Ethynylene)-*alt*-(Arylene-Ethynylene) Copolymers

2.1: Introduction

The majority of Moore group's research efforts on synthesizing arylene-ethynylene macrocycles (AEMs) via alkyne metathesis have focused on systems containing one type of aryl monomer. As a result, the effective angle between the alkynes on the monomer significantly biases the product distribution at thermodynamic equilibrium (see Figure 2.1).[1-3] With the development of the depolymerization-macrocyclization method, we became interested in the depolymerization of copolymers since changing monomers was shorter and more modular relative to the older, precipitation-driven method. The initial experiment involved the depolymerization of an alternating carbazole-based copolymer with comonomers bearing different solubilizing chains, and the product distribution consisted of a statistical mixture of macrocycles with all possible connectivities.[4] This result piqued our interest because this method can be efficiently applied to construct libraries of novel AEMs from comonomers of various geometries, leading to interesting electronic or self-assembly properties while providing insights into the structure-function relationship in macrocycle properties.

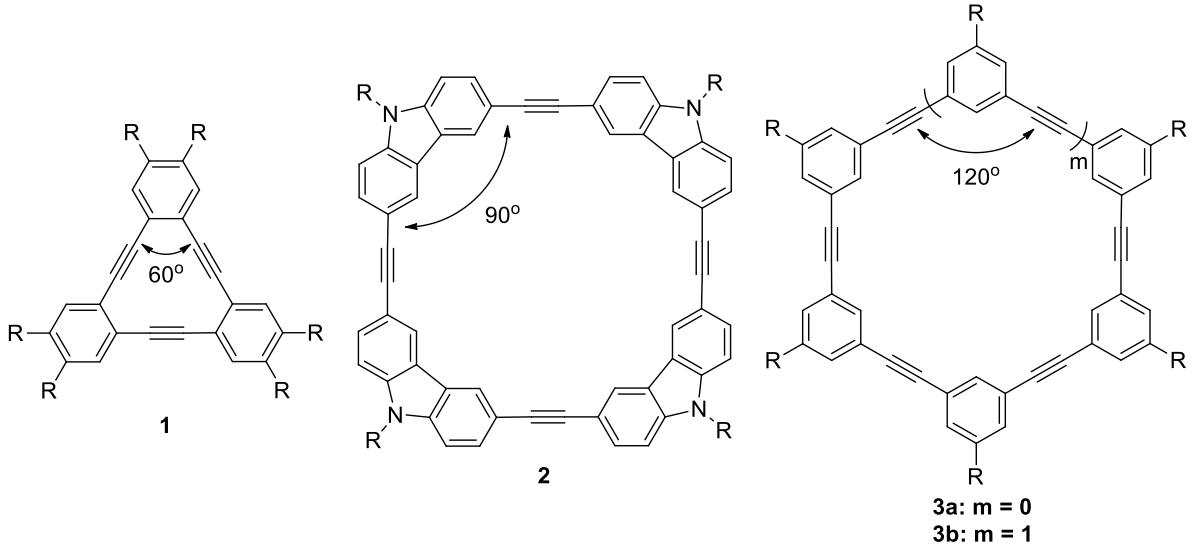

Figure 2.1: Representative single-monomer ("parent") AEMs

Many macrocycles containing two monomers with different geometries have been previously synthesized in order to study their properties. However, these molecules were mostly synthesized by kinetic methods, which are long and tedious to perform, and resulted only in the target compound. We hypothesized was that the thermodynamically driven depolymerization method would provide novel macrocycles in a faster and easier way than the kinetic approach. This principle has since been demonstrated by the depolymerization macrocyclization of alternating copolymers containing carbazole/*para*-phenyl and carbazole/*meta*-phenyl monomer combinations.[4]

2.2: Monomer and Polymer Design and Synthesis

We aimed to investigate the effects of monomers with different geometry on the product distribution of AEMs synthesized by depolymerization-macrocyclization. Alternating copolymers were chosen for their ease of synthesis; under the principals of dynamic covalent chemistry, the starting polymer would have no effect on the distribution. The requisite copolymers **6a-11**were readily available via Sonogashira-type polycondensations of dihaloarenes and diethynylarenes (see Figure 2.2 and Scheme 2.1), and were easily isolated as brown to off-white solids by precipitation from methanol. Molecular weight measurements for these polymers were derived from gel permeation chromatography (GPC) using linear polystyrene standards (see Table 2.1).

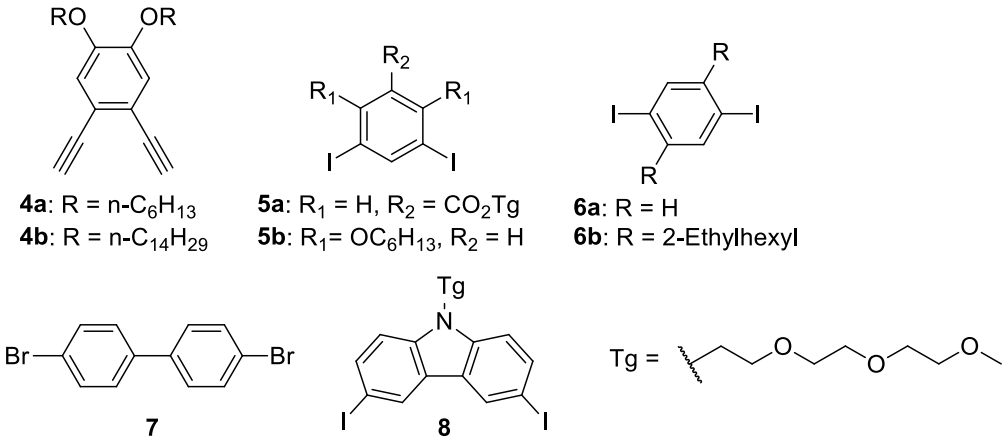

Figure 2.2: Arylene building blocks.

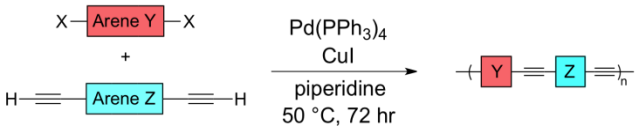

Scheme 2.1: General synthesis of alternating copolymers.

Polymer	Arene Y	Arene Z	Yield (%)[a]	M_n (kDa)[b]	PDI[b]
9a	5a	4a	48	6.9	2.1
9b	5a	4b	100	4.6	1.4
9c	5b	4a	100	4.1	1.5
10a	6a	4b	66	4.8	1.5
10b	6b	4b	70	6.2	1.7
10c	7	4b	75	3.2	1.4
11	8	4a	91	7.1	1.6

Table 2.1: Alternating arylene-ethynylene copolymers synthesized.

(a) Yield is based on a 1:1 ratio of monomers minus 2 equivalents of HX.

(b) Derived from GPC calibrated with linear polystyrene standards.

2.3: Depolymerization-Macrocyclization of Copolymers

We began our investigation with the *o*-phenylene-ethynylene (*o*-PE)/*m*-phenylene-ethynylene (*m*-PE) pair as a model system because it was the only combination previously studied with alkyne metathesis.[5,6] Copolymer **9a** was subjected to depolymerization conditions at room temperature,[3] and a white precipitate formed during the reaction was collected and identified by NMR and FD-MS to be the macrocycle **12a** in 55% yield (Scheme 2.2). The triethylene glycol solubilizing chain was chosen for its polarity, which aids in the separation of different products by column chromatography. The hexyl solubilizing chains on the *ortho*-phenylene monomer were used so that the monomers would have approximately the same molar mass for mass spectrometry analysis. Surprisingly, analysis of the filtrate showed no evidence that any of the single-monomer AEMs (**1**, **3a**, or **3b**) was formed. To ensure that the macrocycles were being formed through metathesis, the starting polymer was separated from macrocyclic byproducts formed kinetically during the polymerization step by preparative GPC. The purified polymer was then depolymerized at room temperature and the appearance of the white precipitate and GPC analysis of the product confirmed the formation of the alternating macrocycle **12a** via depolymerization (see Experimental Section).

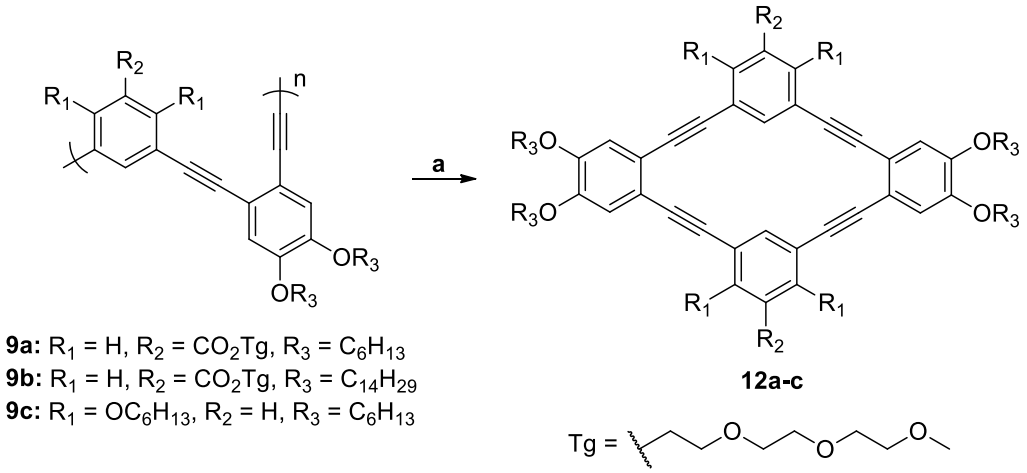

Scheme 2.2: Depolymerization-macrocyclization of (*o*-PE)-*alt*-(*m*-PE) copolymers.

a) EtCMo[N(Ar)t-Bu]$_3$ (10 wt%), Ph_3SiOH (20 wt%), 1,2,4-trichlorobenzene, 23 or 50 °C, 24 h; Ar = 3,5-dimethylbenzene

To determine if the precipitation could have biased the product distribution toward the tetracycle, copolymer **9b** was synthesized with longer alkyl chains to increase the solubility of the product macrocycles and subjected to metathesis. Analysis of the crude product mixture by GPC indicated the emergence of a narrow peak with a substantial shoulder that is broader and of higher molecular weight (Figure 2.3). This shoulder was attributed to linear oligomers formed during the reaction that may account for lost material. Matrix-assisted laser desorption/ionization mass spectrometry (MALDI-TOF MS) of the crude mixture showed that macrocycle **12b** was again the only macrocyclic species present. Upon purification by silica gel chromatography, **12b** was isolated in 79% yield. The depolymerization was repeated on gram-scale to demonstrate the preparative utility of this method and resulted in isolation of the tetracycle product in 49% yield.[7]

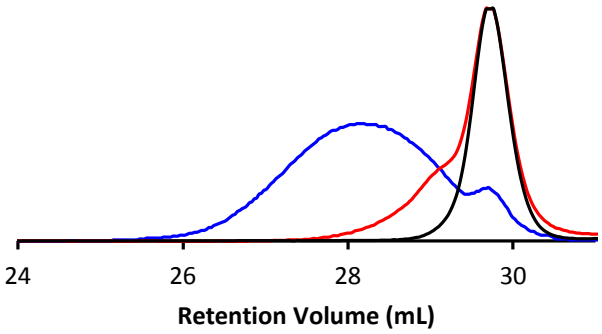

Figure 2.3. GPC traces of a general (*o*-PE)-*alt*-(*m*-PE) copolymer depolymerization reaction showing starting polymer (blue), crude product (red), and purified macrocycle (black). The depolymerization reactions of (*o*-PE)-*alt*-(*p*-PE) followed the same trends.

The observed selectivity for the alternating macrocycle may have been due to a donor-acceptor effect of substituent electronics, where one monomer bears electron-donating ether groups while the other bears electron-withdrawing ester functionality. To test if electronic effects could be favoring the alternating tetracycle structure over the single-monomer macrocycles, copolymer **9c**, in which both monomers are electron rich, was subjected to depolymerization. The hexyl solubilizing chains were chosen so that the monomers had the same molar mass and to more readily compare the results to a previous study on the metathesis of a mixture containing both *m*-PE and *o*-PE monomers.[6] Characterization showed that the alternating AEM **12c** was the only macrocycle product in the crude mixture and was isolated by precipitation from ether in 33% yield.[7]

To investigate whether the observed selectivity was general or not, the depolymerization of (*o*-phenylene-ethynylene)-*alt*-(*p*-phenylene-ethynylene) copolymers was also studied (Scheme 2.3).[8] Through the study of various monomer combinations, it was found that the alternating macrocycle was the sole AEM product and that the *o*-PE/*p*-PE monomer combination behaved the same way as the *ortho*/*meta* pair.

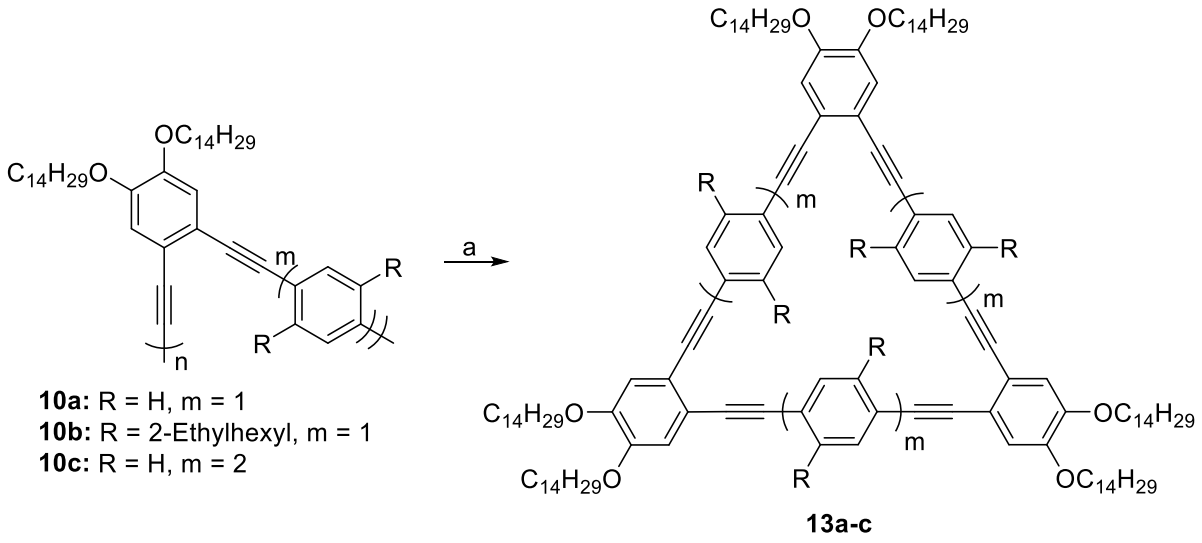

Scheme 2.3: Depolymerization-macrocyclization of (*o*-PE)-*alt*-(*p*-PE) copolymers.

a) EtCMo[N(Ar)t-Bu]$_3$ (10 wt%), Ph_3SiOH (20 wt%), 1,2,4-trichlorobenzene, 23 or 50 °C, 24 h; Ar = 3,5-dimethylbenzene

The last combination studied was the (*o*-phenylene-ethynylene)-*alt*-(carbazolyl-ethynylene) pair. Since all monomer combinations lead to significantly strained, non-planar macrocycles, the depolymerization was expected to result in exclusive formation of the single-

monomer AEMs (**1** and **2**). Just as in the case of *p*-PE- and *m*-PE-CE systems this combination had not previously been incorporated into AEM frameworks, and could lead to novel AEMs if mixing did occur.[4] To test this hypothesis, polymer **11** was subjected to metathesis conditions (Scheme 2.4). A GPC trace of the crude product (Figure 2.4) shows two overlapping peaks, suggesting that more than one small oligomeric products were formed. This result was confirmed by ^{1}H NMR and MALDI-TOF MS. The major components of the product mixture were identified as the alternating tetracycle **14a** and the alternating hexacycle **14b**. Upon purification using silica gel chromatography the two macrocycles co-eluted to give 40% yield of a mixture. However, a small amount of the tetracycle **14a** was separated to permit assignment of the ^{1}H NMR resonances. This result indicated that the tetracycle was the major product in a 2:1 molar ratio.

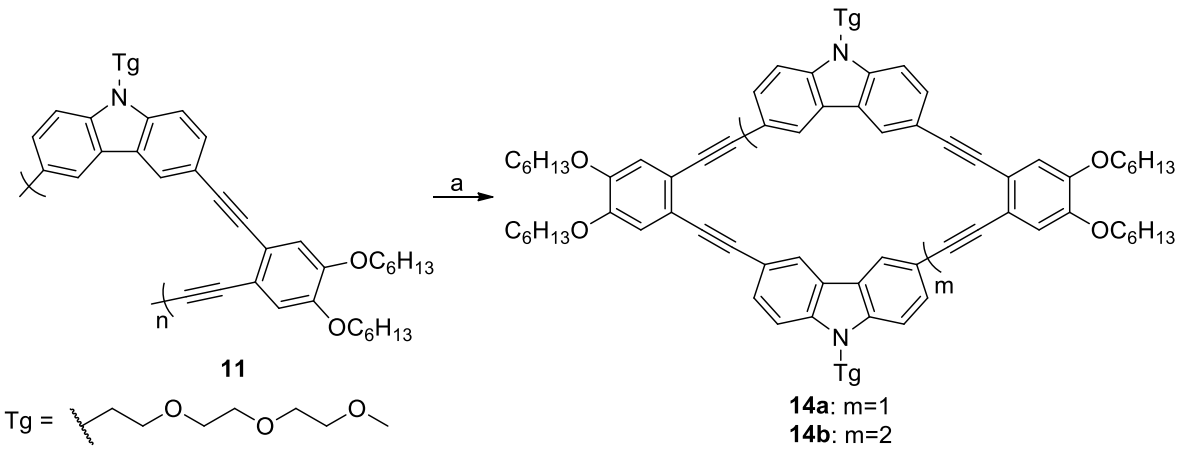

Scheme 2.4: Depolymerization-Macrocyclization of an (*o*-PE)-*alt*-(CE) copolymer.
a) EtCMo[N(Ar)t-Bu]$_3$ (10 wt%), Ph_3SiOH (20 wt%), 1,2,4-trichlorobenzene, 23 °C, 24 h; Ar = 3,5-dimethylbenzene

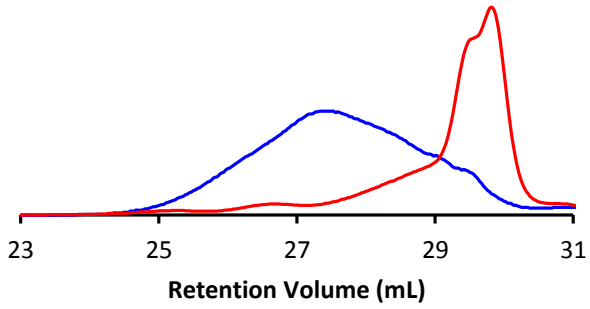

Figure 2.4: GPC traces showing the depolymerization of the (*o*-PE)-*alt*-(CE) copolymer (blue) and the two overlapping peaks in the crude product mixture (red).

Semi-empirical molecular modeling[9] of **14a** results in a curved, saddle-shaped structure, while modeling of **14b** suggests a non-planar crown-type structure with the *o*-PE units on one side and the carbazole units on the other (see Experimental Section). This shape for **14b** is supported by the NMR resonance values for the aromatic protons, all of which are shielded relative to the peaks from the more planar tetracycle (see Experimental Section).

2.4: Investigating the Origin of Selectivity

Intrigued by the lack of single-monomer AEM formation during the depolymerization of (*o*-phenylene-ethynylene)-*alt*-(arylene-ethynylene) copolymers, we set out to determine the source of the observed selectivity. We first hypothesized was that the alternating macrocycles were the thermodynamically or statistically favored product, even though it was not readily apparent. Because alkyne metathesis is a dynamic reaction and should reach equilibrium, the nature of the starting material (copolymers vs. monomers) should be irrelevant and the reaction should reach the same equilibrium product distribution. Therefore, we tested our first hypothesis by performing the metathesis reaction using monomers functionalized with benzoylbiphenyl groups under the precipitation-driven conditions[1] and determined if the product distribution was the same as from depolymerization-macrocyclization.

Monomers **15** and **16** were mixed in equimolar amounts and subjected to metathesis conditions to mimic the depolymerization of copolymer **9c** (Scheme 2.5). Field-desorption mass spectrometry (FD-MS) analysis of the crude product mixture showed that, in contrast to the depolymerization conditions, a much broader distribution of macrocycles was formed under these conditions (Figure 2.5). This result indicates that the tetracycle is not the most thermodynamically stable product to appear as the sole AEM in the depolymerization. Therefore, the depolymerization reaction on (*o*-phenylene-ethynylene)-*alt*-(arylene-ethynylene) copolymers is not operating under thermodynamic control as we originally assumed, and must be falling into a kinetic trap. This observation is unique since all of the depolymerization reactions previously studied were operating under thermodynamic control. It also suggests that the *o*-PE monomer does not behave the same as other arylene-ethynylene monomers toward alkyne metathesis.

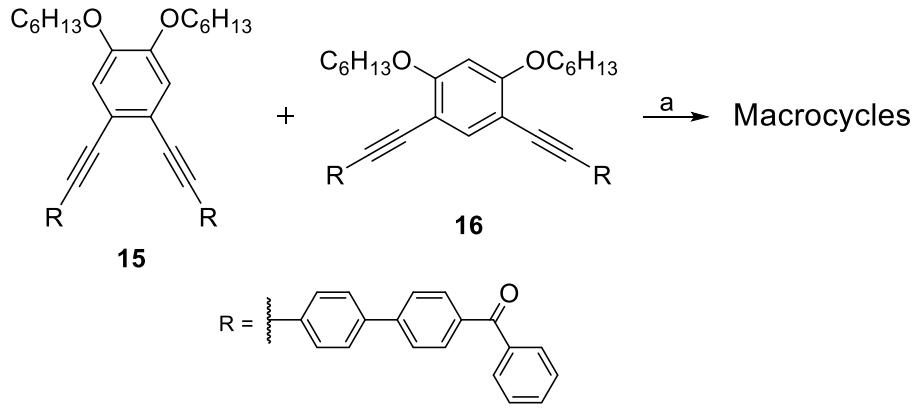

Scheme 2.5: Metathesis of a monomer-based mixture.

a) EtCMo[N(Ar)t-Bu]$_3$ (10 mol%), Ph_3SiOH (50 mol%), 1,2,4-trichlorobenzene, 50 °C, 24 h; Ar = 3,5-dimethylbenzene

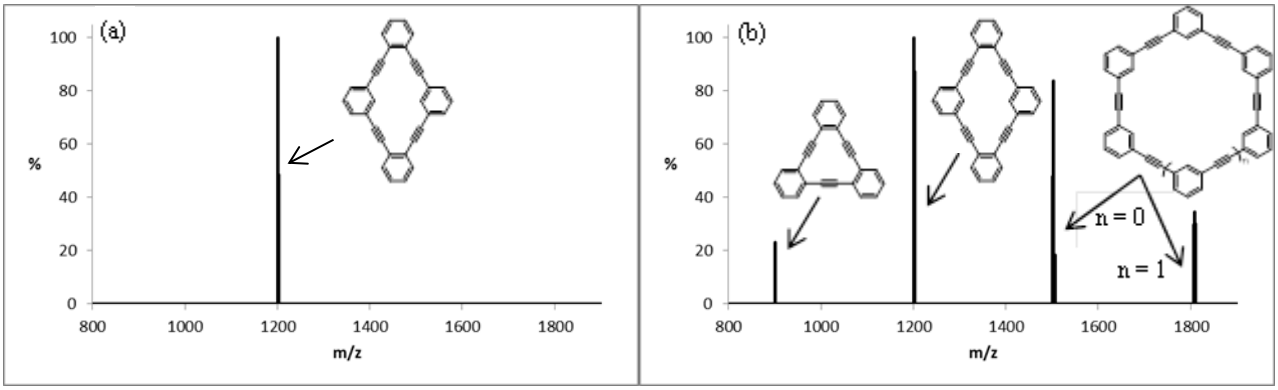

Figure 2.5: FD-MS of the crude product mixtures from (a) the depolymerization of copolymer **9c** and (b) equimolar mixing of monomers **15** and **16**.

Since the depolymerization-macrocyclization in this system is not thermodynamically controlled, we then hypothesized was that the small angle of the *o*-PE monomer was causing the polymer to be predisposed or preorganized to form the tetracycle, which may then be too unreactive toward metathesis for the reaction to progress further. We envisioned that the starting copolymer could fold into a helical conformation[10], thereby increasing the likelihood of intramolecular "back-biting" by the catalyst due to higher effective concentration to produce only the tetracycle. If the tetracycle is relatively unreactive toward further metathesis, then the reaction would be trapped at the tetracycle and unable to progress to form the other AEMs.

We tested this hypothesis by synthesizing an alternating ABAB'-type copolymer by polymerizing a diethynyl-terminated trimer unit with the corresponding diiodide monomer (**17**: M_n = 6.0 kDa, PDI = 2.5; see Experimental Section for detailed synthesis) and subjected it to

depolymerization conditions (Scheme 2.6). Assuming that back-biting is the predominant mechanism for depolymerization and no scrambling can occur between tetracycles, hybrid macrocycle **18** should be the only AEM present in the product mixture.

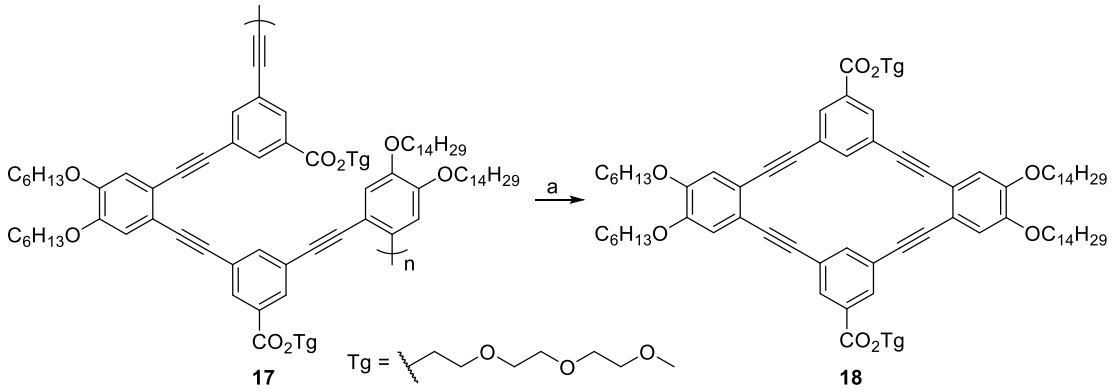

Scheme 2.6: Depolymerization-macrocyclization of an ABAB'-type (*o*-PE)-*alt*-(*m*-PE) copolymer.
a) EtCMo[N(Ar)t-Bu]$_3$ (10 wt%), Ph_3SiOH (20 wt%), 1,2,4-trichlorobenzene, 50 °C, 24 h; Ar = 3,5-dimethylbenzene

Analysis by MALDI-TOF MS showed the presence of **12b** as well as **18**, suggesting that scrambling occurs to some extent during the depolymerization; however, we only observed the formation of tetracyclic products. To determine whether mixing occurred during the depolymerization or between macrocycles, an equimolar amount of **12a** and **12b** was subjected to metathesis and **18** was observed as one species of the tetracycles by MALDI-TOF MS. This result suggests that tetracycle can be opened by the catalyst and scramble under metathesis conditions. Even if back-biting occurs to form the tetracycle, further reaction is possible and should reach the equilibrium product distribution. Thus preorganization is not the origin of the observed selectivity.

We also wanted to determine whether the selectivity was caused by the small angle of the *o*-phenylene-ethynylene monomer or from the steric hindrance due to the close proximity of the alkynes. To study this, a copolymer was synthesized (**19**; M_n=4.0 kDa, PDI=1.3; see Experimental Section for synthesis) with a 3,6-phenanthrene-based monomer in place of the *o*-PE unit. The structure of phenanthrene allows for a monomer that has the same 60° effective angle between the alkynes but with greater distance between them to eliminate any steric effects. Copolymer **19** was subjected to depolymerization (Scheme 2.7) and peaks for the all *m*-PE pentamer and the phenanthrene-based trimer were observed by FD-MS analysis of the crude product mixture.

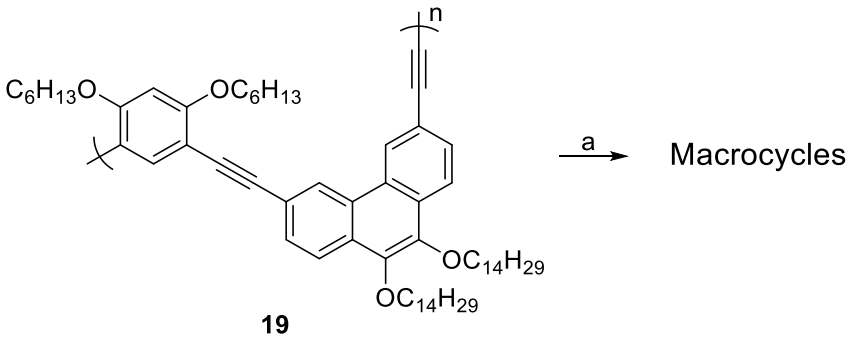

19

Scheme 2.7: Depolymerization-Macrocyclization of a (3,6-phenanthrenyl-ethynyl)-*alt*-(*m*-PE) copolymer.
a) EtCMo[N(Ar)t-Bu]$_3$ (10 wt%), Ph_3SiOH (20 wt%), 1,2,4-trichlorobenzene, 50 °C, 24 h; Ar = 3,5-dimethylbenzene

Based on the results from these three experiments, the depolymerization-macrocyclization selectivity of (*o*-phenylene-ethynylene)-*alt*-(arylene-ethynylene) copolymers is not a consequence of copolymer preorganization or the tetracycle product's lack of reactivity toward metathesis. It is possible that the scrambling of the tetracycle is too slow for the reaction to reach equilibrium, but no difference has yet been observed with increased time or temperature while other copolymers appear to reach equilibrium under standard conditions.[4] Aggregation also does not seem to play a role since the selectivity has not changed with variations in solvent, concentration, or temperature. We also conclude that, instead of the small angle between the monomer substituents, the steric hindrance from close proximity of the alkynes induces the observed selectivity.

Our third hypothesis was that the molybdenum is reacting selectively with one side of the non-symmetric alkyne. This type of selective alkyne metathesis has not been previously reported, though Vollhardt and coworkers noted chemoselective metathesis between two different alkynes based on *ortho*- versus *meta*-substituted functional groups.[5] It is less sterically demanding for the bulky catalyst to approach and react with the non-symmetric alkyne from the *m*-PE side because of the wider 120° angle between the alkynes. Assuming a completely selective interaction between the catalyst and the alkyne, the alternating structure of the copolymer could not be disrupted because it would be unable to connect two units of the same type of monomer (Figure 2.6).

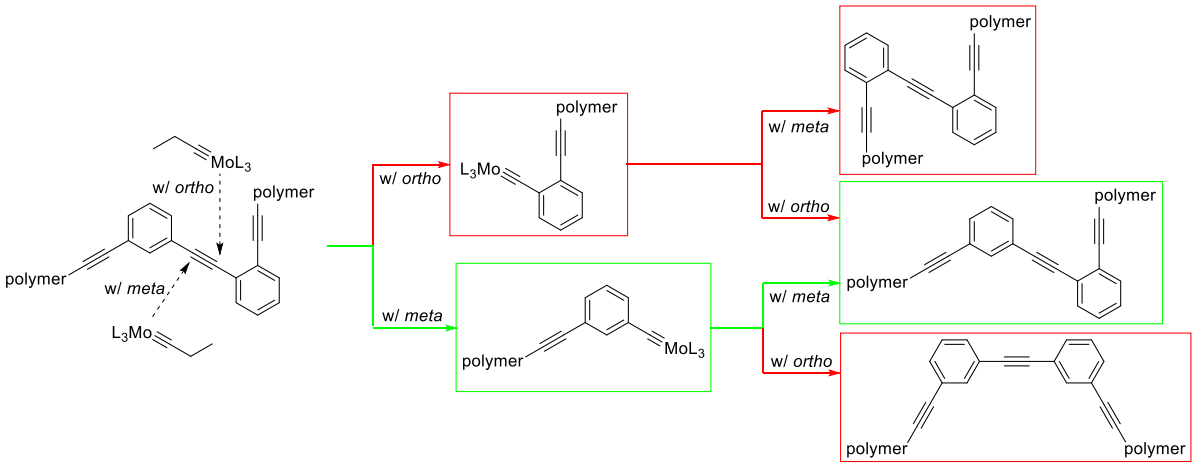

Figure 2.6: The possible products from the reaction of the molybdenum catalyst with each side of the non-symmetric alkyne. The green pathway highlights the compounds formed during the reaction assuming a completely selective reaction of the molybdenum with the *meta*-substituted monomer.

Since the copolymer system is complex and poorly defined due to sample molecular weight and polydispersity, a model compound was used to test this hypothesis (**20**; Figure 2.7). The model compound is based on diphenylacetylene, as it is the simplest unit of the copolymer and has no electronic contribution that can bias the product distribution of the metathesis reaction. Alkynes with trimethylsilyl (TMS) end-caps were chosen for the *ortho*- and *meta*-substituents because, like tert-butyl groups, they were expected to be inert toward the metathesis reaction and they exhibit little electronic impact on the compound.[11] With only one active alkyne in the model compound, the cross-metathesis reaction produces only three compounds (Figure 2.7) that are easily observed by gas chromatography (GC). If the metathesis were completely selctive, only the model compound would be present in the product mixture due to the inability of the catalyst to disrupt the heterodimer. All three of the compounds would be formed if the reaction favored one orientation over the other, but still reacted with both. However, the product distribution should significantly favor the model compound.

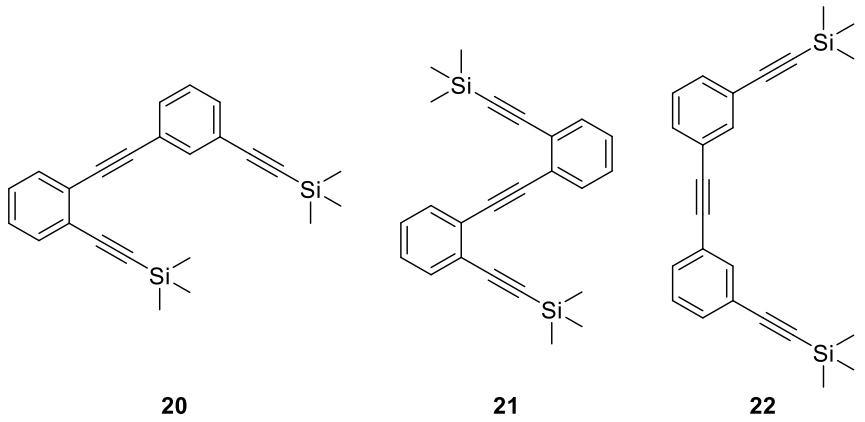

20 **21** **22**

Figure 2.7: Possible products from cross-metathesis of the model compound.

Compound **20** was subjected to metathesis and the reaction mixture was analyzed by gas chromatography (GC) (Scheme 2.8). The chromatograms were compared to standards of the model compound as well as **21** and **22** that were synthesized via an independent route (Figure 2.8). The TMS-alkynes were not completely inert toward metathesis using our catalyst, which made alternative pathways to compound **22** possible even assuming a completely selective reaction. However, the only way to form compound **21** is for the molybdenum catalyst to react on the *o*-PE side of the alkyne. While the presence of **21** in the reaction mixture shows that the metathesis reaction is not totally selective, it does react preferentially with one side because compound **20** is still the major product by a significant margin.

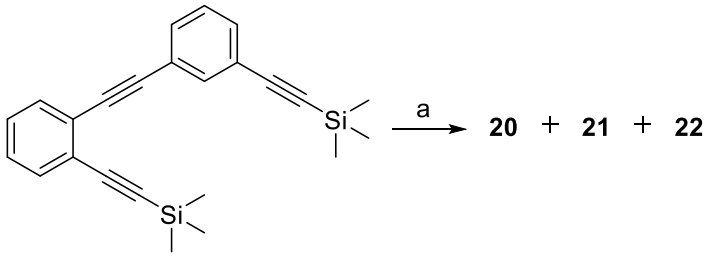

20

Scheme 2.8: Metathesis of a model compound to determine selectivity.

a) EtCMo[N(Ar)t-Bu]$_3$ (10 wt%), Ph_3SiOH (18 wt%), 1,2,4-trichlorobenzene, 50 °C, 24 h; Ar = 3,5-dimethylbenzene

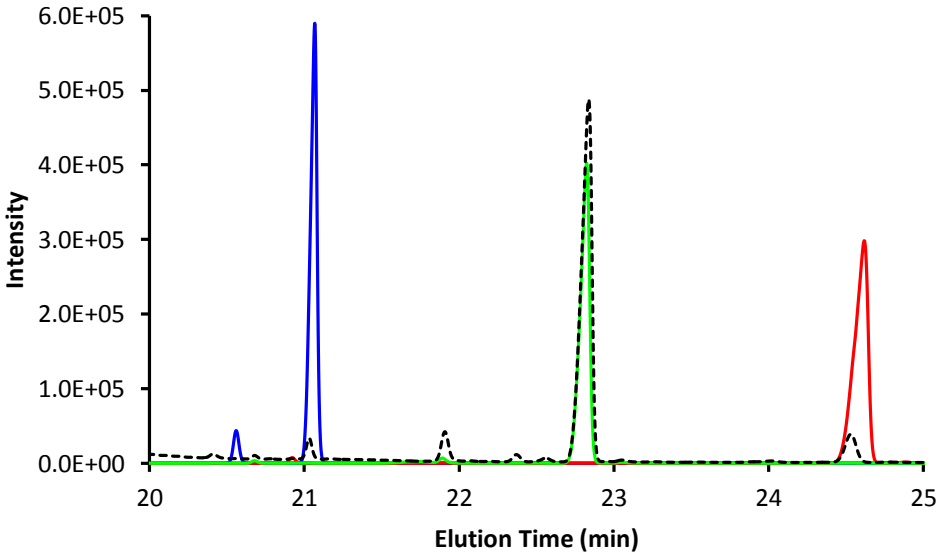

Figure 2.8: Gas chromatograms of the reaction mixture from the metathesis of the model compound (black dashed) showing the presence of all three cross-metathesis products, overlaid with standards of each compound (compound 20 – green; compound 21 – blue; compound 22 – red).

Since compound **20** in the crude mixture could be either the cross-metathesis product or unreacted starting material, it was necessary to demonstrate that it is indeed the major product of the cross-metathesis. Thus the reaction was repeated and monitored every five minutes by GC to determine when it reached equilibrium (see Experimental Section). It was found that the reaction reaches equilibrium in approximately 80 minutes with the catalyst determined to be active over 4 hours into the reaction. This result suggests that the all of the starting material **20** has undergone metathesis and is the major product, demonstrating that the catalyst does react preferentially with only one side of the non-symmetric alkyne. Extending the insights from this study to the depolymerization reaction, our result indicates that the alternating structure can be disrupted but it is difficult for the single-monomer macrocycles to form. Multiple metathesis steps with the disfavored orientation would be necessary to form one of the single-monomer AEMs, which could be present at a concentration too low to be detected. In addition, the homodimer connections that are made could also be in the various linear oligomers formed during the reaction.

2.5: Conclusions

We have found that depolymerization-macrocyclization of (*o*-phenylene-ethynylene)-*alt*-(arylene-ethynylene) copolymers results in the selective formation of alternating arylene-

ethynylene macrocycles. By testing various hypotheses about the origin of this selectivity, we have concluded that it stems from a selective reaction of the molybdenum alkyne metathesis catalyst with the copolymer that disfavors association of the molybdenum with the *o*-PE side of the alkynes. This does not allow for disruption of the alternating structure from the starting copolymer and gives rise to the observed selectivity. The small amount of disfavored reactions that occur is most likely lost in the linear oligomers that are in the crude product of each depolymerization-macrocyclization and do not result in the single-monomer AEMs because of the number of such reactions that would need to occur.

2.6: Experimental Section

All air or moisture-sensitive manipulations were performed under an atmosphere of argon or nitrogen using standard Schlenk techniques or in an argon filled glove box. Analytical thin-layer chromatography (TLC) was performed on Kieselgel F-254 precoated silica gel plates. Visualization was performed with UV light (254 nm) or iodine stain. Flash chromatography was performed using 60 Å silica gel from Silicycle, Inc. All polymerization and metathesis reactions were prepared in an argon-filled glove box and run under an inert atmosphere. The reaction vessels used, unless otherwise specified, were 20 mL vials fitted with PTFE/silicone septa. All glassware was oven-dried before use.

Unless otherwise stated, all starting materials and reagents were purchased from commercial sources and used without further purification. Carbazole (Acros 96%), CuI (99.999%, PURATREM grade, Strem), piperidine (Aldrich, redistilled 99.5%). N,N-Dimethylformamide (DMF) and tetrahydrofuran (THF) were obtained from a Solvent Delivery System (SDS) equipped with activated neutral alumina columns. Triethylamine was freshly distilled from CaH_2 under a nitrogen atmosphere. CCl_4 was distilled over P_2O_5 and degassed before use. Compound **16** was previously synthesized by a former graduate student (Wei Zhang) and used without purification.[2]

^{1}H and ^{13}C NMR spectra were obtained on Varian Unity 400, Unity 500, and VXR 500 spectrometers. Chemical shifts are reported in δ (ppm) relative to the residual solvent protons ($CDCl_3$: 7.26 for ^{1}H, 77.0 for ^{13}C). Coupling constants (*J*) are expressed in hertz (Hz). Splitting patterns are designated as s (singlet); d (doublet); t (triplet); dd (doublet of doublets); td (triplet of doublets); m (multiplet). Low resolution ESI mass spectra were recorded on a Waters Quattro

II spectrometer. High resolution ESI mass spectra were recorded on a Micromass Q-Tof Ultima spectrometer. MALDI mass spectra were recorded on an Applied Biosystems Voyager-DE STR spectrometer. MALDI analysis of macrocycles was carried out using the dithranol matrix. FD mass spectra were recorded on a Micromass 70-VSE EI/CI/FD/FI spectrometer. Analytical gel permeation chromatography (GPC) analyses were performed on a system composed of a Waters 515 HPLC pump, a Thermoseparations Trace series AS100 autosampler, a series of three Waters HR Styragel columns (7.8 × 300 mm, HR3, HR4, and HR5), and a Viscotek TDA Model 300 triple detector array, in HPLC grade THF (flow rate = 1.0 mL/min) at 30 °C. The GPC was calibrated using a series of monodisperse polystyrene standards. Melting points were measured on a Electrothermal Mel-Temp 1001 apparatus. Gas chromatograpy (GC) was performed on a Shimadzu GC-2010 Plus gas chromatograph with SHRXI-MS-15m × 0.25 mm × 0.25 µm column with nitrogen carrier gas and a flame ionization detector (FID). All GC samples were analyzed with the following method: total gas flow rate = 28.3 mL/min (column flow = 1.20mL/min, linear velocity = 35.0 cm/sec, purge flow = 3.0 mL/min); split ratio = 20; initial temp. = 50.0 °C (hold 1 minute); rate = 10 °C/min; final temp. = 250.0 °C (hold 9 minutes).

2.6.1: Synthesis and Characterization of Monomers/Small Molecules

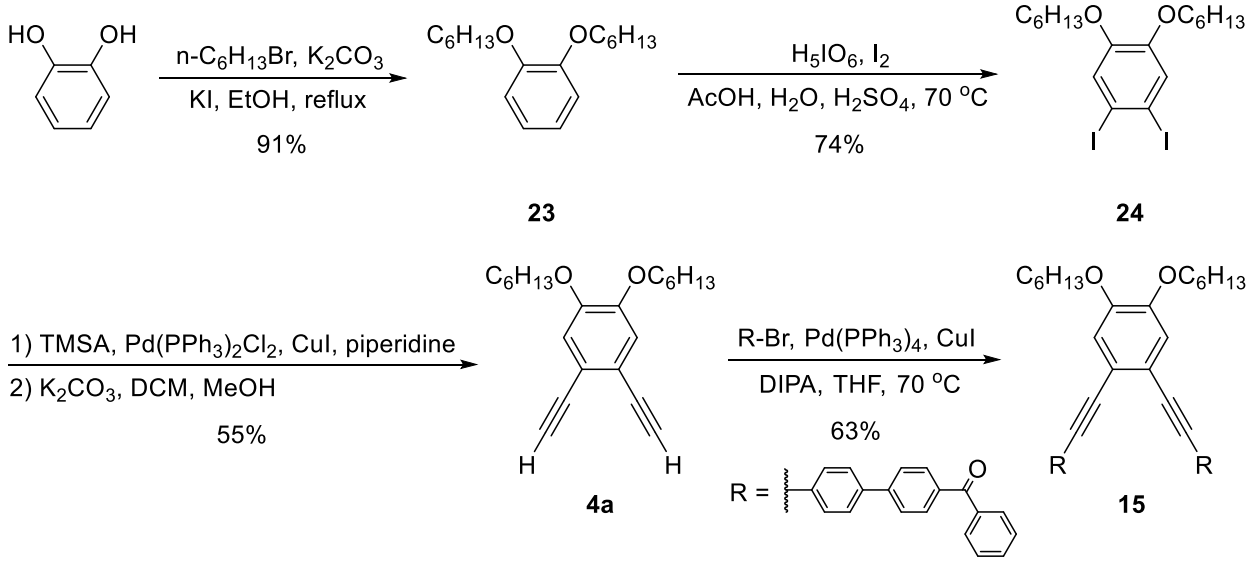

1,2-Bis(hexyloxy)benzene (23)[2]**:** 1-Bromohexane (31.9 mL, 227 mmol) was added to a stirring mixture of catechol (10.0 g, 90.8 mmol), K_2CO_3 (50.3 g, 364 mmol), and KI (1.51 g, 9.10 mmol) in ethanol (90 mL). The mixture was refluxed under nitrogen for 16 hours. The reaction mixture was cooled to room temperature before dichloromethane (250 mL) was added and was filtered

through a pad of silica gel with DCM eluting. The solvent was removed in *vacuo* and the product was purified by column chromatography (silica gel, 85:15 hexanes:DCM) to yield the product as a pale yellow oil (23.1 g, 91%) ^{1}H NMR ($CDCl_3$, 500 MHz) δ: 6.89 (s, 4H), 4.0 (t, 4H, *J* = 6.5 Hz), 1.82 (p, 4H, *J* = 7.5 Hz), 1.48 (m, 4H), 1.35 (m, 8H) 0.91 (t, 6H, *J* = 7.0 Hz); ^{13}C NMR ($CDCl_3$, 125 MHz) δ: 149.2, 121.0, 114.1, 69.2, 31.6, 29.3, 25.7, 22.6, 14.0; HRMS (EI^+): Calcd. for $C_{18}H_{30}O_2$ 278.2246, Found 278.2243.

1,2-Bis(hexyloxy)-4,5-diiodobenzene (24)[2]: 1,2-Bis(hexyloxy)benzene (8.36 g, 30.0 mmol) was slowly added to a stirring mixture of iodine (6.85 g, 27.0 mmol) periodic acid (2.74 g, 12.0 mmol) and a 100:20:3 mixture of AcOH:H_2O:H_2SO_4 (60 mL) in a round-bottomed flask. A reflux condenser was fitted to the flask and the reaction mixture was stirred at 70 °C for 7 hours. The reaction was cooled to room temperature and concentrated in *vacuo*. The residue was dissolved in DCM (50 mL) and washed sequentially with water (100 mL), a saturated solution of $NaHCO_3$ (2×50 mL), a saturated solution of $Na_2S_2O_3$ (2×50 mL), and water again (2×50 mL). The organic layer was then dried ($MgSO_4$), the solvent was removed in *vacuo*, and the product was purified by column chromatography (silica gel, 80:20 hexanes:DCM) to yield the product as a pale orange oil (11.7 g, 74%). ^{1}H NMR ($CDCl_3$, 500 MHz) δ: 7.24 (s, 2H), 3.92 (t, 4H, *J* = 6.5 Hz), 1.79 (p, 4H, *J* = 7 Hz), 1.45 (m, 4H), 1.33 (m, 8H) 0.90 (t, 6H, *J* = 7.0 Hz); ^{13}C NMR ($CDCl_3$, 125 MHz) δ: 149.6, 123.6, 96.0, 69.3, 31.4, 28.9, 25.5, 22.5, 13.9; HRMS (EI^+): Calcd. for $C_{18}H_{28}O_2I_2$ 530.0179, Found 530.0173.

1,2-Diethynyl-4,5-bis(hexyloxy)benzene (4a)[2]: Trimethylsilylacetylene (6.0 mL, 42 mmol) was added dropwise to a stirring mixture of 1,2-bis(hexyloxy)benzene (4.45 g, 8.39 mmol), bis(triphenylphosphine)palladium(II) dichloride (294 mg, 0.42 mmol), and copper(I) iodide (79.8 mg, 0.42 mmol) in piperidine (28 mL, 280 mmol) under nitrogen in a Schlenk flask. The reaction contents were then stirred at room temperature for 16 hours. The mixture was diluted with ethyl acetate (50 mL) and filtered through a pad of silica gel with ethyl acetate eluting. The solvent was removed from the filtrate in *vacuo* and the product was purified by column chromatography (silica gel, 75:25 hexanes:DCM) to yield an orange oil. The TMS-protected intermediate was dissolved in a 1:1 methanol:DCM mixture (340 mL), K_2CO_3 (3.52 g, 25.5 mmol) was added, and the mixture was stirred at room temperature for 3 hours. The reaction mixture was then diluted

with DCM (300 mL) and filtered through a pad of silica gel with DCM eluting. The solvent was removed from the filtrate in *vacuo* and the product was purified by column chromatography (silica gel, 75:25 hexanes:DCM) to yield a pale yellow oil that quickly darkened to a red oil (1.51 g, 55% over two steps). ^{1}H NMR ($CDCl_3$, 500 MHz) δ: 6.95 (s, 2H), 4.0 (t, 4H, *J* = 6.5 Hz), 3.25 (s, 2H), 1.81 (p, 4H, *J* = 7.5 Hz), 1.48 (m, 4H), 1.33 (m, 8H) 0.90 (t, 6H, *J* = 7.0 Hz); ^{13}C NMR ($CDCl_3$, 125 MHz) δ: 149.4, 117.8, 116.5, 82.2, 79.4, 69.1, 31.5, 29.0, 25.6, 22.6, 14.0; HRMS (EI^+): Calcd. for $C_{22}H_{30}O_2$ 326.2246, Found 326.2250; Anal. Calc'd for $C_{22}H_{30}O_2$: C 80.94, H 9.26; Found: C 80.71, H 9.35.

1,2-Bis(2-(4-benzoylbiphen-4'-yl)ethynyl)-4,5-bis(hexyloxy)benzene (15a)[2]: In an argon-filled glove box, 1,2-diethynyl-4,5-bis(hexyloxy)benzene (0.65g, 1.99 mmol), 4-benzoyl-4'-bromobiphenyl (1.48 g, 4.39 mmol), tetrakis(triphenylphosphine)palladium(0) (116 mg, 0.10 mmol), copper(I) iodide (19.0 mg, 0.10 mmol) were combined in an oven-dried vial and suspended in diisopropylamine (2.0 mL, 14 mmol) and THF (4.5 mL). The reaction was then sealed, removed from the glove box, and stirred at 70 °C for 16 hours. The mixture was cooled to room temperature, diluted with ethyl acetate (20 mL), and filtered through a pad of silica gel with ethyl acetate eluting. The solvent was removed from the filtrate in *vacuo* and the product was purified by column chromatography (silica gel, 3:2 to 7:3 DCM:hexanes) to yield an orange solid (1.06 g, 63%). ^{1}H NMR ($CDCl_3$, 500 MHz) δ: 7.90 (d, 4H, *J* = 8 Hz), 7.84 (d, 4H, *J* = 7 Hz), 7.73 (d, 4H, *J* = 8 Hz), 7.67 (m, 8H), 7.61 (m, 2H), 7.51 (t, 4H, *J* = 8 Hz), 7.07 (s, 2H), 4.06 (t, 4H, *J* = 6.5 Hz), 1.87 (p, 4H, *J* = 7.5 Hz), 1.50 (m, 4H), 1.37 (m, 8H) 0.92 (t, 6H, *J* = 7.0 Hz); ^{13}C NMR ($CDCl_3$, 125 MHz) δ: 195.9, 149.2, 144.0, 139.3, 137.5, 136.3, 132.3, 131.9, 130.6, 129.8, 128.2, 127.1, 126.6, 123.4, 118.5, 115.7, 91.8, 90.0, 69.1, 31.5, 29.0, 25.6, 22.5, 13.9; M.P. = 126-128 °C; HRMS (FAB^+): Calcd. for $C_{60}H_{55}O_4$ 839.4100, Found 839.4094.

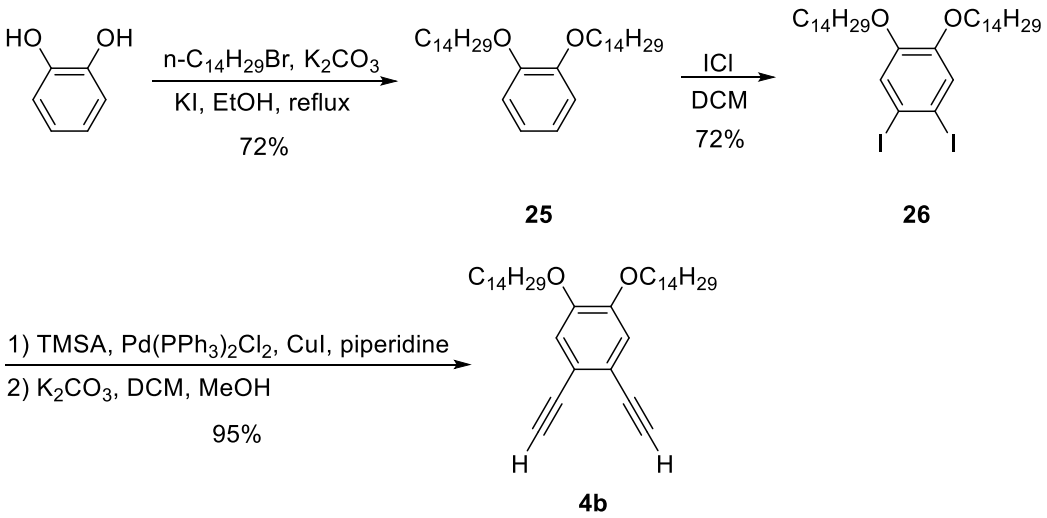

1,2-Bis(tetradecyloxy)benzene (25): To a round-bottomed flask, catechol (10.0 g, 90.8 mmol), 1-bromotetradecane (67.5 mL, 227 mmol), K_2CO_3 (50.2 g, 363 mmol), and KI (1.51 g, 9.10 mmol) were added followed by ethanol (90 mL). The mixture was refluxed under nitrogen for 16 hours. The reaction mixture was cooled to room temperature before dichloromethane (250 mL) was added and the mixture was filtered through a pad of silica gel with DCM eluting. The solvent was removed in *vacuo* and the product was purified by recrystallization from acetone to yield the product as a light tan solid (32.8 g, 72%) ^{1}H NMR ($CDCl_3$, 500 MHz) δ: 6.89 (s, 4H), 4.0 (t, 4H, *J* = 6.5 Hz), 1.82 (p, 4H, *J* = 6.5 Hz), 1.48 (p, 4H, *J* = 6.5 Hz), 1.38-1.27 (m, 40H), 0.90 (t, 6H, *J* = 7.0 Hz); ^{13}C NMR ($CDCl_3$, 125 MHz) δ: 149.2, 121.0, 114.1, 69.3, 31.9, 29.71, 29.67, 29.67, 29.65, 29.64, 29.64 29.45, 29.38, 29.35, 26.1, 22.7, 14.1; HRMS (EI^+): Calcd. for $C_{34}H_{62}O_2$ 502.4749, Found 502.4736.

1,2-Bis(tetradecyloxy)-4,5-diiodobenzene (26): To a stirring solution of 1,2-bis(tetradecyloxy)benzene (5.03 g, 10.0 mmol) dissolved in DCM (100 mL), a solution of ICl (1.0 M solution in DCM, 26.7 mL, 26.7 mmol) was added dropwise in the dark. The reaction mixture was left to stir for 2 hours before quenching with water (100 mL) and extracting with DCM (200 mL). The extract was washed with a saturated solution of $Na_2S_2O_3$ (150 mL) and brine (100 mL) and dried (Na_2SO_4). The solvent was removed in *vacuo* and the product was purified by recrystallization from acetone to yield the product as a tan solid (5.4 g, 72%). ^{1}H NMR ($CDCl_3$, 500 MHz) δ: 7.24 (s, 2H), 3.92 (t, 4H, *J* = 7.5 Hz), 1.78 (m, 4H), 1.45-1.25 (m, 44H), 0.88 (t, 6H, *J* = 10.0 Hz); ^{13}C NMR ($CDCl_3$, 125 MHz) δ: 149.7, 123.7, 95.9, 69.4, 29.7,

29.68, 29.66, 29.66 29.59, 29.58, 29.58, 29.36, 29.32, 29.0, 25.9, 22.7, 14.1; HRMS (EI^+): Calcd. for $C_{34}H_{60}O_2I_2$ 754.2683, Found 754.2668.

1,2-Diethynyl-4,5-bis(tetradecyloxy)benzene (4b): 1,2-Bis(tetradecyloxy)-4,5-diiodobenzene (10.0 g, 13.3 mmol), bis(triphenylphosphine)palladium(II) dichloride (470 mg, 0.66 mmol, 5 mol% equiv.), and copper(I) iodide (75 mg, 0.78 mmol, 3 mol% equiv.) were added to a round-bottomed flask, suspended in piperdine (80 mL), and left to bubble under nitrogen for 20 minutes. At this time, trimethylsilylacetylene (18 mL, 133 mmol) was slowly added, and the mixture was left to stir at room temperature under nitrogen for 24 hours. The mixture was filtered through a pad of silica gel with ethyl acetate eluting. The solvent was removed from the filtrate in *vacuo*, and the product was purified by column chromatography (silica gel, 10:1 hexanes:DCM). The TMS-protected intermediate was dissolved in a 4:1 mixture of DCM:methanol (400 mL) and K_2CO_3 (5.35 g, 39 mmol) was added. The mixture was left to stir at room temperature under nitrogen for 24 hours. The mixture was quenched with water (200 mL) extracted with DCM (300 mL), rinsed with brine (150 mL), and dried over $MgSO_4$. The solvent was removed in *vacuo* to yield the product as a light brown solid (7.0 g, 95%). ^{1}H NMR ($CDCl_3$, 500 MHz) δ: 6.95 (s, 2H), 3.98 (t, 4H, *J* = 10 Hz), 3.25 (s, 2H), 1.83 (m, 4H), 1.35-1.25 (m, 44H), 0.88 (t, 6H, *J* = 7.5 Hz); ^{13}C NMR ($CDCl_3$, 125 MHz) δ: 149.4, 117.7, 116.5, 82.2, 79.4, 69.1, 31.9, 29.7, 29.70, 29.66, 29.66, 29.66, 29.60, 29.60 29.36, 29.0, 25.9, 22.7, 14.1; m.p. = 60-62 °C; HRMS (EI^+): Calcd. for $C_{38}H_{62}O_2$ 550.4749, Found 550.4762.

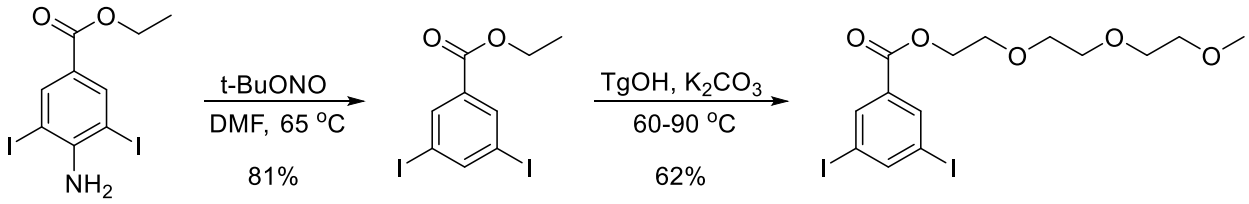

Ethyl 3,5-diiodobenzoate (27)[12]**:** A solution of ethyl 4-amino-3,5-diiodobenzoate (2.09 g, 5.01 mmol) in DMF (20 mL) under nitrogen was slowly added via cannula to a 65 °C solution of *tert*-butyl nitrite (0.89 mL, 7.48 mmol) in DMF in a two-necked flask equipped with a reflux condenser, which was also under nitrogen. The reaction mixture was then stirred at 65 °C for 1 hour before it was cooled to room temperature, diluted with DCM (50 mL) and poured into 3M HCl (125 mL). The layers were separated and the organic layer was washed with more 3M HCl

(2×50 mL) and water (3×100 mL) before it was dried ($MgSO_4$). The solvent was removed in *vacuo*, and the product was purified by column chromatography (silica gel, 97:3 hexanes:ethyl acetate) to yield a pale yellow solid (1.63 g, 81%). NOTE: Contained ~10% inseparable impurity believed to be ethyl 3,4,5-triiodobenzoate that was carried through to the next step.^{1}H NMR ($CDCl_3$, 500 MHz) δ: 8.30 (d, 2H, *J* = 1.5 Hz), 8.20 (t, 1H, *J* = 1.5 Hz), 4.37 (q, 2H, *J* = 7.5 Hz), 1.38 (t, 3H, *J* = 7.5 Hz); ^{13}C NMR ($CDCl_3$, 125 MHz) δ: 163.6, 149.0, 137.6, 133.5, 94.3, 61.7, 14.2; HRMS (EI^+): Calcd. for $C_9H_8O_2I_2$ 401.8614, Found 401.8621.

2-(2-(2-Methoxyethoxy)ethoxy)ethyl 3,5-diiodobenzoate (5a)[13]: To a round-bottomed flask, ethyl 3,5-diiodobenzoate (1.41 g, 3.51 mmol), K_2CO_3 (96.7 mg, 0.70 mmol), and triethylene glycol monomethyl ether (2.8 mL, 17 mmol) were added. The mixture was placed on a Kugelrohr apparatus and the reaction was performed under vacuum (0.7 mmHg) at 60 °C for 2 hours with ethanol distilled off as it formed. The temperature was increased to 90 °C and the excess triethylene glycol monomethyl ether was distilled off. The product was then purified by column chromatography (silica gel, 3:2 hexanes:ethyl acetate) to yield a white solid (1.13 g, 62%). ^{1}H NMR ($CDCl_3$, 500 MHz) δ: 8.29 (d, 2H, *J* = 1.5 Hz), 8.19 (t, 1H, *J* = 1.5 Hz), 4.44 (m, 2H), 3.79 (m, 2H), 3.70-3.61 (m, 6H), 3.51 (m, 2H), 3.34 (s, 3H); ^{13}C NMR ($CDCl_3$, 125 MHz) δ: 163.5, 149.1, 137.6, 133.1, 94.3, 71.8, 70.5, 70.5, 70.5, 68.9, 64.7, 59.0; m.p. = 67-69 °C; HRMS (EI^+): Calcd. for $C_{14}H_{19}O_5I_2$ 520.9323, Found 520.9319.

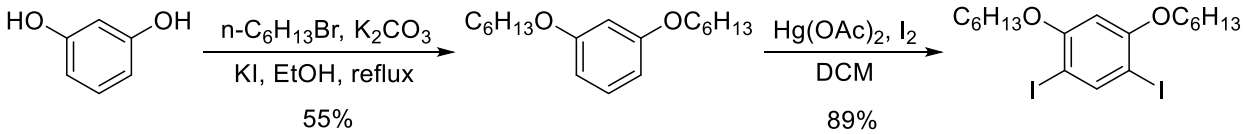

28 **5b**

1,3-Bis(hexyloxy)benzene (28)[2]: 1-Bromohexane (16.0 mL; 114 mmol) was added to a stirring mixture of resorcinol (5.00 g; 45.4 mmol), K_2CO_3 (25.2 g; 182 mmol), and KI (0.75 g; 4.5 mmol) in ethanol (50 mL). The mixture was refluxed under nitrogen for 16 hours. The reaction mixture was cooled to room temperature before dichloromethane (150 mL) was added and the mixture was filtered through a pad of silica gel with DCM eluting. The solvent was removed in *vacuo* and the product was purified by column chromatography (silica gel, 9:1 hexanes:DCM) to yield the product as a clear oil (7.01 g, 55%) ^{1}H NMR ($CDCl_3$, 500 MHz) δ: 7.16 (t, 1H, *J* = 8.5 Hz), 6.49 (m, 3H), 3.95 (t, 4H, *J* = 6.5 Hz), 1.78 (m, 4H), 1.47 (m, 4H), 1.35 (m, 8H), 0.93 (t,

6H, *J* = 7.0 Hz); ^{13}C NMR ($CDCl_3$, 125 MHz) δ:160.4, 129.7, 106.6, 101.4, 67.9, 31.6, 29.2, 25.7, 22.6, 14.0; FD-MS: *m/z* = 279.1 (10%), 278.1 (100%), 278.0 (10%), 117.0 (5%).

1,5-Bis(hexyloxy)-2,4-diiodobenzene (5b)[14]: A solution of iodine (12.7 g; 50.0 mmol) in dichloromethane (150 mL) was added dropwise via an addition funnel to a stirring mixture of 1,3-bis(hexyloxy)benzene (6.96 g; 25.0 mmol) and $Hg(OAc)_2$ (15.9 g; 49.9 mmol) in DCM (350 mL). The reaction mixture was then stirred in the dark and under nitrogen for 5 hours. The mixture was filtered through Celite 545 and the filter cake was rinsed with DCM. The filtrate was washed with saturated $Na_2S_2O_3$ (200 mL), saturated $NaHCO_3$ (200 mL), water (3 × 200 mL), and brine (200 mL). The organic layer was dried ($MgSO_4$), the solvent was removed in *vacuo*, and the product was purified by recrystallization from methanol to yield a white solid (11.77 g; 89%). ^{1}H NMR ($CDCl_3$, 500 MHz) δ: 8.02 (s, 1H), 6.32 (s, 1H), 3.98 (t, 4H, *J* = 6.5 Hz), 1.83 (m, 4H), 1.52 (m, 4H), 1.35 (m, 8H) 0.92 (t, 6H, *J* = 7.0 Hz); ^{13}C NMR ($CDCl_3$, 125 MHz) δ:159.0, 146.6, 97.9, 76.0, 69.5, 31.5, 29.0, 25.7, 22.6, 14.0; m.p. = 73-74 °C FD-MS: *m/z* = 351.8 (53%), 350.8 (100%).

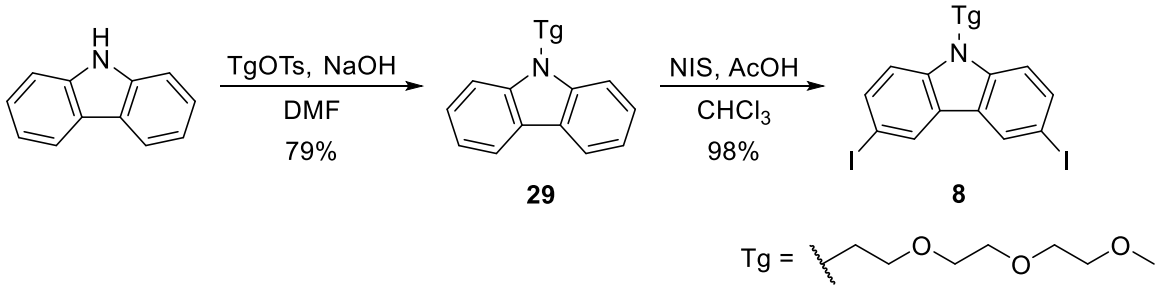

9-(2-(2-(2-Methoxyethoxy)ethoxy)ethyl)carbazole (29)[3,8]: To a round-bottomed flask, carbazole (1.67 g, 10.0 mmol), sodium hydroxide (0.62 g, 15.5 mmol), 2-(2-(2-methoxyethoxy)ethoxy)ethyl 4-methylbenzene sulfonate (4.80 g, 15.1 mmol) and DMF (30 mL) were added. The mixture was stirred for 24 hours at room temperature. Water (100 mL) was then added and the aqueous solution was extracted with DCM. The organic layer was washed with water (2×100 mL), dried (Na_2SO_4), and the solvent was removed in *vacuo*. The product was then purified by column chromatography (silica gel, 4:1 to 1:1 hexanes:ethyl acetate) to yield a yellow oil (2.47 g, 79%). ^{1}H NMR ($CDCl_3$, 500 MHz) δ: 8.10 (d, 2H, *J* = 8.0 Hz), 7.49-7.45 (m, 4H), 7.26-7.28 (m, 2H), 4.51 (t, 2H, *J* = 6.3 Hz), 3.88 (t, 2H, *J* = 6.3 Hz), 3.56-3.9 (m, 6H), 3.49-

3.44 (m, 2H), 3.45 (s, 3H); ^{13}C NMR ($CDCl_3$, 125 MHz) δ: 140.6, 125.6, 122.9, 120.2, 118.9, 108.8, 71.8, 71.0, 70.6, 70., 69.2, 58.9, 43.1; HRMS (EI^+): Calcd. for $C_{19}H_{24}NO_3$ 314.1756, Found 314.1754.

3,6-Diiodo-9-(2-(2-(2-methoxyethoxy)ethoxy)ethyl)carbazole (8)[3,8]**:** To a round-bottomed flask, 9-(2-(2-(2-Methoxyethoxy)ethoxy)ethyl)carbazole (12.54 g, 40.0 mmol), N-iodosuccinimide (18.2 g, 81.0 mmol), acetic acid (100 mL) and chloroform (280 mL) were added. The mixture was stirred in the dark, under nitrogen, at room temperature for 22 hours. The solvent was removed in *vacuo* and water (400 mL) was added to the residue to form a slurry before the water was decanted off. The solid was then extracted with chloroform (300 mL) and the organic solution was washed with a saturated solution of $Na_2S_2O_3$ (2×70 mL) and brine (2×100 mL). The organic layer was dried (Na_2SO_4) and the solvent was removed in *vacuo* to yield a yellow oil that solidified upon standing (22.18 g, 98%). ^{1}H NMR ($CDCl_3$, 500 MHz) δ: 8.29 (d, 2H, *J* = 1.5 Hz), 7.69 (dd, 2H, *J* = 8.5, 1.5 Hz), 7.20 (d, 2H, *J* = 9.0 Hz), 4.40 (t, 2H, *J* = 5.5 Hz), 3.81 (t, 2H, *J* = 5.8 Hz), 3.50-3.39 (m, 10H), 3.33 (s, 3H); ^{13}C NMR ($CDCl_3$, 125 MHz) δ: 139.7, 134.5, 129.2, 124.0, 111.3, 81.9, 71.8, 70.9, 70.6, 70.5, 69.3, 59.0, 43.4; m.p. = 43-46 °C; HRMS (EI^+): Calcd. for $C_{19}H_{22}NO_3I_2$ 565.9689, Found 565.9687.

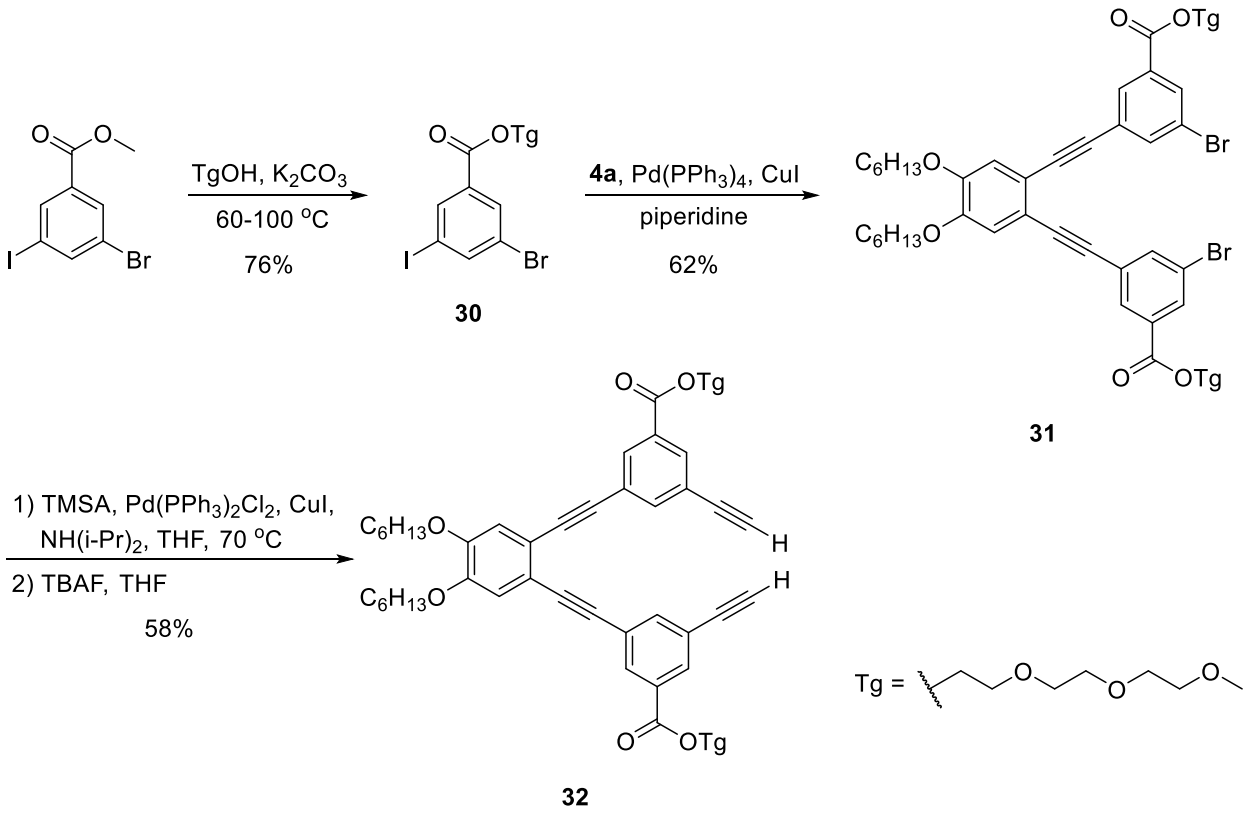

2-(2-(2-Methoxyethoxy)ethoxy)ethyl 3-bromo-5-iodobenzoate (30)[13]**:** To a round-bottomed flask, methyl 3-bromo-5-diiodobenzoate (6.82 g, 20.0 mmol), K_2CO_3 (550 mg, 3.98 mmol), and triethylene glycol monomethyl ether (32 mL, 0.20 mol) were added. A short path distillation head was attached and the mixture was stirred under vacuum (0.2 mmHg) at 60 °C for 2 hours with methanol distilled off as it formed. The temperature was increased to 100 °C and the excess triethylene glycol monomethyl ether was distilled off. The product was then purified by column chromatography (silica gel, 65:35 hexanes:ethyl acetate) to yield a pale yellow solid (7.20 g, 76%). ^{1}H NMR ($CDCl_3$, 500 MHz) δ: 8.27 (t, 1H, *J* = 1.5 Hz), 8.11 (t, 1H, *J* = 1.5 Hz), 8.00 (t, 1H, *J* = 1.5 Hz), 4.45 (m, 2H), 3.80 (m, 2H), 3.62-3.52 (m, 6H), 3.52 (m, 2H), 3.34 (s, 3H); ^{13}C NMR ($CDCl_3$, 125 MHz) δ: 163.7, 143.7, 137.1, 133.2, 131.9, 122.9, 93.9, 71.8, 70.6, 70.5, 70.5, 68.9, 64.7, 59.0; HRMS (EI^+): Calcd. for $C_{14}H_{18}O_5IBr$ 471.9383, Found 471.9376.

Bis(2-(2-(2-methoxyethoxy)ethoxy)ethyl) 5,5'-((4,5-bis(hexyloxy)-1,2-phenylene)bis(ethyne-2,1-diyl))bis(3-bromobenzoate) (31): In an argon-filled glove box, 1,2-diethynyl-4,5-bis(hexyloxy)benzene (1.63 g, 4.99 mmol), 2-(2-(2-methoxyethoxy)ethoxy)ethyl 3-bromo-5-iodobenzoate (5.20 g, 11.0 mmol), tetrakis(triphenylphosphine)palladium(0) (289 mg, 0.25

mmol), and copper(I) iodide (47.8 mg, 0.25 mmol) were combined in an oven-dried vial and suspended in piperidine (15 mL, 0.15 mol). The reaction was sealed, removed from the glove box, and stirred at room temperature for 16 hours. The mixture was diluted with ethyl acetate (30 mL) and filtered through a pad of silica gel with ethyl acetate eluting. The solvent was then removed from the filtrate in *vacuo* and the product was purified by column chromatography (silica gel, chloroform to 9:1 chloroform:ethyl acetate) to yield a tan solid (3.16 g, 62%). ^{1}H NMR ($CDCl_3$, 500 MHz) δ: 8.12 (t, 2H, *J* = 1.5 Hz), 8.11 (t, 2H, *J* = 1.5 Hz), 7.81 (t, 2H, *J* = 1.5 Hz), 7.01 (s, 2H), 4.46 (m, 4H), 4.03 (t, 4H, *J* = 7.0 Hz), 3.79 (m, 4H), 3.70-3.62 (m, 12H), 3.51 (m, 4H), 3.34 (s, 6H), 1.84 (p, 4H, *J* = 7.5 Hz), 1.48 (m, 4H), 1.35 (m, 8H), 0.90 (t, 6H, *J* = 7.0 Hz); ^{13}C NMR ($CDCl_3$, 125 MHz) δ: 164.5, 149.6, 138.0, 132.1, 131.0, 125.6, 122.3, 117.9, 115.6, 90.7, 89.8, 71.9, 70.6, 70.5, 69.2, 68.9, 64.5, 59.0, 31.5, 28.9, 25.6, 22.5, 14.0; FD-MS: *m/z* = 1016.5 (100%).

Bis(2-(2-(2-methoxyethoxy)ethoxy)ethyl) 5,5'-((4,5-bis(hexyloxy)-1,2-phenylene)bis(ethyne-2,1-diyl))bis(3-ethynylbenzoate) (32): Trimethylsilylacetylene (2.1 mL, 15 mmol) was added dropwise to a stirring mixture of **S7** (2.85 g, 2.80 mmol), bis(triphenylphosphine)palladium(II) dichloride (105 mg, 0.15 mmol), and copper(I) iodide (28.6 mg, 0.15 mmol) in THF (7.0mL) and diisopropylamine (3.0 mL, 21.4 mmol) under nitrogen in a Schlenk flask. The reaction was then stirred at 70 °C for 16 hours. The mixture was diluted with ethyl acetate (20 mL) and filtered through a pad of silica gel with ethyl acetate eluting. The solvent was removed from the filtrate in *vacuo* and the TMS-protected intermediate was dissolved in THF (80 mL) under nitrogen. A 1.0M solution of TBAF in THF (7.3 mL, 7.3 mmol) was added dropwise and the reaction was stirred for 1 minute. It was then filtered through a pad of silica gel with THF eluting, and the solvent was removed from the filtrate in *vacuo*. The product was purified by column chromatography (silica gel, 9:1 chloroform:ethyl acetate) to yield an orange solid (1.48 g, 58% over two steps). ^{1}H NMR ($CDCl_3$, 500 MHz) δ: 8.17 (t, 2H, *J* = 1.5 Hz), 8.08 (t, 2H, *J* = 1.5 Hz), 7.78 (t, 2H, *J* = 1.5 Hz), 7.02 (s, 2H), 4.45 (m, 4H), 4.04 (t, 4H, *J* = 7.0 Hz), 3.78 (m, 4H), 3.69-3.61 (m, 12H), 3.51 (m, 4H), 3.33 (s, 6H), 3.13 (s, 2H), 1.84 (p, 4H, *J* = 7.5 Hz), 1.48 (m, 4H), 1.35 (m, 8H), 0.90 (t, 6H, *J* = 7.0 Hz); ^{13}C NMR ($CDCl_3$, 125 MHz) δ: 165.2, 149.8, 138.9, 132.8, 131.1, 124.5, 123.3, 118.4, 116.0, 90.5, 90.4, 82.0, 79.1, 72.1, 70.9, 70.8, 70.8, 69.4, 69.3, 64.7, 59.2, 31.8, 29.3, 25.9, 22.8, 14.2; FD-MS: *m/z* = 906.7 (100%).

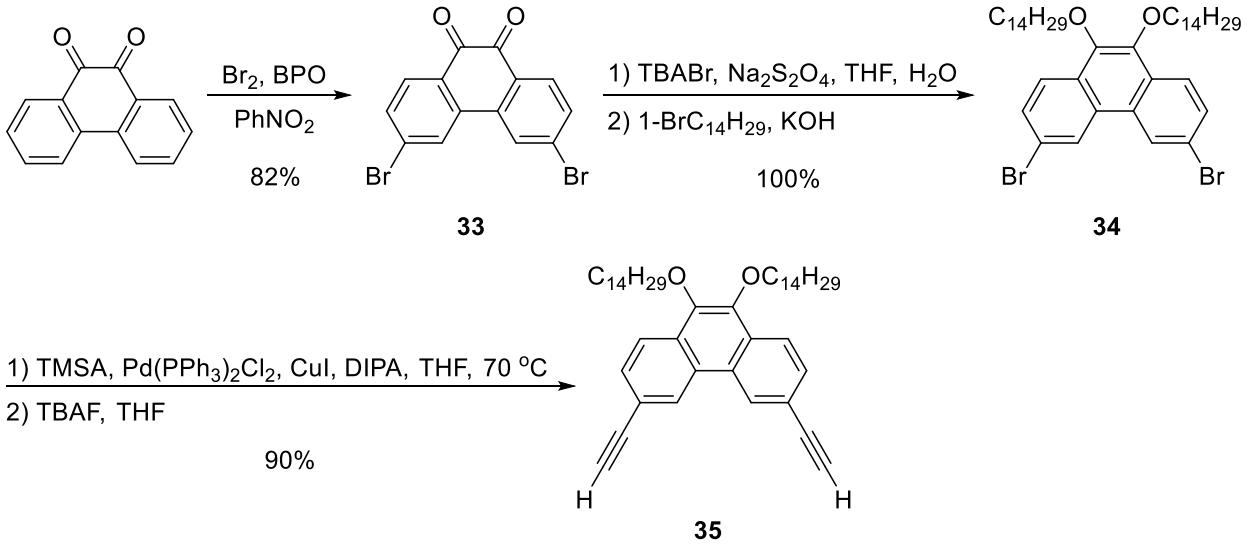

3,6-Dibromo-9,10-phenanthrenequinone (33)[15]**:** Bromine (1.7 mL; 33 mmol) was added to a mixture of 9,10-phenanthrenequinone (3.42 g; 16.4 mmol) and benzoyl peroxide (0.32 g; 1.3 mmol) in nitrobenzene (20 mL) under nitrogen. A KOH trap was attached to the apparatus and the reaction mixture was stirred at 110 °C for 16 hours. The mixture was cooled to room temperature, poured into hexane (150 mL), and filtered. The filter cake was rinsed with hexane until the filtrate ran clear to yield the product as a brown solid (4.89 g; 82%). ^{1}H NMR ($CDCl_3$, 500 MHz) δ: 8.12 (d, 2H, *J* = 2.0 Hz), 8.07 (d, 2H, *J* = 8.5 Hz), 7.67 (dd, 2H, *J* = 8.5 Hz, 2 Hz); FD-MS: *m/z* = 368.0 (57%), 367.0 (20%), 365.9 (100%), 364.0 (66%).

3,6-Dibromo-9,10-bis(tetradecyloxy)phenanthrene (34)[16]**:** A mixture of 3,6-dibromo-9,10-phenanthrenequinone (3.00 g; 8.20 mmol), tetrabutylammonium bromide (3.00 g; 9.31 mmol), and $Na_2S_2O_4$ (14.4 g; 82.7 mmol) in THF (60 mL) and water (60 mL) was stirred vigorously at room temperature for five minutes. 1-Bromotetradecane (64 mL; 215 mmol) and a solution of KOH (12.2 g; 217 mmol) in water (60 mL) were added and the reaction mixture was stirred at room temperature for two days. The mixture was diluted with water (200 mL) and the organic layer was separated and the solvent removed in *vacuo*. The excess 1-bromotetradecane was removed by vacuum distillation and the residue was purified by recrystallization from 3/1 ethanol/hexane to yield a pale yellow solid (6.84 g; quantitative). ^{1}H NMR ($CDCl_3$, 500 MHz) δ: 8.64 (d, 2H, *J* = 2.0 Hz), 8.09 (d, 2H, *J* = 9 Hz), 7.71 (dd, 2H, *J* = 9 Hz, 2 Hz), 4.17 (t, 4H, *J* = 7.0 Hz), 1.88 (m, 4H), 1.56 (m, 4H), 1.48-1.26 (m, 40H), 0.88 (t, 6H, *J* = 7.0 Hz); ^{13}C NMR

($CDCl_3$, 125 MHz) δ: 143.1, 130.4, 128.7, 125.4, 124.2, 120.3, 73.7, 32.2, 31.9, 30.4, 29.7, 29.6, 29.5, 29.4, 26.2, 22.7, 14.1; FD-MS: *m/z* = 760.0 (100%), 682.1 (5%), 426.2 (3%).

3,6-Diethynyl-9,10-bis(tetradecyloxy)phenanthrene (35): In an argon-filled glove box, trimethylsilylacetylene (4.2 mL, 30 mmol) was added dropwise to a stirring mixture of 3,6-dibromo-9,10-bis(tetradecyloxy)phenanthrene (4.56 g, 5.99 mmol), bis(triphenylphosphine)palladium(II) dichloride (.21 g, 0.30 mmol), and copper(I) iodide (57 mg, 0.30 mmol), and diisopropylamine (6.0 mL; 43 mmol) in THF (14 mL) in an oven-dried vial. The reaction was then sealed, removed from the glove box, and stirred at 70 °C for 16 hours. The mixture was cooled to room temperature, diluted with ethyl acetate (40 mL), and filtered through a pad of silica gel with ethyl acetate eluting. The solvent was removed from the filtrate in *vacuo* and the product was purified by column chromatography (silica gel, 85:15 hexanes:DCM) to yield an yellow solid. The TMS-protected intermediate was dissolved in THF (120 mL), a 1.0 M solution of tetrabutylammonium fluoride in THF (13.2 mL, 13.2 mmol) was added, and the mixture was stirred at room temperature for one minute. The reaction mixture was then filtered through a pad of silica gel with THF eluting. The solvent was removed from the filtrate in *vacuo* and the product was purified by recrystallization from ethanol to yield a tan solid (3.51 g, 90% over two steps). ^{1}H NMR ($CDCl_3$, 500 MHz) δ: 8.75 (d, 2H, *J* = 1.5 Hz), 8.18 (d, 2H, *J* = 8.5 Hz), 7.69 (dd, 2H, *J* = 8.5 Hz, 1.5 Hz), 4.19 (t, 4H, *J* = 6.5 Hz), 3.20 (s, 2H), 1.89 (m, 4H), 1.55 (m, 4H), 1.41-1.27 (m, 42H), 0.88 (t, 6H, *J* = 7.0 Hz); ^{13}C NMR ($CDCl_3$, 125 MHz) δ: 143.9, 130.0, 129.9, 127.6, 126.9, 122.5, 119.5, 84.1, 77.8, 77.7, 73.8, 32.2, 31.9, 30.4, 29.7, 29.7, 29.5, 29.4, 29.0, 26.2, 22.7, 14.1; m.p. = 59-62 °C; FD-MS: *m/z* = 652.3 (10%), 651.3 (50%), 650.3 (100%).

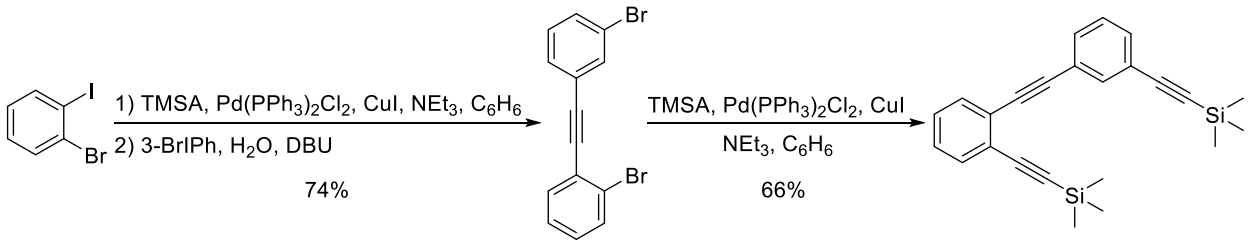

36 **20**

1-Bromo-2-((3-bromophenyl)ethynyl)benzene (36)[17]**:** Trimethylsilylacetylene (1.04 mL; 7.36 mmol) was slowly added to a mixture of 2-bromoiodobenzene (0.90 mL; 7.0 mmol),

bis(triphenylphosphine)palladium(II) dichloride (0.29 g; 0.41 mmol), copper(I) iodide (0.13 g; 0.68 mmol), and triethylamine (5.9 mL; 42 mmol) in benzene (35 mL) under nitrogen. The reaction was sealed and stirred in the dark at 60 °C for 16 hours. The reaction mixture was cooled to room temperature before 3-bromoiodobenzene (0.89 mL; 7.0 mmol), water (50 µL; 2.8 mmol), and DBU (12.6 mL; 84 mmol) were added under nitrogen. The reaction mixture was stirred again in the dark at room temperature for 16 hours. The mixture was diluted with ethyl acetate (80 mL) and filtered through a pad of silica gel with ethyl acetate eluting. The solvent was removed from the filtrate in *vacuo* and the product was purified by column chromatography (silica gel; hexanes) to yield a pale yellow solid (1.73 g; 74%). ^{1}H NMR ($CDCl_3$, 500 MHz) δ: 7.73 (m, 1H), 7.63 (dd, 1H, *J* = 8.0 Hz, 1.0 Hz), 7.55 (dd, 1H, *J* = 8.0 Hz, 1.5 Hz), 7.50 (m, 2H), 7.30 (dt, 1H, *J* = 7.5 Hz, 1.0 Hz), 7.25-7.18 (m, 2H); ^{13}C NMR ($CDCl_3$, 125 MHz) δ: 134.3, 133.3, 132.5, 131.7, 130.2, 129.8, 129.7, 127.1, 125.7, 124.9, 122.2, 92.2, 89.2; FD-MS: *m/z* = 338.0 (45%), 336.0 (100%), 334.0 (45%).

Trimethyl((2-((3-((trimethylsilyl)ethynyl)phenyl)ethynyl)phenyl)ethynyl)silane (20): Trimethylsilylacetylene (3.5 mL; 25 mmol) was slowly added to a mixture of 1-Bromo-2-((3-bromophenyl)ethynyl)benzene (0.84 g; 2.5 mmol), bis(triphenylphosphine)palladium(II) dichloride (91 mg; 0.13 mmol), copper(I) iodide (26 mg; 0.14 mmol), and triethylamine (2.5 mL; 18 mmol) in benzene (6 mL) under nitrogen. The reaction was sealed and stirred at 80 °C for 16 hours. The mixture was cooled to room temperature, diluted with ethyl acetate (20 mL), and filtered through a pad of silica gel with ethyl acetate eluting. The solvent was removed from the filtrate in *vacuo* and the product was purified by column chromatography (silica gel; hexanes) to yield a viscous orange oil that very slowly solidified (0.61 g; 66%). ^{1}H NMR ($CDCl_3$, 500 MHz) δ: 7.70 (m, 1H), 7.50 (m, 3H), 7.43 (m, 1H), 7.29 (m, 3H), 0.29 (s, 9H), 0.26 (s, 9H); ^{13}C NMR ($CDCl_3$, 125 MHz) δ: 135.7, 132.6, 131.8, 131.6, 128.6, 128.5, 128.3, 126.1, 126.0, 123.8, 123.7, 104.3, 103.6, 99.0, 95.2, 92.8, 89.1, 0.3, 0.2; FD-MS: *m/z* = 853.9 (100%), 426.9 (20%).

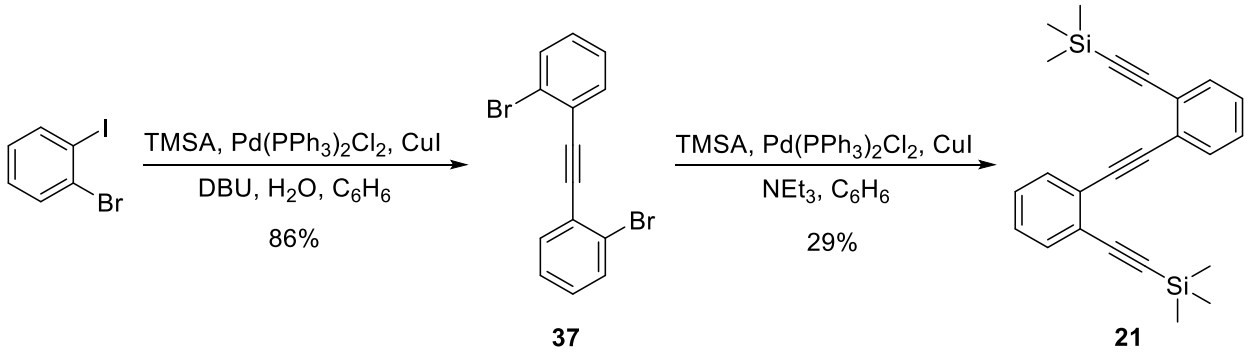

1,2-Bis(2-bromophenyl)ethyne (37)[17]**:** Trimethylsilylacetylene (0.42 mL; 3.0 mmol) was slowly added to a solution of 2-bromoiodobenzene (0.77 mL; 6.0 mmol), bis(triphenylphosphine)palladium(II) dichloride (0.25 g; 0.36 mmol), copper(I) iodide (0.11 g; 0.58 mmol), DBU (5.4 mL; 36 mmol), and water (40 µL; 2.2 mmol) in benzene (30 mL) under nitrogen. The reaction was sealed and stirred in the dark at 60 °C for 18 hours. The reaction mixture was cooled to room temperature, diluted with ethyl acetate (75 mL), and filtered through a pad of silica gel with ethyl acetate eluting. The solvent was removed from the filtrate in *vacuo* and the product was purified by column chromatography (silica gel; 9:1 hexanes:DCM) to yield a white solid (0.87 g; 86%). ^{1}H NMR ($CDCl_3$, 500 MHz) δ: 7.64-7.61 (m, 4H), 7.31 (dt, 2H, J = 7.5 Hz, 1.0 Hz), 7.21 (dt, 2H, J = 8.0 Hz, 2.0 Hz); ^{13}C NMR ($CDCl_3$, 125 MHz) δ: 133.9, 132.8, 130.0, 127.3, 125.8, 125.4, 92.5; FD-MS: *m/z* = 337.8 (10%), 337.8 (25%), 335.8 (100%), 333.8 (50%).

1,2-Bis(2-((trimethylsilyl)ethynyl)phenyl)ethyne (21): Trimethylsilylacetylene (1.6 mL; 11 mmol) was slowly added to a mixture of 1,2-bis(2-bromophenyl)ethyne (0.71 g; 2.1 mmol), bis(triphenylphosphine)palladium(II) dichloride (77 mg; 0.11 mmol), copper(I) iodide (21 mg; 0.11 mmol), and triethylamine (2.0 mL; 18 mmol) in benzene (4.5 mL) under nitrogen. The reaction was sealed and stirred at 80 °C for 16 hours. The mixture was cooled to room temperature, diluted with ethyl acetate (20 mL), and filtered through a pad of silica gel with ethyl acetate eluting. The solvent was removed from the filtrate in *vacuo* and the product was purified by column chromatography (silica gel; 85:15 hexanes:DCM) and further purified by recrystallization from methanol to yield a light orange solid (0.23 g; 29%). ^{1}H NMR ($CDCl_3$, 500 MHz) δ: 7.55 (m, 2H), 7.50 (m, 2H), 7.31-7.25 (m, 4H), 0.26 (s, 18H); ^{13}C NMR ($CDCl_3$, 125

MHz) δ: 132.2, 131.9, 128.1, 128.0, 126.2, 125.6, 103.5, 98.7, 92.1, 0.0; FD-MS: *m/z* = 370.2 (100%), 354.0 (10%), 345.5 (5%).

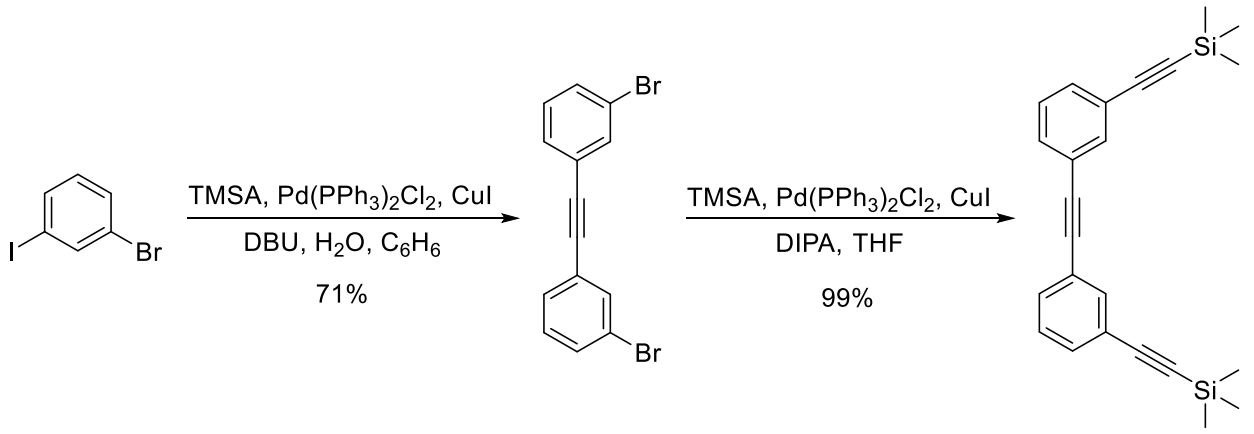

38 **22**

1,2-Bis(3-bromophenyl)ethyne (38)[17]**:** Trimethylsilylacetylene (0.42 mL; 3.0 mmol) was slowly added to a solution of 2-bromoiodobenzene (0.76 mL; 6.0 mmol), bis(triphenylphosphine)palladium(II) dichloride (0.26 g; 0.37 mmol), copper(I) iodide (0.11 g; 0.58 mmol), DBU (5.4 mL; 36 mmol), and water (44 μL; 2.4 mmol) in benzene (30 mL) under nitrogen. The reaction was sealed and stirred in the dark at room temperature for 18 hours. The reaction mixture was diluted with ethyl acetate (75 mL) and filtered through a pad of silica gel with ethyl acetate eluting. The solvent was removed from the filtrate in *vacuo* and the product was purified by column chromatography (silica gel; hexanes) to yield a white solid (0.72 g; 71%). ^{1}H NMR ($CDCl_3$, 500 MHz) δ: 7.68 (t, 2H, *J* = 1.5 Hz), 7.50-7.44 (m, 4H), 7.23 (t, 2H, *J* = 8.0 Hz); ^{13}C NMR ($CDCl_3$, 125 MHz) δ: 134.4, 131.7, 130.2, 129.8, 124.7, 122.2, 89.0; FD-MS: *m/z* = 337.9 (40%), 335.9 (100%), 333.9 (40%).

1,2-Bis(3-((trimethylsilyl)ethynyl)phenyl)ethyne (22): In an argon-filled glove box, trimethylsilylacetylene (1.4 mL; 9.9 mmol) was slowly added to a mixture of 1,2-bis(3-bromophenyl)ethyne (0.67 g; 2.0 mmol), bis(triphenylphosphine)palladium(II) dichloride (71 mg; 0.10 mmol), copper(I) iodide (19 mg; 0.10 mmol), and diisopropylamine (2.0 mL; 14 mmol) in THF (5 mL). The reaction was sealed, removed from the glove box, and stirred at 70 °C for 16 hours. The mixture was cooled to room temperature, diluted with ethyl acetate (20 mL), and filtered through a pad of silica gel with ethyl acetate eluting. The solvent was removed from the

filtrate in *vacuo* and the product was purified by column chromatography (silica gel; 95:5 hexanes:DCM) to yield yellow solid (0.73 g; 99%). ^{1}H NMR ($CDCl_3$, 500 MHz) δ: 7.64 (t, 2H, *J* = 1.5 Hz), 7.46-7.41 (m, 4H), 7.28 (t, 2H, *J* = 7.5 Hz), 0.26 (s, 18H); ^{13}C NMR ($CDCl_3$, 125 MHz) δ: 135.0, 131.7, 131.5, 128.3, 123.5, 123.2, 104.0, 95.0, 89.0, -0.1; FD-MS: *m/z* = 372.1 (10%), 371.1 (40%), 370.1 (100%).

2.6.2: Synthesis and Characterization of Polymers

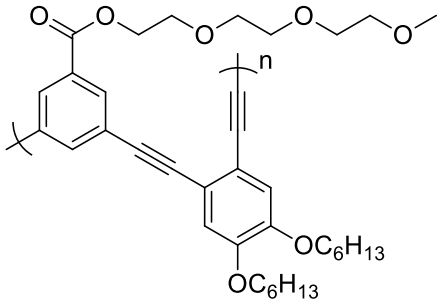

(*o*-Phenylene-ethynylene)-*alt*-(*m*-phenylene-ethynylene) copolymer (9a): In an argon-filled glovebox, 1,2-diethynyl-4,5-bis(hexyloxy)benzene (979 mg, 3.00 mmol), 2-(2-(2-methoxyethoxy)ethoxy)ethyl 3,5-diiodobenzoate (1.64 g, 3.15 mmol), tetrakis(triphenylphosphine)palladium(0) (173 mg, 0.15 mmol), and copper(I) iodide (28.6 mg, 0.15 mmol) were added to an oven-dried vial and suspended in piperdine (9.0 mL, 91 mmol). The reaction mixture was left to stir at 50 °C for 72 hours. The crude reaction mixture was cooled to room temperature and added dropwise to a flask of stirring methanol (150 mL) to precipitate the polymer. The precipitate was collected by vacuum filtration and left to dry overnight under high vacuum to yield a tan solid (852 mg, 48%). GPC (THF): M_n = 6900 g/mol, M_w = 14,200 g/mol, PDI = 2.1, ret. vol. = 27.1 mL).

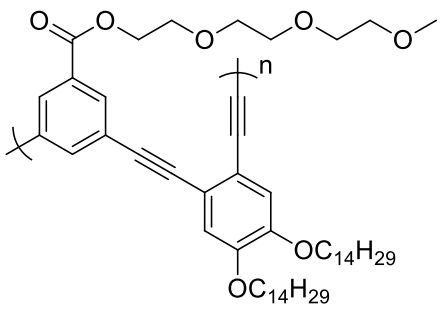

(*o*-Phenylene-ethynylene)-*alt*-(*m*-phenylene-ethynylene) copolymer (9b): In an argon-filled glovebox, 1,2-diethynyl-4,5-bis(tetradecyloxy)benzene (1.65 g, 3.00 mmol), 2-(2-(2-methoxyethoxy)ethoxy)ethyl 3,5-diiodobenzoate (1.64 g, 3.15 mmol), tetrakis(triphenylphosphine)palladium(0) (173 mg, 0.15 mmol), and copper(I) iodide (28.7 mg, 0.15 mmol) were added to an oven-dried vial and suspended in piperdine (9.0 mL, 91 mmol). The reaction mixture was left to stir at 50 °C for 72 hours. The crude reaction mixture was cooled to room temperature and added dropwise to a flask of stirring methanol (150 mL) to precipitate the polymer. The precipitate was collected by vacuum filtration and left to dry overnight under high vacuum to yield a tan solid (2.48 g, 100%). GPC (THF): M_n = 4600 g/mol, M_w = 6300 g/mol, PDI = 1.4, ret. vol. = 28.1 mL).

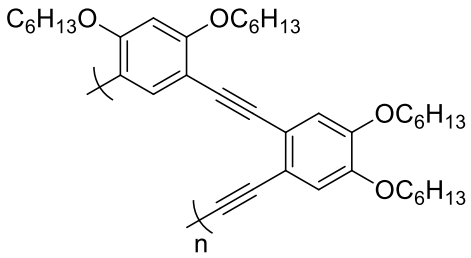

(*o*-Phenylene-ethynylene)-*alt*-(*m*-phenylene-ethynylene) copolymer (9c): In an argon-filled glovebox, 1,2-diethynyl-4,5-bis(hexyloxy)benzene (979 mg, 3.00 mmol), 1,3-bis(hexyloxy)-4,6-diiodobenzene (1.67 g, 3.15 mmol), tetrakis(triphenylphosphine)palladium(0) (173 mg, 0.15 mmol), and copper(I) iodide (28.6 mg, 0.15 mmol) were added to an oven-dried vial and suspended in piperdine (9.0 mL, 91 mmol). The reaction mixture was left to stir at 50 °C for 72 hours. The crude reaction mixture was cooled to room temperature and added dropwise to a flask of stirring methanol (150 mL) to precipitate the polymer. The precipitate was collected by vacuum filtration and left to dry overnight under high vacuum to yield a tan solid (1.86g, 100%). GPC (THF): M_n = 4100 g/mol, M_w = 6000 g/mol, PDI = 1.5, ret. vol. = 28.5 mL).

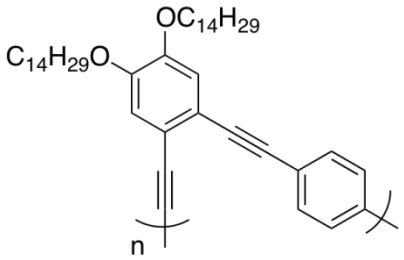

(*o*-Phenylene-ethynylene)-*alt*-(*p*-phenylene-ethynylene) copolymer (10a): In an argon-filled glovebox, 1,2-diethynyl-4,5-bis(tetradecyloxy)benzene (551 mg, 1.0 mmol), 1,4-diiodobenzene (330 mg, 1 mmol), tetrakis(triphenylphosphine)palladium(0) (58 mg, 0.05 mmol), and copper(I) iodide (4 mg, 0.02 mmol) were added to an oven-dried vial and suspended in piperdine (9.0 mL, 91 mmol). The reaction mixture was left to stir at 50 °C for 72 hours. The crude reaction mixture was cooled to room temperature and added dropwise to a flask of stirring methanol (200 mL) to precipitate the polymer. The precipitate was collected by vacuum filtration and left to dry overnight under high vacuum to yield a light brown solid (580 mg, 66%). GPC (THF): M_n = 4800 g/mol, M_w = 3100 g/mol, PDI = 1.5, ret. vol. = 27.9 mL).

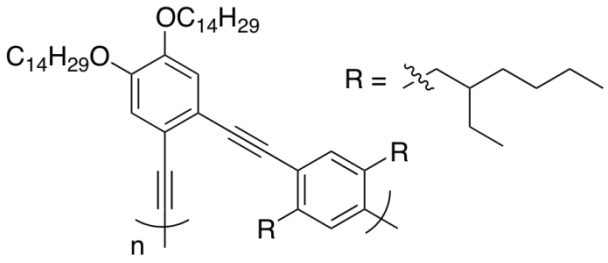

(*o*-Phenylene-ethynylene)-*alt*-(*p*-phenylene-ethynylene) copolymer (10b): In an argon-filled glovebox, 1,2-diethynyl-4,5-bis(tetradecyloxy)benzene (551 mg, 1.0 mmol), 1,4-bis-(2-ethylhexyl)-2,5-diiodobenzene (554 mg, 1 mmol), tetrakis(triphenylphosphine)palladium(0) (58 mg, 0.05 mmol), and copper(I) iodide (4 mg, 0.02 mmol) were added to an oven-dried vial and suspended in piperdine (9.0 mL, 91 mmol). The reaction mixture was left to stir at 50 °C for 72 hours. The crude reaction mixture was left to cool to room temperature and added dropwise to a flask of stirring methanol (200 mL) to precipitate the polymer. The precipitate was collected by vacuum filtration and left to dry overnight under high vacuum to yield a light brown solid (778 mg, 70%). GPC (THF): M_n = 6200 g/mol, M_w = 10500 g/mol, PDI = 1.7, ret. vol. = 28.6 mL).

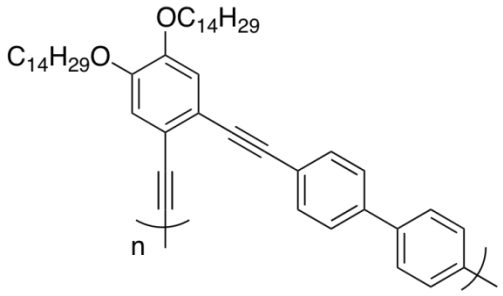

(*o*-Phenylene-ethynylene)-*alt*-(*p*-phenylene-ethynylene) copolymer (10c): In an argon-filled glovebox, 1,2-diethynyl-4,5-di(tetradecyloxy)benzene (551 mg, 1.0 mmol), 4,4'-dibromobiphenyl (312 mg, 1 mmol), tetrakis(triphenylphosphine)palladium(0) (58 mg, 0.05 mmol), and copper(I) iodide (4 mg, 0.02 mmol) were added to an oven-dried vial and suspended in piperdine (9.0 mL, 91 mmol). The reaction mixture was left to stir at 50 °C for 72 hours. The crude reaction mixture was left to cool to room temperature and added dropwise to a flask of stirring methanol (200 mL) to precipitate the polymer. The precipitate was collected by vacuum filtration and left to dry overnight under high vacuum to yield a bright yellow solid (645 mg, 75%). GPC (THF): M_n = 3200 g/mol, M_w = 4400 g/mol, PDI = 1.4, ret. vol. = 28.1 mL).

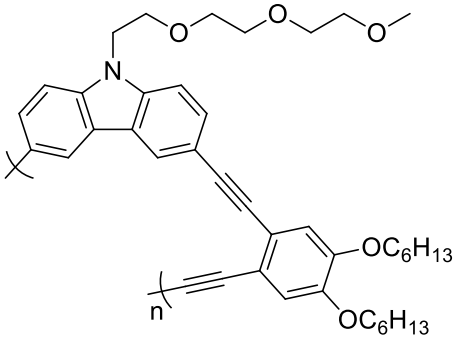

(*o*-Phenylene-ethynylene)-*alt*-(carbazolyl-ethynylene) copolymer (11): In an argon-filled glovebox, 1,2-diethynyl-4,5-di(hexyloxy)benzene (345 mg, 1.06 mmol), 3,6-diiodo-9-(2-(2-(2-methoxyethoxy)ethoxy)ethyl)-9H-carbazole (565 mg,1.00 mmol), tetrakis(triphenylphosphine)palladium(0) (57.8 mg, 0.05 mmol), and copper(I) iodide (10.4 mg, 0.05 mmol) were added to a vial and suspended in piperdine (3.3 mL, 33 mmol). The reaction mixture was left to stir at 70 °C for 72 hours. The crude reaction mixture was left to cool to room temperature and added dropwise to a flask of stirring methanol (70 mL) to precipitate the polymer. The precipitate was collected by vacuum filtration and left to dry overnight under high

vacuum to yield a tan solid (579 mg, 91%). GPC (THF): M_n = 7100 g/mol, M_w = 11,100 g/mol, PDI = 1.6, ret. vol. = 27.4 mL).

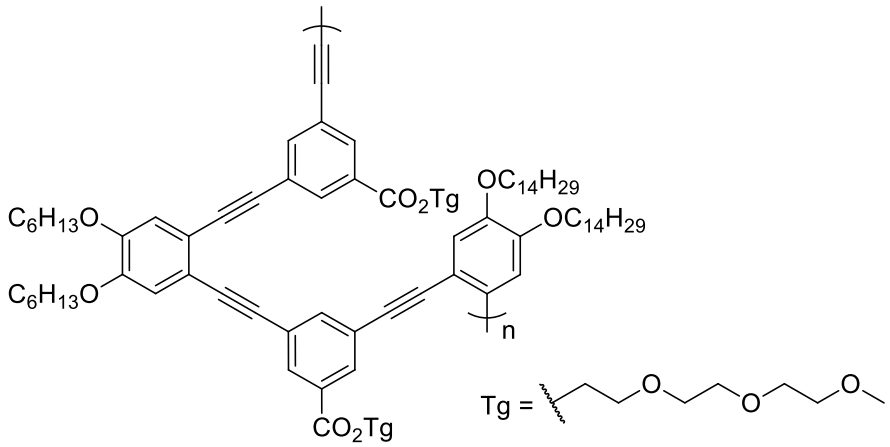

ABAB'-type copolymer (18): In an argon-filled glovebox, **S9** (1.30 g, 1.43 mmol), 1,2-bis(tetradecyoxy)-4,5-diiodobenzene (1.13 g,1.50 mmol), tetrakis(triphenylphosphine)palladium(0) (81.2 mg, 0.07 mmol), and copper(I) iodide (13.3 mg, 0.07 mmol) were added to a vial and suspended in piperdine (4.3 mL, 44 mmol). The reaction mixture was left to stir at 50 °C for 72 hours. The crude reaction mixture was left to cool to room temperature and added dropwise to a flask of stirring methanol (100 mL) to precipitate the polymer. The precipitate was collected by vacuum filtration and left to dry overnight under high vacuum to yield a tan solid (1.92 mg, 93%). GPC (THF): M_n = 8400 g/mol, M_w = 18,400 g/mol, PDI = 2.2, ret. vol. = 26.5 mL).

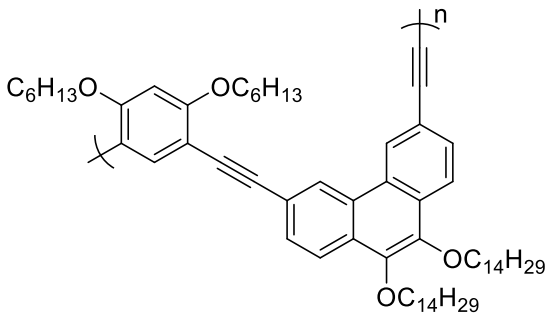

(Phenanthrenyl-ethynylene)-*alt*-(*m*-phenylene-ethynylene) copolymer (19): In an argon-filled glovebox, 1,2-diethynyl-9,10-bis(tetradecyl)phenanthrene (.21 g, 0.32 mmol), 1,5-bis(hexyloxy)-2,4-diiodobenzene (0.18 g, 0.34 mmol), tetrakis(triphenylphosphine)palladium(0) (18 mg, 0.016 mmol), and copper(I) iodide (3.4 mg, 0.018 mmol) were added to an oven-dried vial and

suspended in piperdine (0.3 mL, 3.0 mmol) and THF (0.8 mL). The reaction mixture was sealed, removed from the glove box, and stirred at 50 °C for 72 hours. The crude reaction mixture was cooled to room temperature and added dropwise to a flask of stirring methanol (150 mL) to precipitate the polymer. The precipitate was collected by vacuum filtration and left to dry overnight under high vacuum to yield a tan solid (0.31 g, 100%). GPC (THF): M_n = 3,800 g/mol, M_w = 5,000 g/mol, PDI = 1.3, ret. vol. = 28.8 mL).

2.6.3: Synthesis and Characterization of Macrocycles

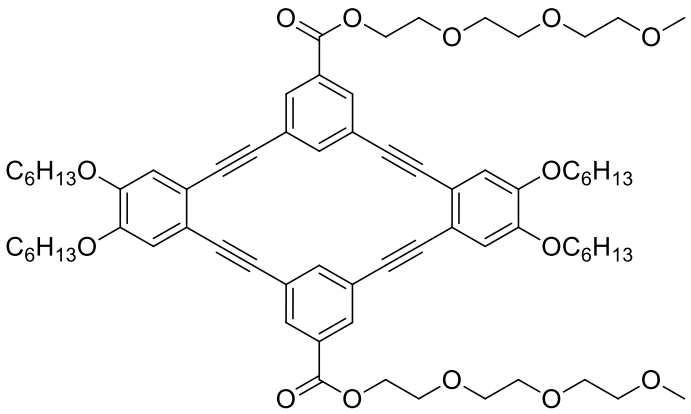

Macrocycle 12a. In an argon-filled glovebox, *o*-phenylene-alt-*m*-phenylene ethynylene copolymer **9a** (100 mg) was dissolved in 1,2,4-trichlorobenzene (3 mL) in an oven-dried vial. In a separate oven dried vial, Mo(VI) alkylidine catalyst (10 mg, 0.015 mmol) and triphenylsilanol (21 mg, 0.076 mmol) were dissolved together in 1,2,4-trichlorobenzene (2 mL). The catalyst solution was added to the dissolved polymer and the reaction was sealed, removed from the glove box, and stirred at 50 °C for 24 hours. The reaction mixture was opened to air and allowed to cool to room temperature, upon which a white precipitate formed. The precipitate was collected by vacuum filtration washed with ether to yield a white solid (55.4 mg, 55%). GPC (THF): M_n = 1500 g/mol, M_w = 1600 g/mol, PDI = 1.0, ret. time = 30.3 min.); ^{1}H NMR ($CDCl_3$, 500 MHz) δ: 8.17 (d, 4H, *J* = 1.5 Hz), 8.07 (t, 2H, *J* = 1.5 Hz), 7.07 (s, 4H), 4.53 (m, 4H), 4.07 (t, 8H, *J* = 7.0 Hz), 3.88 (m, 4H), 3.72 (m, 8H), 3.66 (m, 4H), 3.54 (m, 4H), 3.36 (s, 6H), 1.87 (p, 8H, *J* = 7.5 Hz), 1.51 (m, 8H), 1.37 (m, 16H), 0.92 (t, 12 H, *J* = 7.0 Hz); ^{13}C NMR ($CDCl_3$, 125 MHz) δ: 165.3, 149.6, 138.6, 131.4, 130.9, 124.4, 118.2, 115.9, 90.4, 90.3, 71.9, 70.7, 70.6, 70.6, 69.2, 69.2, 64.4, 59.0, 31.5, 29.0, 25.7, 22.6, 14.0; m.p. = 144-146 °C; MALDI-TOF MS: *m/z* = 1204.

This reaction was repeated using polymer purified by preparatory GPC to demonstrate that the macrocycle is formed through depolymerization.

GPC traces of purified copolymer **9a** and precipitate from the reaction (**12a**).

Purified polymer data: M_n = 22,000 g/mol, M_w = 42,000 g/mol, PDI = 1.9, ret. vol. = 25.01 mL

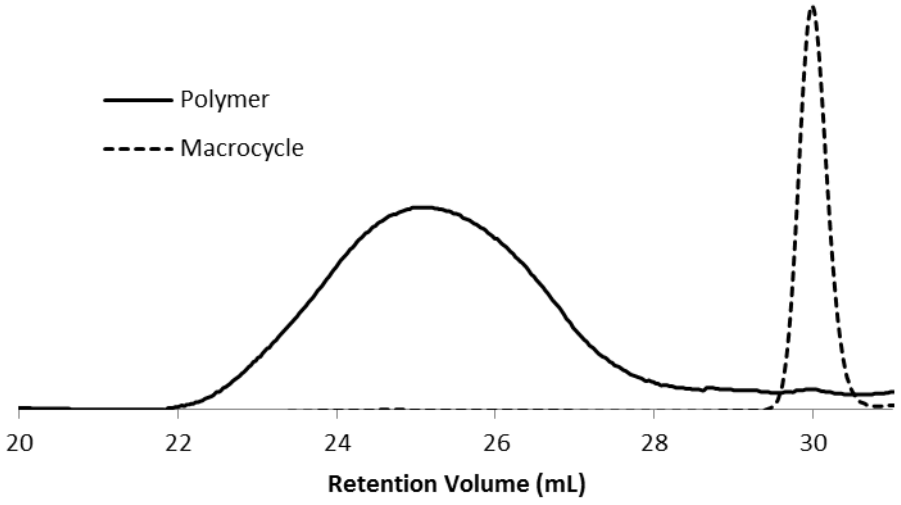

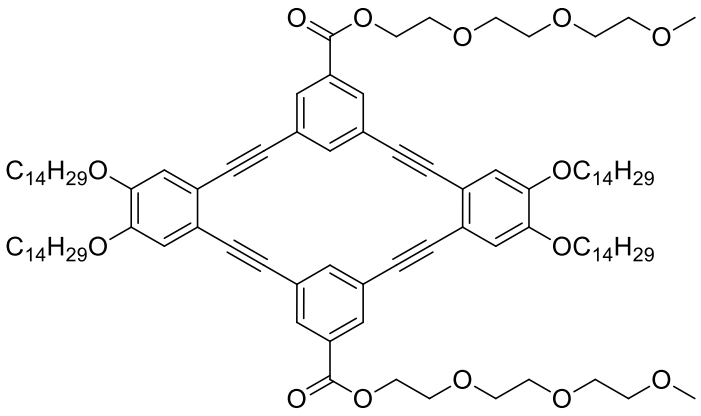

Macrocycle 12b. In an argon-filled glovebox, *o*-phenylene-alt-*m*-phenylene ethynylene copolymer **9b** (200 mg) was dissolved in 1,2,4-trichlorobenzene (6 mL) in an oven-dried vial. In a separate oven dried vial, Mo(VI) alkylidine catalyst (20 mg, 0.030 mmol) and triphenylsilanol (42 mg, 0.15 mmol) were dissolved together in 1,2,4-trichlorobenzene (4 mL). The catalyst solution was added to the dissolved polymer and the reaction was sealed, removed from the glove box, and stirred at 50 °C for 24 hours. The 1,2,4-trichlorobenzene was removed via vacuum distillation and the resulting crude mixture was purified by column chromatography (silica gel, chloroform to 1% methanol/chloroform) to yield a tan solid (157 mg, 79%). GPC

(THF): M_n = 2500 g/mol, M_w = 2600 g/mol, PDI = 1.0, ret. time = 29.7min.); ^{1}H NMR ($CDCl_3$, 500 MHz) δ: 8.16 (d, 4H, *J* = 1.0 Hz), 8.06 (t, 2H, *J* = 1.0 Hz), 7.06 (s, 4H), 4.52 (m, 4H), 4.06 (t, 8H, *J* = 6.5 Hz), 3.88 (m, 4H), 3.72 (m, 8H), 3.66 (m, 4H), 3.54 (m, 4H), 3.35 (s, 6H), 1.87 (p, 8H, *J* = 7.5 Hz), 1.50 (m, 8H), 1.37 (m, 82H), 0.88 (t, 12 H, *J* = 7.0 Hz); ^{13}C NMR ($CDCl_3$, 125 MHz) δ: 165.3, 149.6, 138.5, 131.4, 130.9, 124.3, 118.2, 115.8, 90.4, 90.2, 71.9, 70.7, 70.6, 70.6, 69.2, 69.2, 64.4, 59.0, 31.9, 29.7, 29.7, 29.6, 29.4, 29.4, 29.1, 26.0, 22.7, 14.1; m.p. = 106-108 °C; MALDI-TOF MS: *m/z* = 1652.

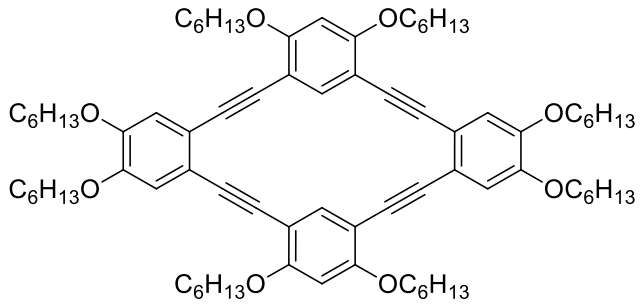

Macrocycle 12c. In an argon-filled glovebox, *o*-phenylene-alt-*m*-phenylene ethynylene copolymer **9c** (200 mg) was dissolved in 1,2,4-trichlorobenzene (6 mL) in an oven-dried vial. In a separate oven dried vial, Mo(VI) alkylidine catalyst (20 mg, 0.030 mmol) and triphenylsilanol (41 mg, 0.15 mmol) were dissolved together in 1,2,4-trichlorobenzene (4 mL). The catalyst solution was added to the dissolved polymer and the reaction was sealed, removed from the glove box, and stirred at 50 °C for 24 hours. The reaction mixture was cooled to room temperature and added dropwise to a flask of stirring ether (125 mL) to precipitate the product. The precipitate was collected by vacuum filtration to yield a white solid (65 mg, 33%). ^{1}H NMR ($CDCl_3$, 500 MHz) δ: 7.90 (s, 2H), 6.97 (s, 4H), 6.44 (s, 2H), 4.10 (t, *J* = 6.5 Hz, 18H), 4.01 (t, *J* = 6.5 Hz, 18H), 1.90 (p, *J* = 7.5 Hz, 8H), 1.83 (p, *J* = 7.5 Hz, 8H), 1.61 (p, *J* = 7.5 Hz, 8H), 1.48 (m, 14H), 1.37 (m, 33H), 0.92 (m, 24H); ^{13}C NMR ($CDCl_3$, 125 MHz, 50^{o}C) δ: 160.7, 149.1, 138.1, 119.4, 116.4, 106.5, 98.4, 91.8, 88.0, 69.4, 69.3, 31.7, 31.6, 29.3, 25.8, 25.7, 22.7, 22.6, 14.0, 13.9; m.p. = 253-255 °C; MALDI-TOF MS: *m/z* = 1201.

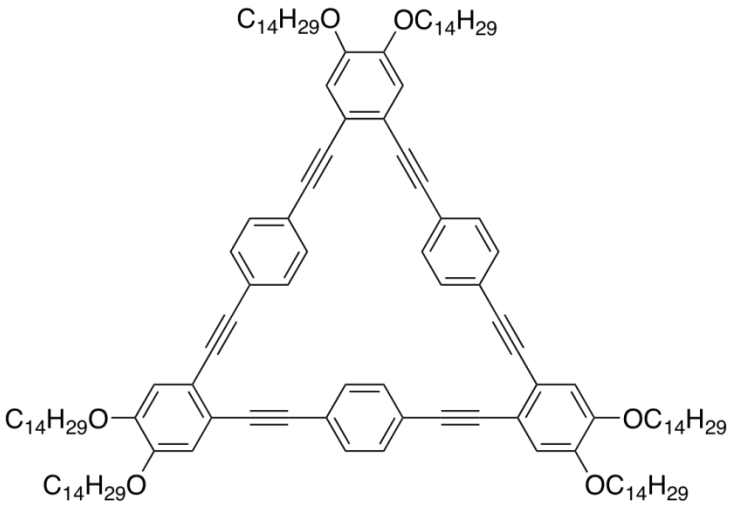

Macrocycle 13a. In an argon-filled glovebox, *o*-phenylene-alt-*p*-phenylene ethynylene copolymer **10a** (100 mg) was dissolved in 1,2,4-trichlorobenzene (8 mL) in an oven-dried vial. In a separate oven dried vial, Mo(VI) alkylidine catalyst (10.0 mg, 0.015 mmol) and triphenylsilanol (20.0 mg, 0.072 mmol) were dissolved together in 1,2,4-trichlorobenzene (8 mL). The dissolved polymer was added to the catalyst solution and left to stir at room temperature for 24 hours. The 1,2,4-trichlorobenzene was removed via vacuum distillation, and the resulting crude mixture was purified by column chromatography (silica gel, 1:2 chloroform:hexanes to yield a yellow solid (60%). GPC (THF): M_n = 2900 g/mol, M_w = 2900 g/mol, PDI = 1.0, ret. time = 28.9 min.); ^{1}H NMR ($CDCl_3$, 500 MHz) δ: 7.57 (s, 12H), 7.04 (s, 6H), 4.05 (t, 12H, J = 6.75 Hz), 1.86 (m, 12H), 1.50 (m, 12H), 1.35-1.26 (m, 120H), 0.88 (t, 18H, J = 6.75 Hz); ^{13}C NMR ($CDCl_3$, 125 MHz) δ: 149.3, 131.3, 123.3, 118.5, 115.7, 92.0, 90.6, 69.2, 31.9, 29.71, 29.71, 29.66, 29.66, 29.62, 29.62, 29.38, 29.37, 29.1, 26.0, 22.7, 14.1; MALDI-TOF MS: *m/z* = 1873.

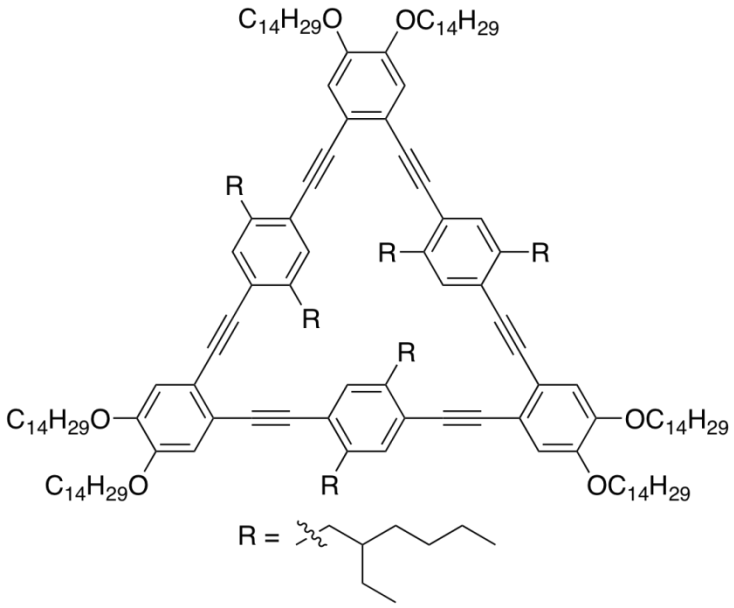

Macrocycle 13b. In an argon-filled glovebox, *o*-phenylene-alt-*p*-phenylene ethynylene copolymer **10b** (100 mg) was dissolved in carbon tetrachloride (8 mL) in a vial. In a separate oven dried vial, Mo(VI) alkylidine catalyst (10.0 mg, 0.015 mmol) and triphenylsilanol (20.0 mg, 0.072 mmol) were dissolved together in carbon tetrachloride (8 mL). The dissolved polymer was added to the catalyst solution and left to stir at room temperature for 24 hours. The carbon tetrachloride was removed in *vacuo* and the resulting crude mixture was purified by column chromatography (silica gel, 1:3 chloroform:hexanes) to yield a yellow oil (24%). GPC (THF): M_n = 3000 g/mol, M_w = 3100 g/mol, PDI = 1.0, ret. time = 28.8 min.); ^{1}H NMR ($CDCl_3$, 500 MHz) δ: 7.31 (s, 6H), 7.03 (s, 6H), 4.03 (t, 12H, J = 6.75 Hz), 2.73 (m, 12H), 1.85 (m, 12H), 1.47 (m, 12H), 1.36-1.15 (m, 192H), 0.88 (t, 18H, J = 6.75 Hz), 0.76 (t, 18H, , J = Hz); ^{13}C NMR ($CDCl_3$, 125 MHz) δ: 149.0, 141.2, 133.6, 125.9, 122.8, 118.8, 115.9, 93.0, 91.2, 69.2, 40.5, 38.5, 32.4, 31.9, 29.71, 29.71, 29.67, 29.67, 29.64, 29.4, 29.4, 29.37, 29.1, 28.8, 26.0, 25.5, 23.1, 22.7, 14.11, 14.06, 10.8; MALDI-TOF MS: *m/z* = 2546.

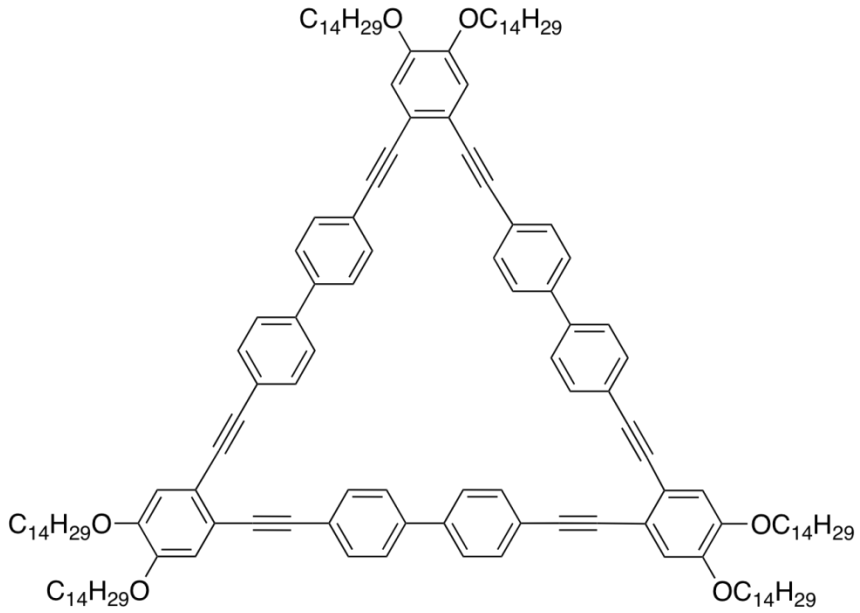

Macrocycle 13c. In an argon-filled glovebox, *o*-phenylene-alt-*p*-biphenylene ethynylene copolymer **10c** (100 mg) was dissolved in 1,2,4-trichlorobenzene (8 mL) in a vial. In a separate oven dried vial, Mo(VI) alkylidine catalyst (10.0 mg, 0.015 mmol) and triphenylsilanol (20.0 mg, 0.072 mmol) were dissolved together in 1,2,4-trichlorobenzene (8 mL). The dissolved polymer was added to the catalyst solution and left to stir at room temperature for 24 hours. The 1,2,4-trichlorobenzene was removed via vacuum distillation, and the resulting crude mixture was purified by column chromatography (silica gel, 1:2 DCM:hexanes) to yield a yellow solid (21%). GPC (THF): M_n = 3500 g/mol, M_w = 3600 g/mol, PDI = 1.0, ret. time = 28.9 min.); ^{1}H NMR ($CDCl_3$, 500 MHz) δ: 7.69 (s, 24H), 7.06 (s, 6H), 4.05 (t, 12H, J = 6.75 Hz), 1.86 (m, 12H), 1.50 (m, 12H), 1.35-1.26 (m, 120H), 0.88 (t, 18H, J = 6.75 Hz); ^{13}C NMR ($CDCl_3$, 125 MHz) δ: 149.2, 139.6, 131.9, 126.8, 122.9, 118.6, 115.7, 91.9, 89.7, 69.2, 31.9, 29.72, 29.72, 29.68, 29.68, 29.63, 29.63, 29.41, 29.38, 29.1, 26.0, 22.7, 14.1; MALDI-TOF MS: *m/z* = 2102.

2.6.4: Depolymerization of Copolymer 11

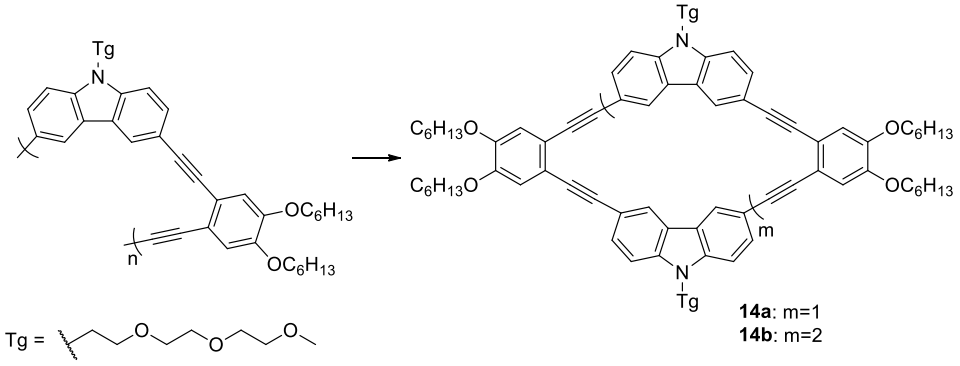

In an argon-filled glovebox, copolymer **11** (200 mg) was suspended in 1,2,4-trichlorobenzene (2 mL) in a vial. In a separate oven dried vial, Mo(VI) alkylidine catalyst (20.2 mg, 0.03 mmol) and triphenylsilanol (42.3 mg, 0.15 mmol) were dissolved together in 1,2,4-trichlorobenzene (8 mL). The dissolved polymer was added to the catalyst solution and left to stir at room temperature for 24 hours before he 1,2,4-trichlorobenzene was removed via vacuum distillation. GPC and MALDI-TOF MS of the crude mixture suggested that two macrocycle products were present, and the compounds were identified as the tetracycle (**14a**) and hexacycle (**14b**) by MALDI-TOF MS. Purification of the crude mixture was attempted by column chromatography (silica gel, chloroform to 95:5 chloroform:methanol). A small, impure sample of **14b** was separated from the mixture and could be used for identification of the upfield aryl peaks by ^{1}H NMR for quantification. The remaining material was collected as a mixture of the two products which were found to be produced in a 2:1 molar ratio (**14a**:**14b**) by ^{1}H NMR. The combined yield of the two products was 40%.

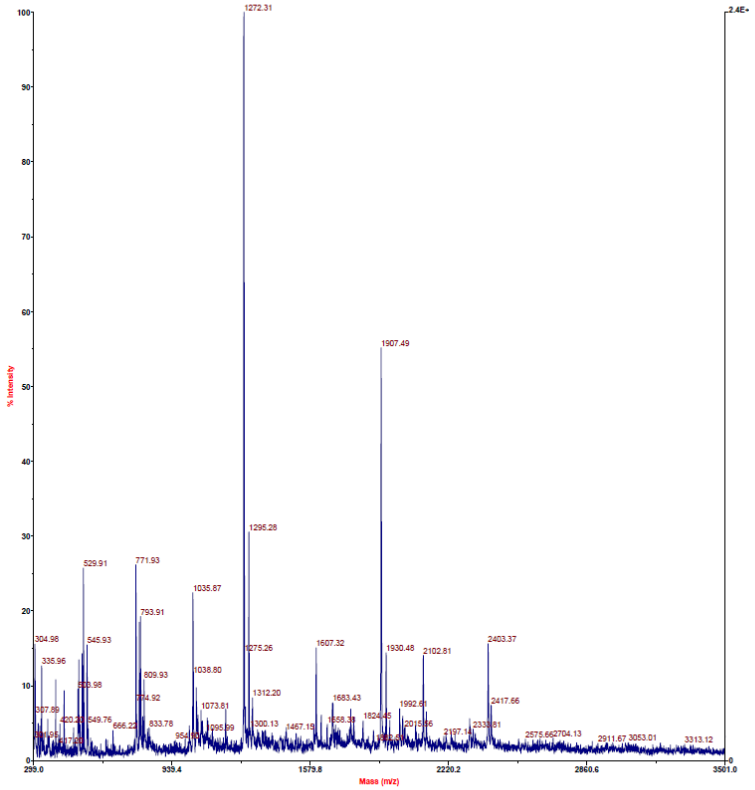

Figure 2.9: MALDI-TOF spectrum of crude mixture from depolymerization of **11**.

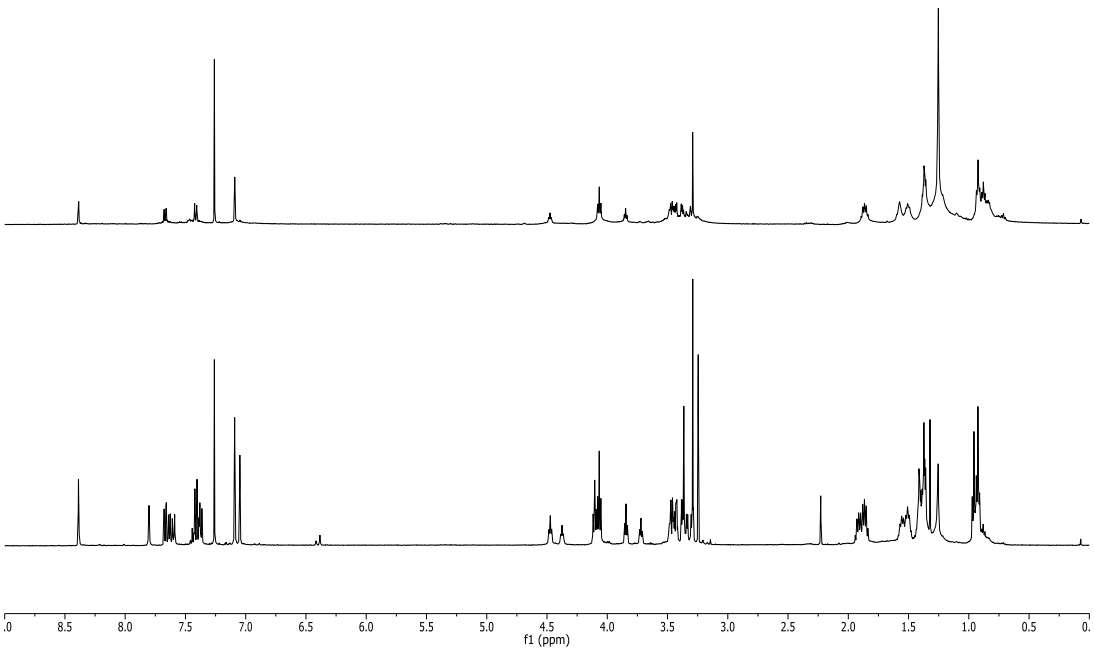

Figure 2.10: ^{1}H NMR spectra of tetracycle (top) and the mixture of macrocycles (bottom).

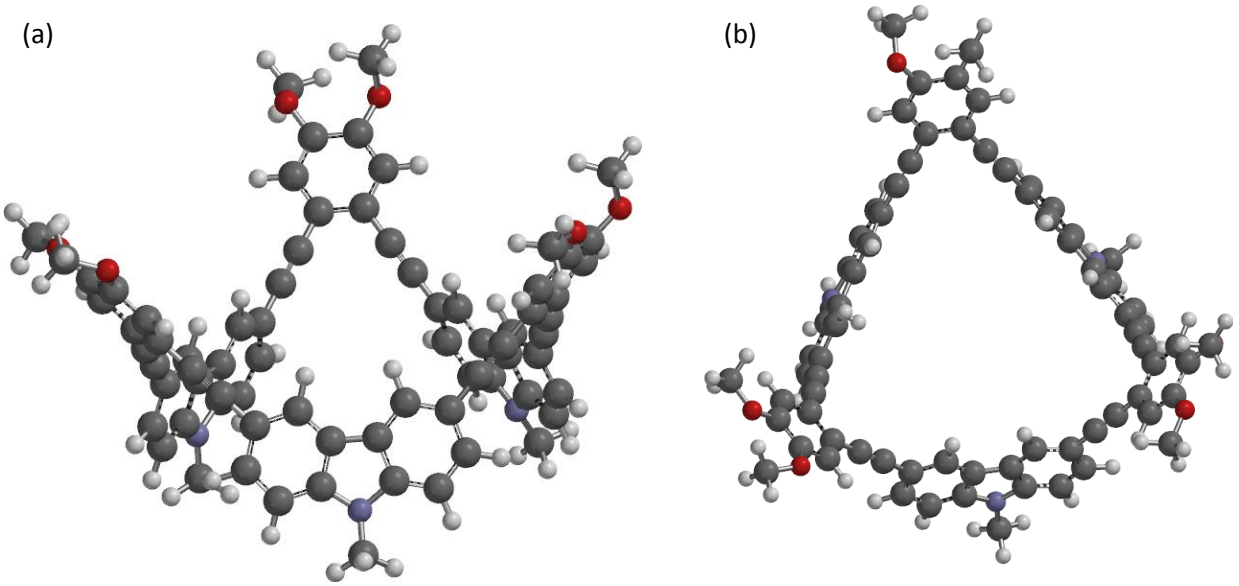

Figure 2.11: AM1 molecular modeling of **14b** from the (a) side and (b) top views (side chains have been shortened for clarity).

2.6.5: Monomer-Based Mixing Study

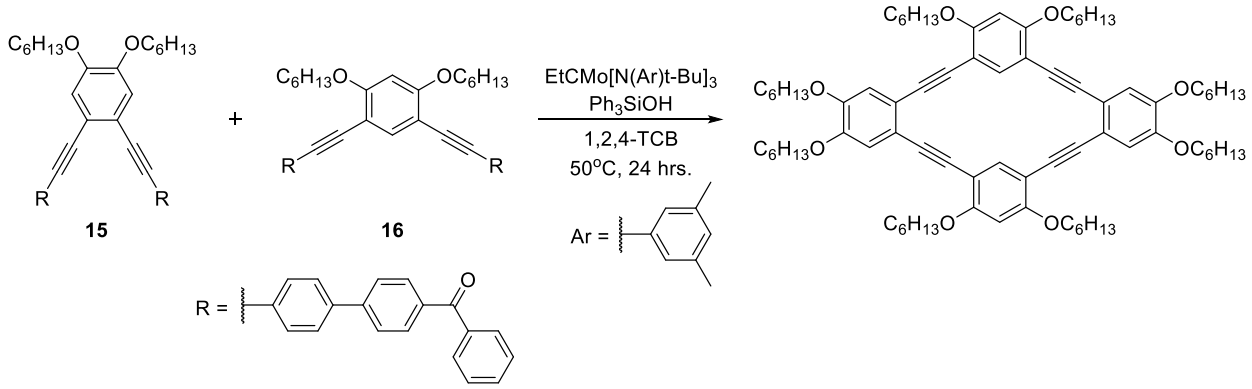

***o*-PE and *m*-PE monomer mixing.** In an argon-filled glove box, **15a** (50.0 mg, 0.06 mmol) and **16** (50.0 mg, 0.06 mmol) were dissolved in 1,2,4-trichlorobenzene (3 mL) in an oven-dried vial. In a separate oven-dried vial, Mo(VI) alkylidine catalyst (10.0 mg, 0.015 mmol) and triphenylsilanol (21.1 mg, 0.075 mmol) were dissolved together in 1,2,4-trichlorobenzene (2 mL). The catalyst solution was added to the solution of monomers, and the reaction was sealed, removed from the glove box, and stirred at 50 °C for 24 hours. The 1,2,4-trichlorobenzene was removed via vacuum distillation and the resulting crude mixture was analyzed by FD-MS. The mass spectrometry analysis shows that the *o*-PE tricycle and the *m*-PE pentacycle and hexacycle

were all formed along with the hybrid tetracycle. This result is in contrast to the depolymerization of copolymer **9c**, in which only the hybrid macrocycle is observed.

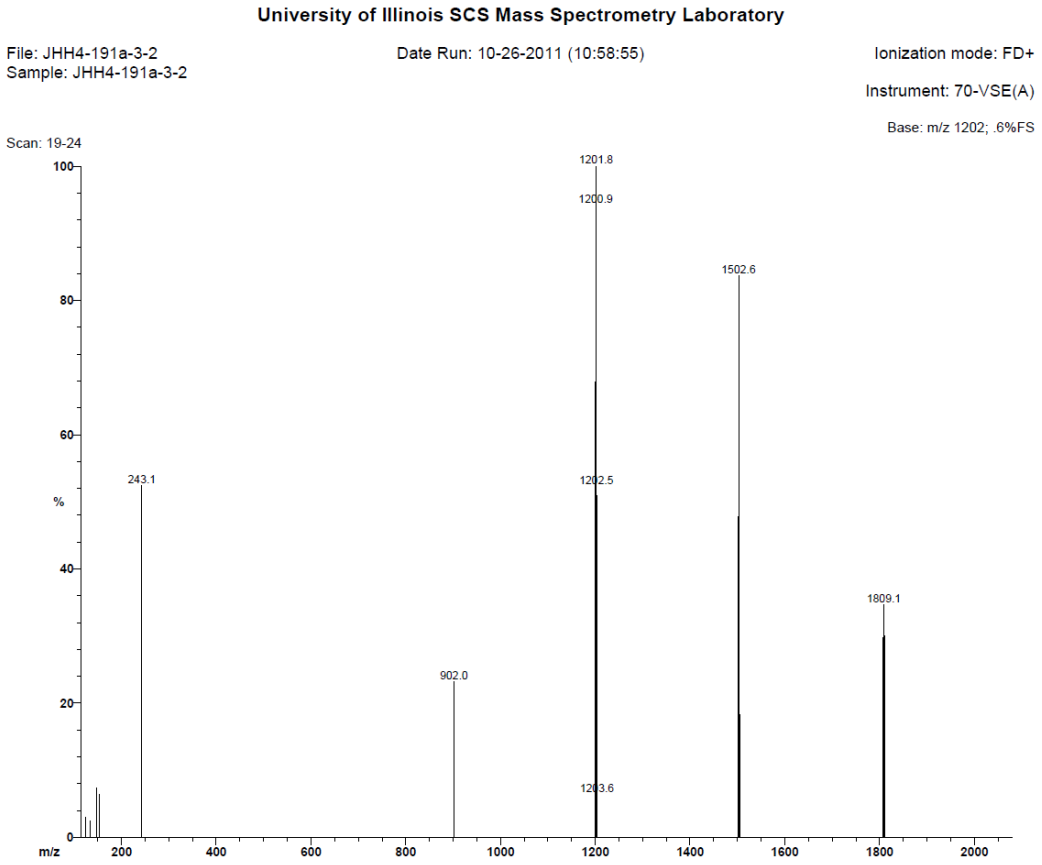

Figure 2.12: Crude FD-MS from *o*-PE and *m*-PE monomer mixing.

2.6.6: ABAB'-Copolymer Depolymerization

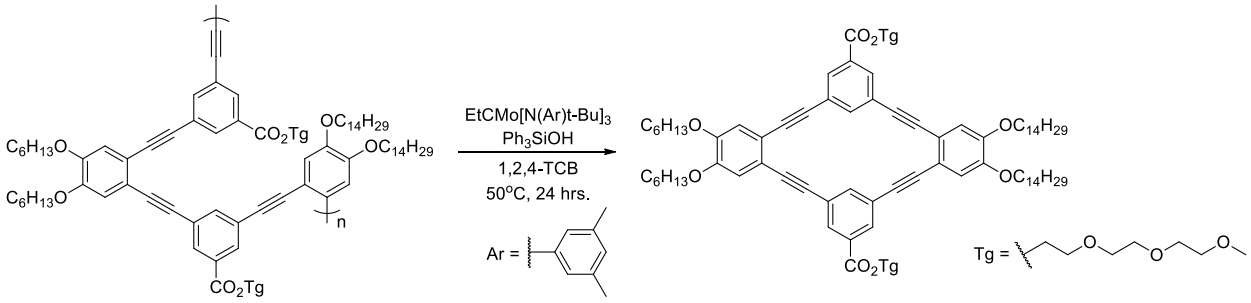

In an argon-filled glovebox, ABAB' copolymer **18** (200 mg) was dissolved in 1,2,4-trichlorobenzene (6 mL) in an oven-dried vial. In a separate vial, Mo(VI) alkylidine catalyst (20.1 mg, 0.03 mmol) and triphenylsilanol (42.1 mg, 0.15 mmol) were dissolved together in 1,2,4-trichlorobenzene (4 mL). The catalyst solution was added to the solution of polymer, and the reaction was sealed, removed from the glove box, and stirred at 50 °C for 24 hours. The

1,2,4-trichlorobenzene was removed via vacuum distillation and the resulting crude mixture was analyzed by mass spectrometry (FD and MALDI-TOF) for the presence of macrocycles **12a** or **12b**.

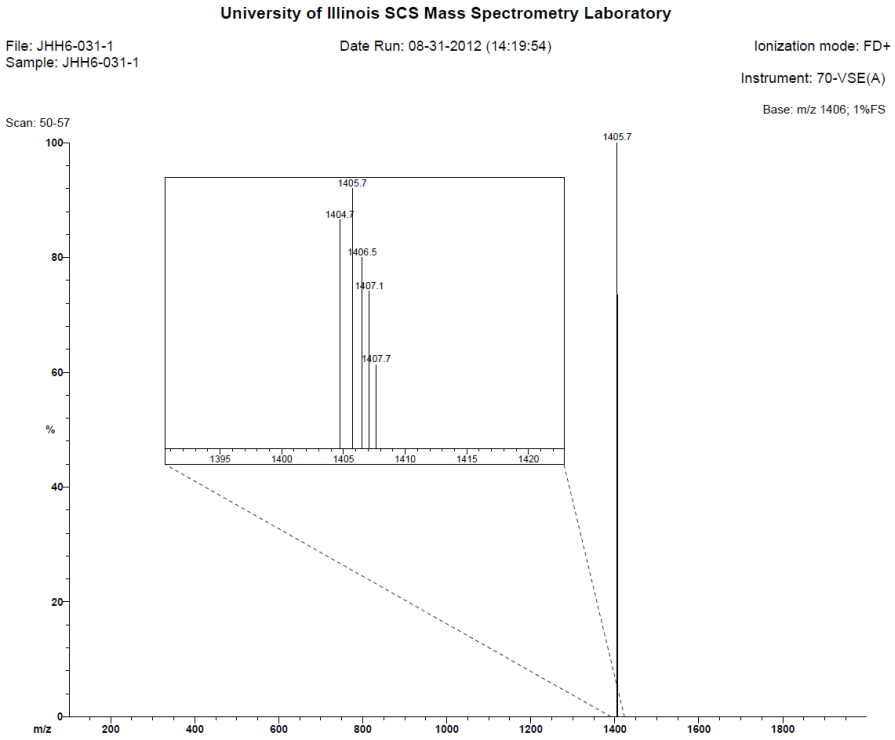

Figure 2.13: FD-MS spectrum of the crude product.

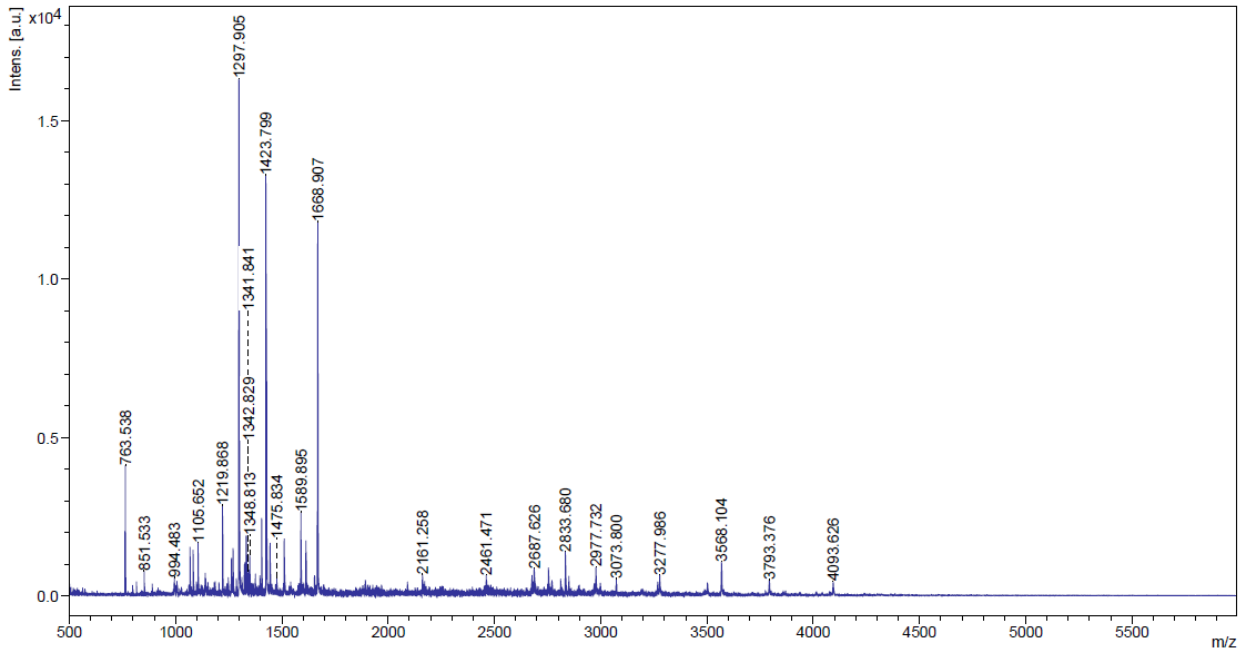

Figure 2.14: MALDI-TOF MS spectrum of the crude product.

2.6.7: Macrocycle-Based Mixing Study

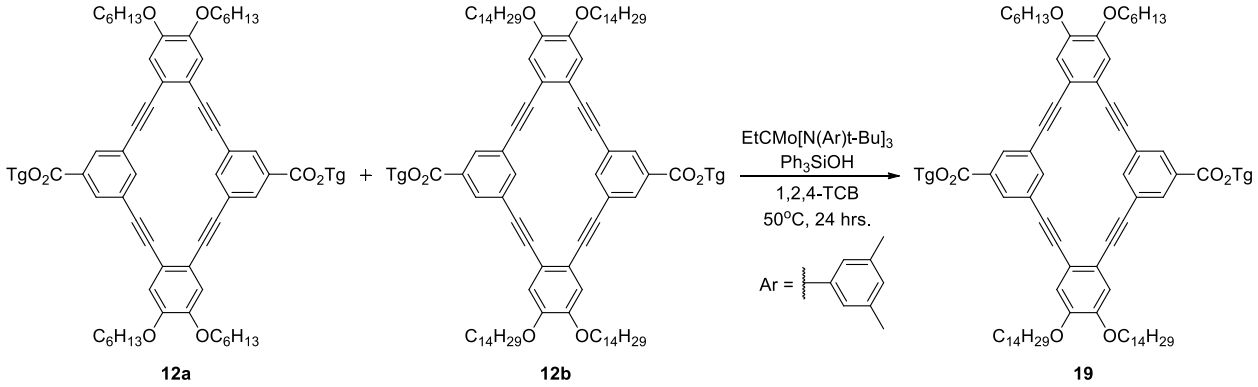

o-PE and m-PE macrocycle mixing. In an argon-filled glove box, macrocycle **12a** (83.9 mg, 0.07 mmol) and macrocycle **12b** (116 mg, 0.07 mmol) were suspended in 1,2,4-trichlorobenzene (6 mL) in an oven-dried vial. In a separate oven-dried vial, Mo(VI) alkylidine catalyst (20.1 mg, 0.03 mmol) and triphenylsilanol (42.1 mg, 0.15 mmol) were dissolved together in 1,2,4-trichlorobenzene (4 mL). The catalyst solution was added to the solution of macrocycles, and the reaction was sealed, removed from the glove box, and stirred at 50 °C for 24 hours. The 1,2,4-trichlorobenzene was removed via vacuum distillation and the resulting crude mixture was analyzed by MALDI-TOF and FD-MS. Analysis by FD shows only the two starting macrocycles, but the MALDI-TOF spectrum indicates the presence of macrocycle **19** as well, suggesting that scrambling of the hybrid macrocycles is possible. The MALDI spectrum also shows the presence of higher molecular weight material which is possibly due to ring-opening of the macrocycles.

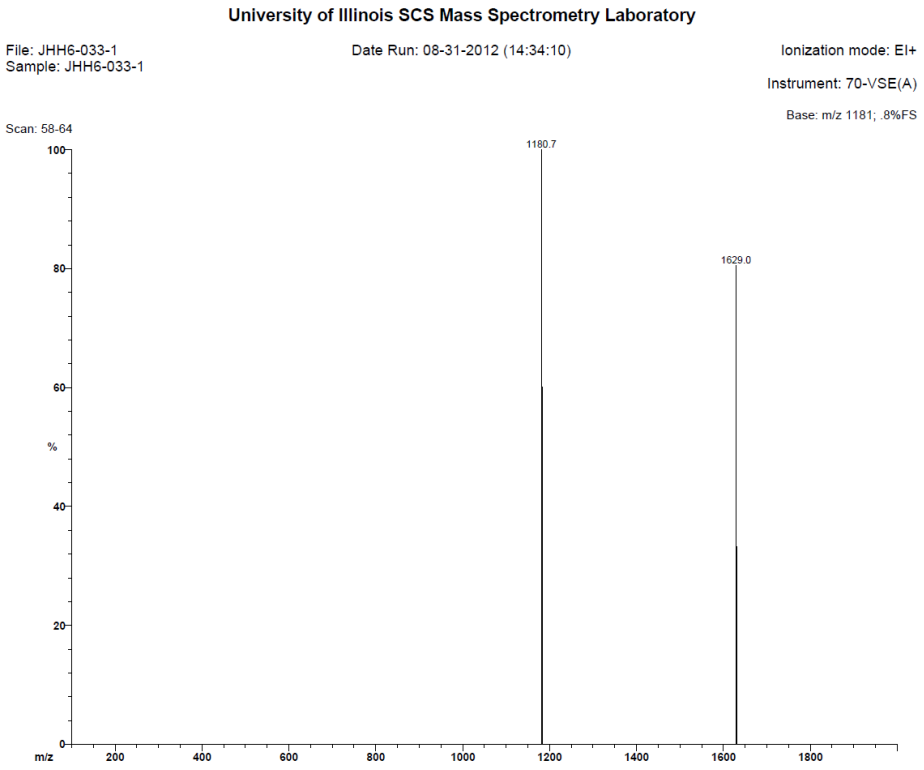

Figure 2.15: Crude FD-MS from *o*-PE and *m*-PE macrocycle mixing.

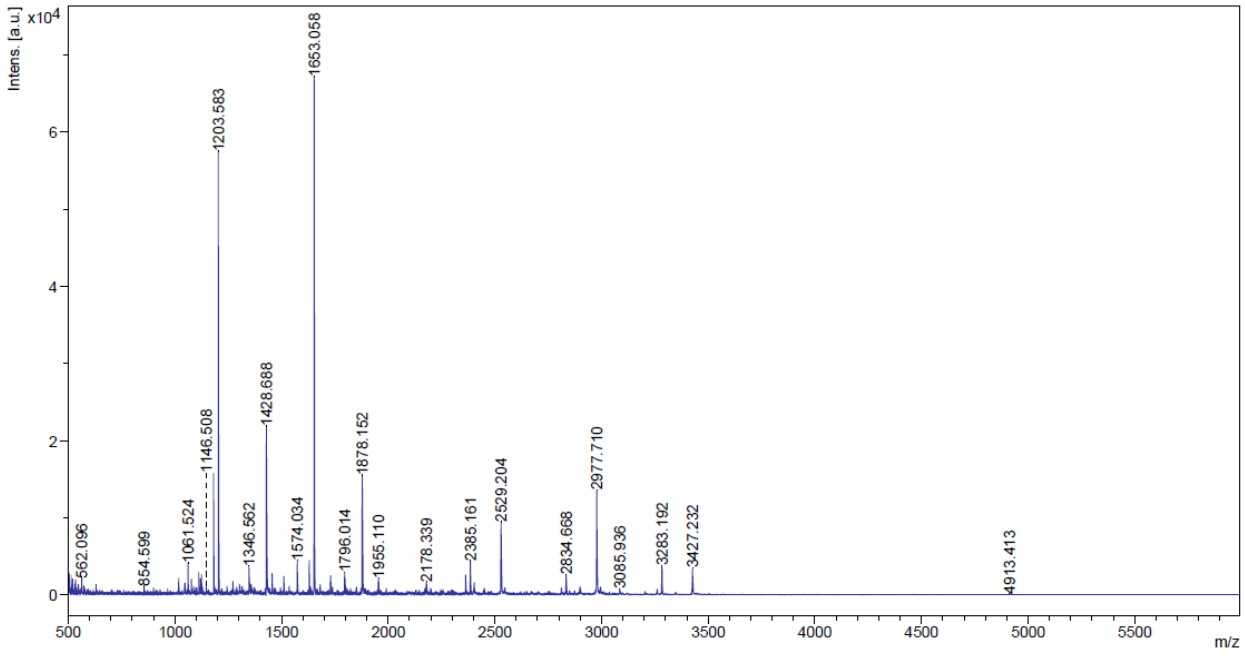

Figure 2.16: Crude MALDI-TOF MS from *o*-PE and *m*-PE macrocycle mixing.

2.6.8: Depolymerization of Copolymer 19

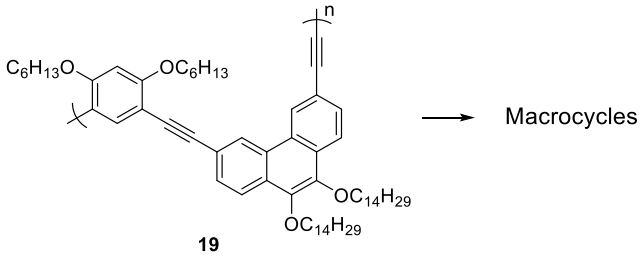

19

In an argon-filled glovebox, (phenanthrenyl-ethynylene)-*alt*-(*m*-phenylene-ethynylene) (100 mg) was suspended in 1,2,4-trichlorobenzene (3 mL) in a vial. In a separate oven dried vial, Mo(VI) alkylidine catalyst (10.0 mg, 0.015 mmol) and triphenylsilanol (21.1 mg, 0.076 mmol) were dissolved together in 1,2,4-trichlorobenzene (2 mL). The catalyst solution was added to the polymer mixture and the reaction was sealed, removed from the glove box, and stirred for 24 hours. The 1,2,4-trichlorobenzene was then removed via vacuum distillation. The crude product was analyzed by FD-MS, which showed the presence of the sodium adduct of the all *m*-phenylene-ethynylene pentamer and the all phenanthrene-ethynylene trimer in addition to the mixed tetramer.

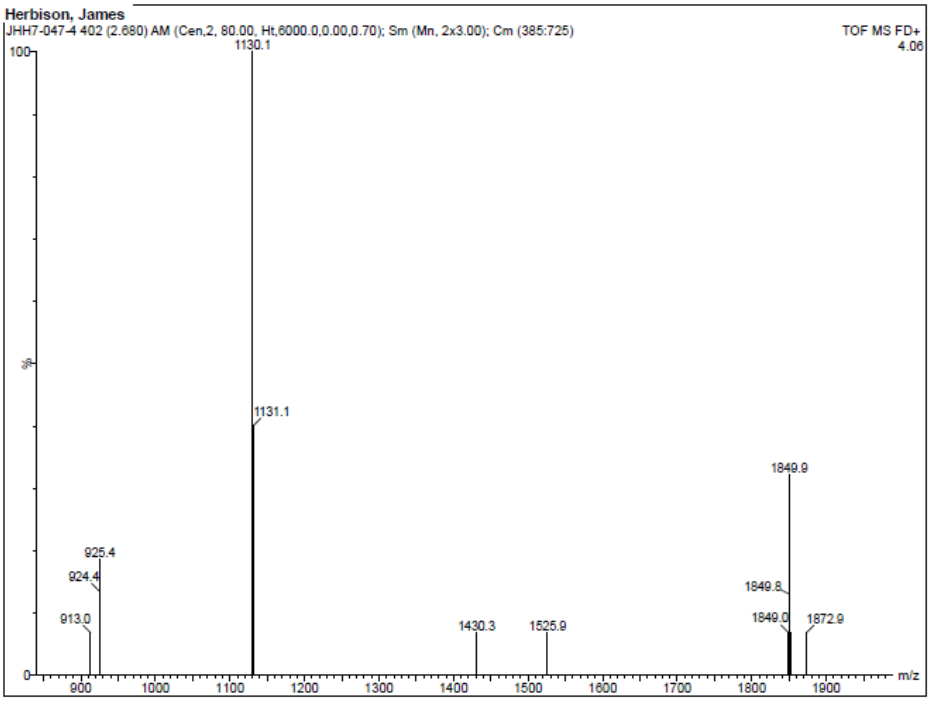

Figure 2.17: Crude FD-MS from the Depolymerization of Copolymer **19.**

2.6.9: Model Compound Metathesis Studies

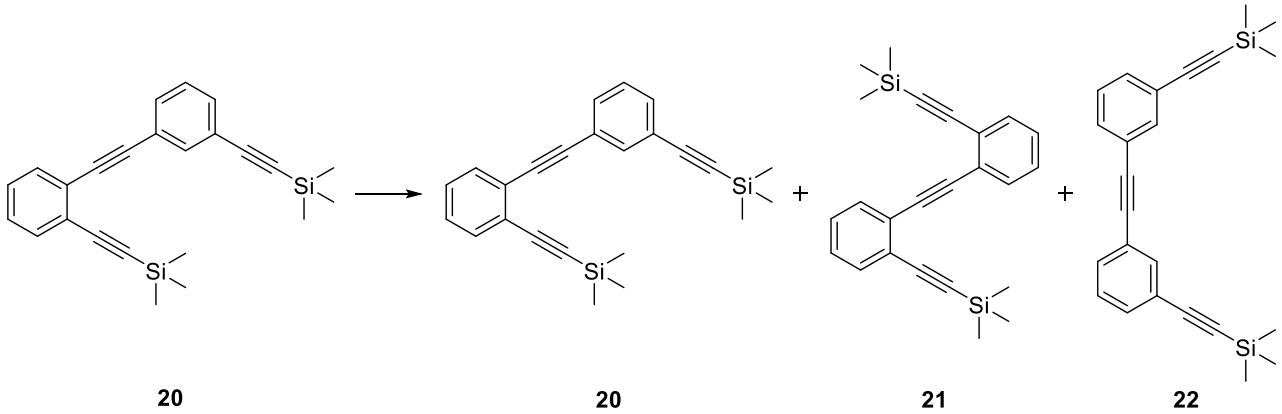

20 **20** **21** **22**

In an argon-filled glove box, model compound **20** (27 mg; 73 µmol) was dissolved in 1,2,4-trichlorobenzene (1.5 mL) before a solution of trisamidomolybdenum(IV) propylidyne (5.0 mg; 7.5 µmol) and triphenylsilanol (11 mg; 40 µmol) in 1,2,4-trichlorobenzene (1 mL) was added. The reaction was then sealed, removed from the glove box, and stirred at 50 °C for 24 hours. The reaction mixture was then analyzed by GC and compared to standards synthesized independently (see Figure 2.8). Due to the presence of all three possible cross-metathesis products, the reaction was repeated in triplicate on a larger scale (0.30 mmol of compound **20**) and the progress of the reaction was monitored every five minutes to determine when the reaction reached equilibrium. To determine if the catalyst was still active after that point, the reaction was repeated once more and compound **16** (0.21g; 0.25 mmol) was added after four hours. The formation of a precipitate demonstrated that the catalyst was still active four hours into the reaction.

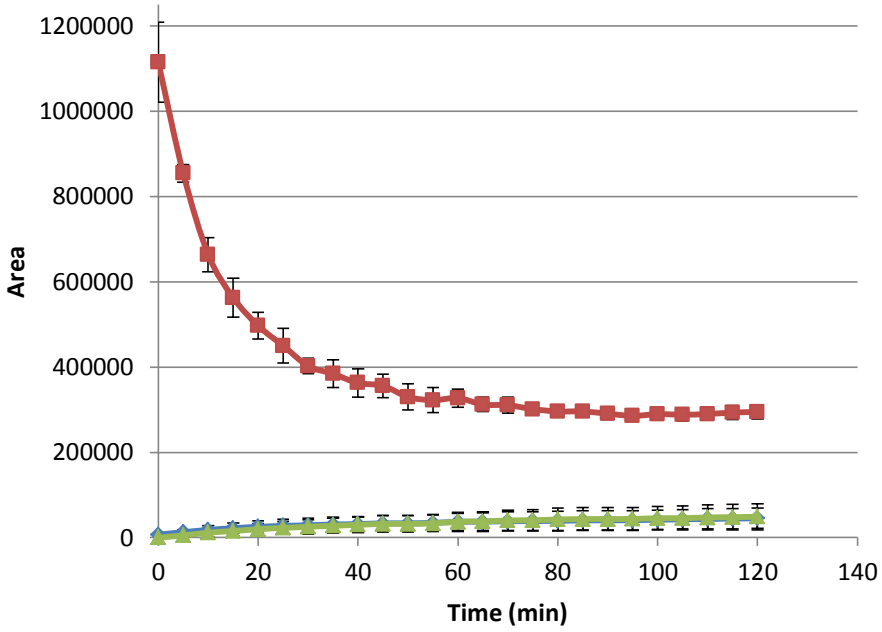

Figure 2.18: Reaction progress of the metathesis of the model compound showing the reaction reaching equilibrium and the decrease in concentration of **20** (red) and the increase in concentration of **21** (blue) and **22** (green). The graph only depicts the cross-metathesis products, while products from consumption of the starting material that does not result in one of the diphenylacetylene derivatives is not shown. These compounds are the butyne-functionalized fragment from metathesis with the original catalytic species and the bis(trimethylsilyl)ethynyl-derivatives resulting from the side reactions with the TMS-capped alkynes.

2.7: References and Notes

1) Zhang, W.; Moore, J.S. *J. Am. Chem. Soc.* **2004**, *126*, 12796.

2) Zhang, W.; Brombosz, S.M.; Mendoza, J.L.; Moore, J.S. *J. Org. Chem.* **2005**, *70*, 10198-10201.

3) Gross, D.E.; Moore, J.S. *Macromolecules* **2011**, *44*, 3685-3687.

4) Gross, D.E.; Discekici, E.; Moore, J.S. *Chem. Commun.* **2012**, *48*, 4426-4428.

5) Miljanić, O.Š.; Vollhardt, K.P.C.; Whitener, G.D. *Synlett* **2003**, 29-34.

6) Zhang, W.; Moore, J.S. *J. Am. Chem. Soc.* **2005**, *127*, 11862-11870.

7) It was found that all of the tetracycle compounds synthesized were mostly insoluble in diethyl ether, while the linear oligomers and polymers were fully soluble. For compounds with poor solubility that precluded purification by conventional methods, washing or precipitating the compound with ether resulted in the pure compound (determined by ^{1}H NMR and GPC).

8) This work was performed by Dr. Dustin Gross and his undergraduate researcher Emre Discekici.

9) Molecular modelling and geometry optimizations were performed using Spartan ’10 Quantum Mechanics Program (Version 1.1.0; Wavefunction, Inc.) at the AM1 level using semi-empirical calculations.

10) Moore, J. S. Foldamers Based on Solvophobic Effects. In *Foldamers: Structure, Properties, and Applications;* Hecht, S., Huc, I., Eds; Wiley-VCH: Verlag, 2007.

11) Zhang, W.; Kraft, S.; Moore, J.S. *J. Am. Chem. Soc.* **2004**, *126*, 329-335.

12) Khan, A.; Hecht, S. *Chem. Commun.* **2004**, *3*, 300-301.

13) Elliot, E.L.; Ray, C.R.; Kraft, S.; Atkins, J.R.; Moore, J.S. *J. Org. Chem.* **2006**, *71*, 5282-5290.

14) Zhou, Q.; Carroll, P.J.; Swager, T.M. *J. Org. Chem.* **1994**, *59*, 1294-1301.

15) Kobin, B.; Grubert, L.; Blumstengel, S.; Henneberger, F.; Hecht, S. *J. Mater. Chem.* **2012**, *22*, 4383.

16) Maran, U.; Britt, D.; Fox, C.B.; Harris, J.M.; Orendt, A.M.; Conley, H.; Davis, R.; Hlady, V.; Stang, P.J. *Chem. Eur. J.* **2009**, *15*, 8566-8577.

17) Mio, M.J.; Kopel, L.C.; Braun, J.B.; Gadzikwa, T.L.; Hull, K.L.; Brisbois, R.G.; Markworth, C.J.; Grieco, P.A. *J. Org. Chem.* **2002**, *4*, 3199-3202.

Chapter 3

Water Filtration and Improving Current Membranes

3.1: The Importance of Water Filtration

Access to safe drinking water is rapidly becoming a worldwide crisis, and in many regions it is already a significant problem. According to the United Nations; "Water scarcity already affects every continent. Around **1.2 billion** people, or almost one-fifth of the world's population, live in areas of physical scarcity, and 500 million people are approaching this situation. Another 1.6 billion people, or almost one quarter of the world's population, face economic water shortage."[1] Part of this problem is due to shortfalls in infrastructure and the lack of capabilities to transport water efficiently to arid regions where it is needed most. However, a significant contribution to this problem results from an increasing amount of contaminated drinking water containing various toxins and the difficulties associated with removing those toxins. Targeting this problem requires an efficient and sustainable method for large-scale water purification.[2]

One of the issues in water purification is the variety of toxins that need to be removed and the wide range of properties that these toxins exhibit. Both organic and inorganic impurities need to be removed in order to make water sufficiently clean and safe for daily use.[3] The organic toxins include compounds from natural contaminants to pharmaceutical wastes introduced into water sources via pollution and runoff from landfills. Inorganic contaminants are just as varied, and pressing issues range from the need to remove arsenates from groundwater in some regions to the highly sought desalination of ocean water.

The most straightforward method for purifying water is distillation. Volatile contaminants can be removed by the same techniques that chemists have used for over a century to purify compounds. Non-volatile compounds, such as inorganic salts, would simply be left behind after evaporation so that the collected water would be completely pure. The major problem with distillation is the extremely large amount of energy required to distill any significant amount of water due to its high specific heat. On a scale necessary to curb the water crisis, the energetic and monetary costs are prohibitively high.

Alternatives to distillation include reverse osmosis (RO) or nanofiltration (NF), which work by forcing water through a semi-permeable membrane that restricts the passage of

contaminants. Because of the high pressure used to push the water through the membranes, reverse osmosis also requires a significant amount of energy. However, the membrane properties, such as water flux and rejection of different solutes, can be modified by changing its composition, thickness, and film processing methods.[4-7] Therefore, reverse osmosis and nanofiltration have attracted increasing attention due to their versatility along with potential cost efficiency.

3.2: Polyaramide Nanofiltration and Reverse Osmosis Membranes

Thin-film composites (TFC) are used in the majority of commercial membranes for reverse osmosis and nanofiltration to reject salts.[4] The first layer (*ca.* 50 μm) of the composite is a porous, asymmetric polysulfone (PSU) that has large pores near the bottom of the film and small pores near the top.[8] This layer simply acts as a mechanical support for the active layer, which is composed of a highly cross-linked polyamide film with thickness of 50-200 nm.[9] This layer is responsible for the filtration properties of the composite including the water flux of the membrane and the rejection of solutes. Aromatic polyamide (polyaramide) membranes are commonly used as the active layer material for their favorable filtration properties. The filtration properties of the membrane are typically related to the thickness of the active layer, with thicker layers able to reject a higher percentage of contaminants but resulting in a lower water flux.

Polyaramide membranes are synthesized through interfacial polymerization (IP) between an aniline monomer dissolved in water and an organic solution of an acyl chloride (Figure 3.1). Commonly used monomers are *m*-phenylene diamine (MPD) and trimesoyl chloride (TMC). The reaction is carried out by first immersing the porous polysulfone support in the aqueous solution containing the diamine, filling the pores of the PSU. The support is then dried to remove droplets containing the aniline on the surface of the support that would cause deformities in the membrane before it is immersed in the acyl chloride solution. Polymerization occurs at the interface between the organic and aqueous solutions inside the pores of the PSU. As the polymerization progresses, the aniline monomer diffuses through the polymer matrix and forms the active layer on top of the support.

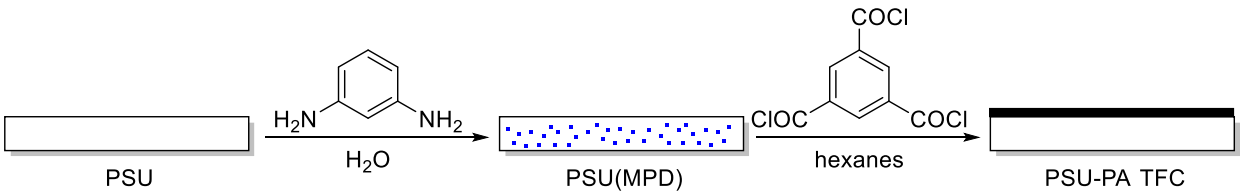

Figure 3.1: Schematic of the synthesis of the polyaramide active layer by interfacial polymerization with the support (PSU) first immersed in MPD and then reacted with TMC to form the active layer.

The interfacial polymerization allows for the formation of very thin active layers, which would be difficult to produce by physical processing methods, such as spin-coating or melt-based processing techniques. Polyaramides also exhibit low solubility in organic solvents, thereby limiting its solution processability. As an additional benefit, this approach enables strong adhesion between the support and the active layers as polymerization initiates from the PSU pores. One challenge of the interfacial polymerization is the limited control over active layer thickness and morphology. Incomplete cross-linking of the active layer is significant because the residual amine and carboxylate groups contribute to pH-dependent membrane charges, which play a large role in salt rejection by electrostatic repulsion, or the Donnan effect. Therefore it is important to optimize the reaction conditions in order to allow for reproducible fabrication of an acceptable membrane.

3.3: Improving Polyamide Membranes

Polyaramide membranes have seen significant development in the past decades, but most of them exhibit similar physiochemical properties and thus the same drawbacks, particularly insufficient rejection of certain contaminants such as arsenates[10] and fouling.[11-15] Because of these challenges, research in this area has been devoted to improving the separation and anti-fouling properties of the membranes. Many ways to improve membranes have been studied, and the two main approaches include: (1) new membrane compositions and (2) surface modification of existing membranes.

3.3.1: New Membrane Compositions

Compared to chemically modifying existing active layer materials, designing and synthesizing new polymeric membranes enable the tailoring of chemical structures for specific functions and chemistries. It can also keep the membrane system simple with fewer components that could be prone to mechanical failure, such as delamination between layers. However, the

successful development of a new membrane material will depend on extensive material characterization to determine its separation efficacy. It will also rely on optimization of polymerization because any changes in the reaction conditions may drastically alter the final membrane properties. In addition, the target monomers are required to be accessed on a large scale through efficient synthetic routes if the compounds are not commercially available.

Despite these synthetic challenges, many new active layer materials display significantly improved anti-fouling properties compared current polyaramide materials. Chlorination of polyaramide with hypochlorite is one of the major contributors to membrane fouling, which decreases membrane efficacy overtime.[16] This process is hypothesized to occur through N-chlorination of the amide followed by an Orton rearrangement reaction to chlorinate the *ortho*-position of the attached phenyl ring.[16] Chlorination of the aromatic moiety is the irreversible step and reduces the ability to rejuvenate the membrane by chemical rinsing. Thus, minimizing chlorine-based fouling by inhibiting this mechanism has become a major research focus.

The approach taken by La *et al.* involved the synthesis of a new active layer material by substituting MPD with a hexafluoroalcohol (HFA)-functionalized aryl diamine (Figure 3.2).[17] The authors rationalized that the steric bulk and electron withdrawing character of the HFA functionality would reduce the nucleophilicity of the aromatic rings toward electrophilic aromatic substitution, thereby preventing the Orton rearrangement from occurring. Analysis of a linear analog and of the membrane after chlorine exposure showed a significant improvement in chlorine resistance of the new material relative to traditional MPD-TMC membranes, even though the salt rejection efficiency of the new membrane was lower.

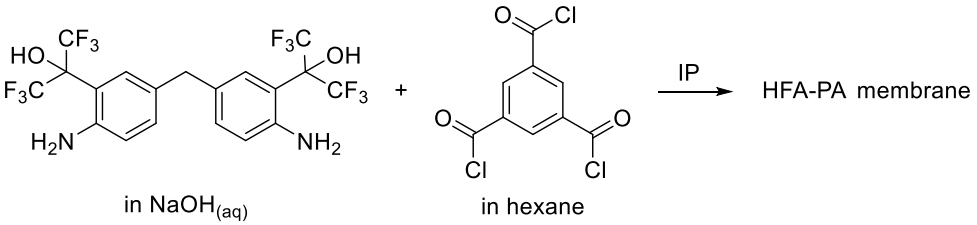

Figure 3.2: Synthesis of a new membrane material utilizing bulky, electron-withdrawing groups to improve chlorine resistance.

In another approach, Yu and coworkers studied new composite materials by comparing permutations of MPD or 4-methyl-1,3-diaminobenzene (MMPD) as the amine component and TMC or 1,3,5-cyclohexanetriacyl chloride (HTC) as the acyl chloride component (Figure 3.3).[18] The authors found that a combination of the *ortho*-methylated aniline and the cycloaliphatic acyl

chloride monomers resulted in a membrane with a higher chlorine resistance relative to MPD/TMC materials. By comparing MMPD/TMC to MPD/HTC composites, it was found that installing an additional methyl substituent on the aryl diamine led to greater chlorine resistance than using an aliphatic acyl chloride comonomer. As with the work of La and coworkers, the membranes synthesized in this study also had lower salt rejection, though the MPD/HTC membrane had a significantly higher water flux.

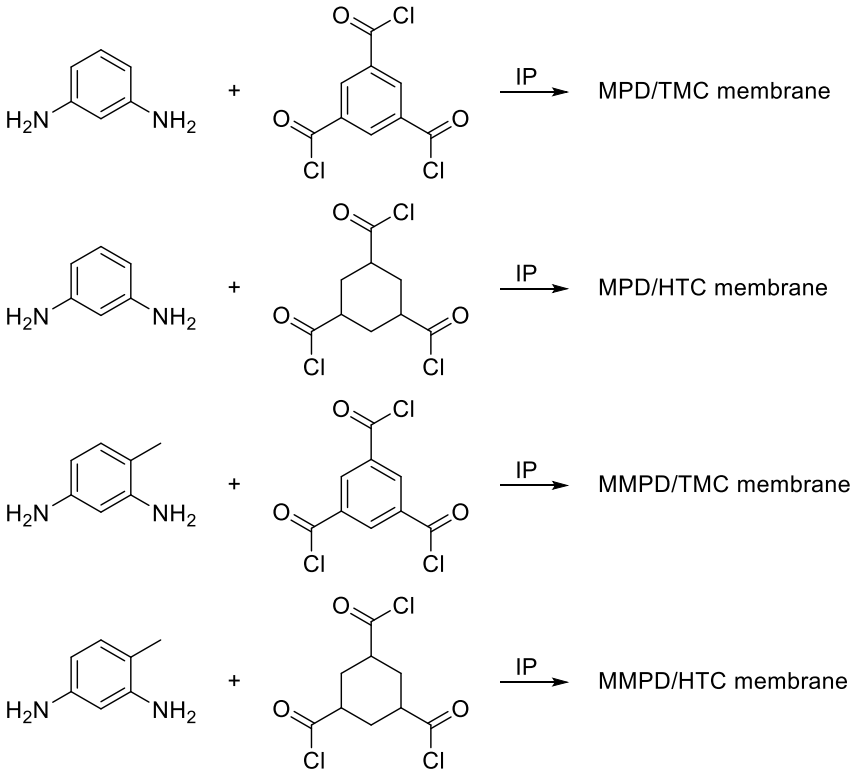

Figure 3.3: Membranes synthesized by interfacial polymerization using a methylated aryl diamine and an aliphatic triacyl chloride to study their effects on chlorine resistance.

Many other groups have focused on synthesizing new materials in order to afford improved filtration properties relative to MPD/TMC membranes. Gao and coworkers have extensively studied the effect of replacing one of the acyl chloride groups on trimesoyl chloride with isocyanate or chloroformate to afford a mixture of amide bonds and either urea or urethane groups.[19] The authors found that a composite with amide/urea linkages exhibit the highest water flux and intermediate salt rejection (at low NaCl concentrations), while a composite with amide/urethane groups has the highest salt rejection but the lowest flux. These results can be attributed to both the hydrophilic character of the membrane, where amide/urea is the most hydrophilic and amide/urethane is the least, and the membrane thickness which follows the order

of amide/urethane>amide>amide/urea. The urea composite was also more susceptible to chlorine fouling, which is consistent with the accepted mechanism due to the higher number of C(O)-N-H bonds in the material.

Zhang and coworkers have extensively studied the use of various monomers with additional aryl rings, increased number of functional groups, or both properties relative to MPD and TMC (Figure 3.4).[20-22] In general, the monomers with more functional groups than the reference monomers formed smoother membranes with a tighter morphology, which is typically attributed to an enhanced degree of cross-linking, affecting diffusion of the aqueous monomer to the reaction interface during polymerization. The low diffusion of the aniline monomer through the polymer matrix also led to the formation of active layers thinner than the MPD/TMC composite, contributing to the improved water flux. In the case of the amine monomer DABA, the authors also hypothesize that the low monomer diffusion through the growing membrane has an impact on the flux due to reduced cross-linking on the surface, allowing for hydrolysis of more acyl chloride groups, yielding membranes with higher hydrophilicity. For monomers with a higher number of acyl chloride groups, the authors observed a comparable rejection of salts compared to a TMC-based membrane but with much higher flux, which was attributed to the increased spacing of the monomer, a higher carboxylate concentration, and the Donnan exclusion effect.

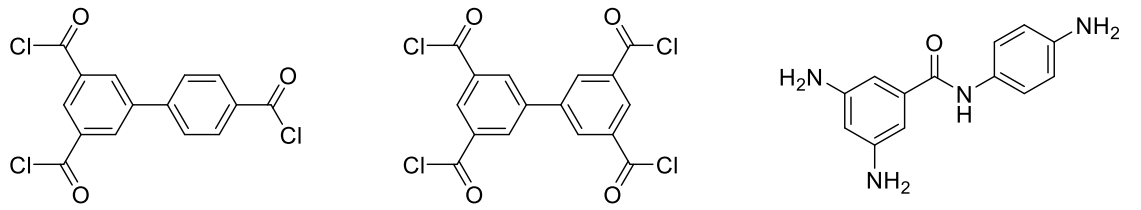

Figure 3.4: Monomers with larger size, increased functionality, or both tested to synthesize membranes with improved filtration properties.

3.3.2: Surface Modification of Existing Membranes

Surface modification of existing polyaramide membranes is often less synthetically involved than the development of a novel membrane. The properties of the original membrane are typically preserved while new functionality can be added to achieve the desired effect. Modification can be accomplished through either coating the membrane with a new material or

covalently attaching the additive to the existing material. The former relies on physiochemical effects to keep the new coating in place while the latter is more difficult to perform but results in a more stable attachment of the modification.

Polymer coatings have attracted attention for their potential to improve the fouling resistance of membranes. Reinhard and coworkers demonstrated this capability by coating a polyaramide membrane with a polyether-polyamide block copolymer with a high hydrophilic character that had previously shown to improve gas separation and ultrafiltration membranes.[23] The hydrophilicity of the coating was expected to prevent contact between the active layer and hydrophobic foulants. In agreement with their hypothesis, the coated membranes were significantly less susceptible to fouling with an oil-containing mixture. However, the flux of the membranes was much lower and the membrane did not recover after rinsing which suggests that any fouling of the active layer that occurs is irreversible. Yu and coworkers have developed similar anti-fouling coatings using *N*-isopropylacrylamide-*co*-acrylamide and *N*-isopropylacrylamide-*co*-acrylic acid copolymers. These coatings have minimal effect on the flux of the membrane and show better recovery of the membrane after fouling.[24,25]

Feng et al. and Gao et al. have also demonstrated the use of polymer coatings to improve both the anti-fouling and filtration properties using polymers functionalized with pendant amine groups that provide positive charge to the coating.[26,27] The positively charged side chains were hypothesized to repel positively charged foulants, along with the cations of dissolved salts, from the negatively charged active layer. The resulting membranes displayed improved fouling resistance and salt rejection and the high degree of hydrophilicity of the coating offset the flux reduction from making the membrane thicker.

While coatings have traditionally been fabricated using polymers, dendrimers have drawn increasing attention because of their modularity and monodispersity. In addition to the tunability of desired properties based on composition and functionality, the size of dendrimers is easily controlled, which can significantly affect their molecular packing in the coating and interactions with the active layer surface. Dendrimers can also display a greater number of functionalities on the surface than traditional polymers, subsequently allowing for a higher functional group density in the coating. Sarkar *et al.* studied coatings analogous to the hydrophilic polymer coatings but with PEG-terminated polyamidoamine-based dendrimers that were either cross-linked with the PEG chain or with PEG chains on the periphery of the dendrimer that did not

cross-link the dendrimers. In this initial test, the coated membranes showed slightly lower water flux than the uncoated membrane and no improvement of the salt rejection. The anti-fouling properties of the coating were not explored.[28]

Covalent modification of a membrane requires the additive to be reactive toward functionalities on the polymer membrane, yielding for stable attachment of the new layer upon chemical reactions. Although this technique is not as widely used as coating, there have been examples of grafting poly(ethylene glycol) chains to the surface of membranes to improve the water flux while restricting passage of ionic species, achieving similar effects as the other hydrophilic polymeric coatings mentioned above.[32,33]

Wang and coworkers have demonstrated both covalent attachment of a small molecule to membrane surfaces and surface graft polymerization using hydantoin derivatives to prevent membrane fouling.[34,35] The amide groups present on the small molecule and monomers of the graft polymer were designed to react with hypochlorite more rapidly to avoid chlorination of the membrane, Since the hydantoin does not have an aromatic ring for the Orton rearrangement to occur, the chlorination is reversible, protecting the polyaramide layer and allowing for facile removal of the foulant. These successful studies proved the feasibility of using the residual functional groups in the material from incomplete cross-linking for the attachment of compounds to modify the properties of the membrane.

Building on their work with rigid-star ampiphiles,[29,30] Moore and Mariñas studied the use of polyaramide dendrimers as coatings toward improving water filtration (Figure 3.5).[31] The dendrimers chosen were structurally similar to a fragment of MPD/TMC membranes and were hypothesized to exhibit filtration properties by constricting the membrane pores rather than through physiochemical interactions. For polyaramide membranes coated with **G2** and **G3**, the dendrimeric coating improved the rejection of an organic surrogate (rhodamine WT), arsenate and salts with a slight reduction in water flux. Dendrimer **G1** was too small to coat the membrane effectively, broke through the membrane at high pressure, and could not be used reliably.

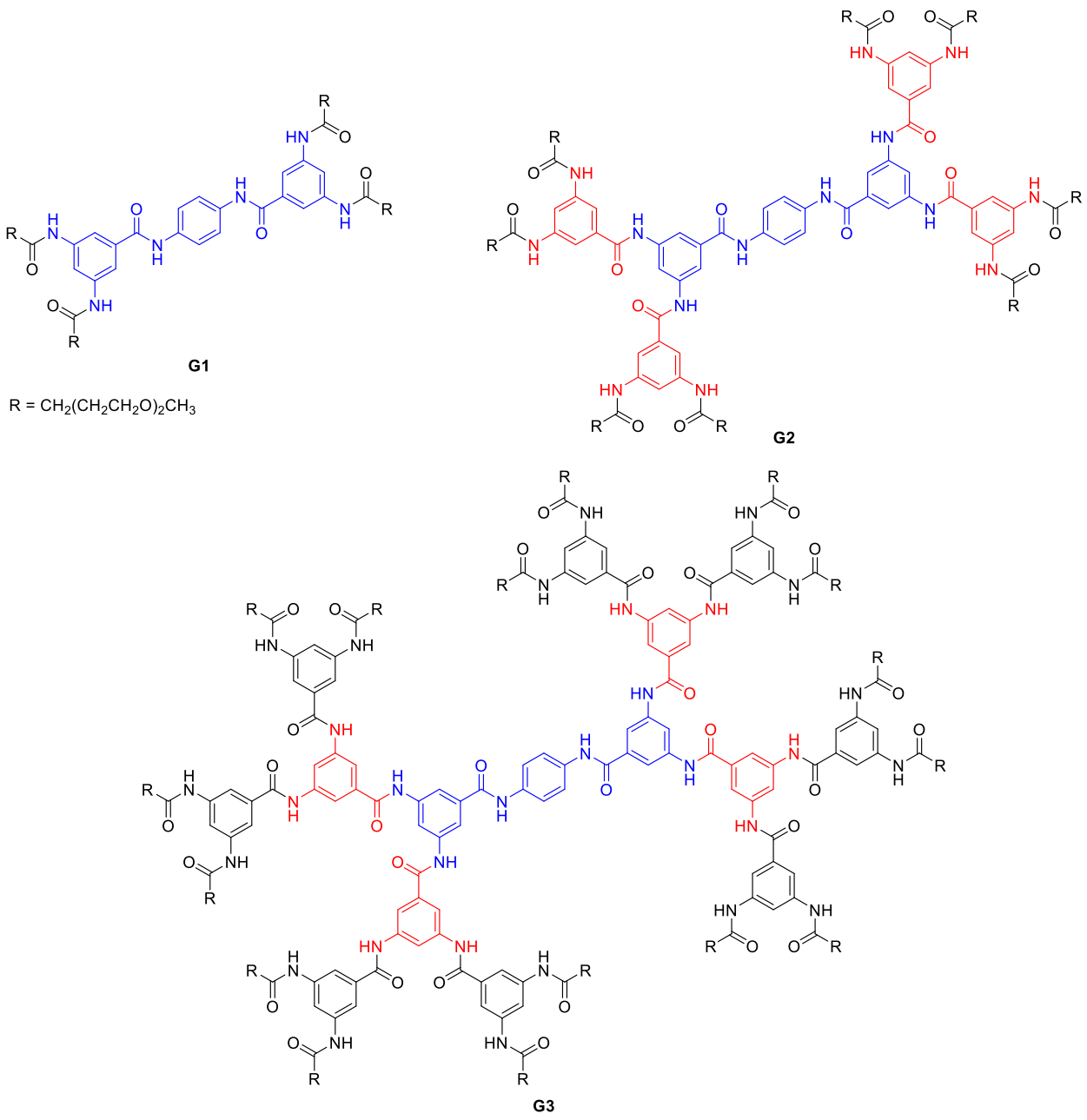

Figure 3.5: Polyaramide dendrimers used to fabricate coatings to improve existing membranes.

We have recently discovered that these dendrimeric coatings are unstable, and the modified membranes lose their efficacy over time. These findings and our attempts to account for the instability by covalently attaching the dendrimers to the polyaramide are detailed in Chapter 4.

3.4: References

1) Water scarcity | International Decade for Action 'Water for Life' 2005-2015. http://www.un.org/waterforlifedecade/scarcity.shtml (accessed June 14, 2014).

2) Shannon, M.A.; Bohn, P.W.; Elimelech, M.; Georgiadis, J.G.; Mariñas, B.J.; Mayes, A.M. *Nature* **2008**, *452*, 301-310.

3) United States Environmental Protection Agency (US EPA), Drinking Water Contaminant Candidate List 2: Final Notice. In Federal Register: 2005; Vol. 70(36), 9071-9077.

4) Ghosh, A.K.; Jeong, B.H.; Huang, X.; Hoek, E.M.V. *J. Membr. Sci.* **2008**, *311*, 34-45.

5) Jin, Y.; Su, Z. *J. Membr. Sci.* **2009**, *330*, 175-179.

6) Geise, G.M.; Park, H.B.; Sagle, A.C.; Freeman, B.D.; McGrath, J.E. *J. Membr. Sci.* **2011**, *369*, 130-138.

7) Kim, Y.K.; Lee, S.Y.; Kim, D.H.; Lee, B.S.; Nam, S.Y.; Rhim, J.W. *Desalination* **2010**, *250*, 865-867.

8) Petersen, R.J. *J. Membr. Sci.* **1993**, *83*, 81-150.

9) Mi, B.; Coronell, O.; Mariñas, B.J.; Watanabe, F.; Cahill, D.G., Petrov, I. *J. Membr. Sci.* **2006**, *282*, 71-81.

10) Sen, M.; Manna, A.; Pal, P. *J. Membr. Sci.* **2010**, *354*, 108-113.

11) Xu, P.; Drewes, J.E.; Kim, T.U.; Bellona, C.; Amy, G. *J. Membr. Sci.* **2006**, *279*, 165-175.

12) Kipper da Silva, M.; Tessaro, I.C.; Wada, K. *J. Membr. Sci.* **2006**, *282*, 375-382.

13) Zhu, X.; Elimelech, M. *Environ. Sci. Technol.* **1997**, *31*, 3654-3662.

14) Kim, M.M.; Lin, N.H.; Lewis, G.T.; Cohen, Y. *J. Membr. Sci.* **2010**, *354*, 142-149.

15) Arsuaga, J.M.; Sotto, A.; López-Muñoz, M.J.; Braeken, L. *J. Membr. Sci.* **2011**, *372*, 380-386.

16) Powell, J.; Luh, J.; Coronell, O. *Environ. Sci. Technol.* **2014**, *48*, 2741-2749.

17) La, Y.H.; Sooriyakumaran, R.; Miller, D.C.; Fujiwara, M.; Terui, Y.; Yamanaka, K.; McCloskey, B.D.; Freeman, B.D.; Allen, R.D. *J. Mater. Chem.* **2010**, *20*, 4615-4620.

18) Yu, S.; Liu, M.; Lü, Z.; Zhou, Y.; Gao, C. *J. Membr. Sci.* **2009**, *344*, 155-164.

19) Liu, M.; Wu D.; Yu, S.; Gao, C. *J. Membr. Sci.* **2009**, *326*, 205-214.

20) Li, L.; Zhang, S.; Zhang, X.; Zheng, G. *J. Membr. Sci.* **2007**, *289*, 258-267.

21) Li, L.; Zhang, S.; Zhang, X. *J. Membr. Sci.* **2009**, *335*, 133-139.

22) Wang, H.; Li, L.; Zhang, X.; Zhang, S. *J. Membr. Sci.* **2010**, *353*, 78-84.

23) Louie, J.S.; Pinnau, I.; Ciobanu, I.; Ishida, K.P.; Ng, A.; Reinhard, M. *J. Membr. Sci.* **2006**, *280*, 762-770.

24) Liu, M.; Chen, Z.; Yu, S.; Wu, D.; Gao, C. *Desalination* **2011**, *270*, 248-257.

25) Yu, S.; Lü, Z.; Chen, Z.; Liu, X.; Liu, M.; Gao. C. *J. Membr. Sci.* **2011**, *371*, 293-306.

26) Zhou, Y.; Yu, S.; Gao, C.; Feng, X. *Sep. Purif. Technol.* **2009**, *66*, 287-294.

27) Xu, J.; Feng, X.; Gao, C. *J. Membr. Sci.* **2011**, *370*, 116-123.

28) Sarkar, A.; Carver, P.I.; Zhang, T.; Merrington, A.; Bruza, K.J.; Rousseau, J.L.; Keinath, S.E.; Dvornic, P.R. *J. Membr. Sci.* **2010**, *349*, 421-428.

29) Lu, Y.; Suzuki, T.; Zhang, W.; Moore, J.S.; Mariñas, B.J. *Chem. Mater.* **2007**, *19*, 3194-3204.

30) Suzuki, T.; Lu, Y. Zhang, W.; Moore, J.S.; Mariñas, B.J. *Environ. Sci. Technol.* **2007**, *41*, 6246-6252.

31) Saenz de Jubera, A.M.; Gao, Y.; Moore, J.S.; Cahill, D.G.; Mariñas, B.J. *Environ. Sci. Technol.* **2012**, *46*, 9592-9599.

32) Kang, G.; Liu, M.; Lin, B.; Cao, Y.; Yuan, Q. Polymer 2007, 48, 1165-1170.

33) Van Wagner, E.M.; Sagle, A.C.; Sharma, M.M.; La, Y.H.; Freeman, B.D. *J. Membr. Sci.* **2011**, *367*, 273-287.

34) Wei, X.; Wang, Z.; Chen, J.; Wang, J.; Wang, S. *J. Membr. Sci.* **2010**, *346*, 152-162.

35) Wei, X.; Wang, Z.; Zhang, Z.; Wang, J.; Wang, S. *J. Membr. Sci.* **2010**, *351*, 222-233.

Chapter 4

Improving Existing Water Filtration Membranes via Covalent Modification[1]

4.1: Disclaimer

The work reported in this chapter is the result of collaboration between Ana Martinez Saenz de Jubera in the Mariñas group in the Environmental Engineering Department and me. Synthesis and characterization of the dendrimers, as well as the synthesis and attempted attachment of solubilizing chains, were performed by me. Attachment of the dendrimers, characterization of the membranes, and membrane performance tests were performed by Ana, and the data from these experiments have been reproduced with her permission. Development and optimization of the attachment reaction and the method for measuring the number of attachment points was the product of discussions between both of us.

4.2 Introduction

Collaborative work between the Mariñas and Moore groups has recently demonstrated that coating polyaramide dendrimers on the surface of a polyaramide water filtration membrane can improve the filtration properties of the membrane.[2,3] Characterization of iodine-labelled dendrimers by Rutherford backscattering spectrometry (RBS) shows that this coating was unstable and the dendrimers were removed membrane surface upon stirring in water over ten days (Figure 4.1). The loss of the dendrimer layer corresponded to a decrease in the performance in the membrane, negating any of the beneficial effects of the dendrimers.

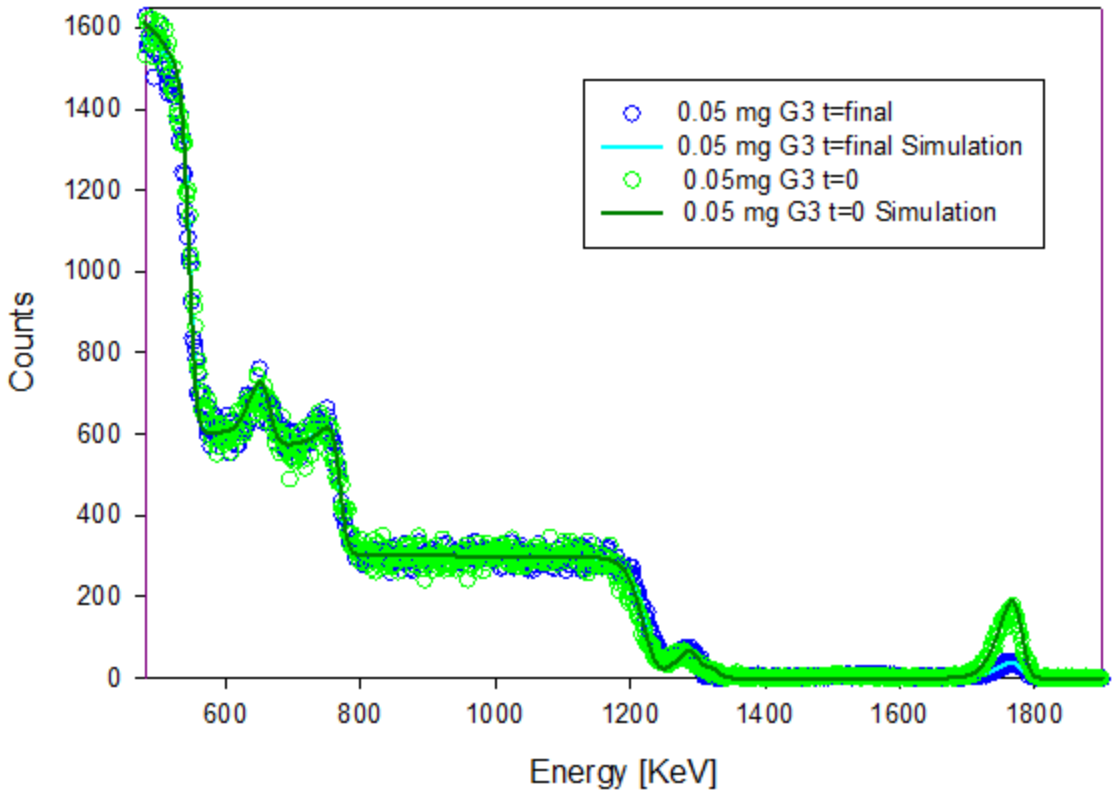

Figure 4.1: RBS data using iodine (~1750 KeV) showing the loss of the dendrimer layer from the initial 5.8 nm layer (green) to the final 0.6 nm layer (blue) after stirring in water for ten days.

Previous reports have shown that residual functional groups in the membrane due to incomplete cross-linking can be used for the attachment of compounds.[4-6] This result lead toan appealing solution to the instability of the dendrimer layer since the residual carboxylates could easily be coupled to amines and form stable amide bonds that covalently attach the dendrimers. There was also a concern regarding the scalability of our method using dendrimers, so we aimed to optimize the dendrimer synthesis and develop new syntheses that are feasible for large-scale production and manufacture.

4.3: Dendrimer Design and Synthesis

The synthesis of the polyaramide dendrimer was originally reported by Ueda *et al.* as a facile, high-yielding procedure (Scheme 4.1).[7] These dendrimers were ideal for our purposes because they high structural similarity to the active layer of the membrane and contained amine functionality at the periphery. The amine functionality was desired for the formation of an amide

bond with the residual carboxylate functional groups in the membrane. This approach is advantageous since the functionalization does not introduce new reactivity or chemical sensitivity to the membrane.

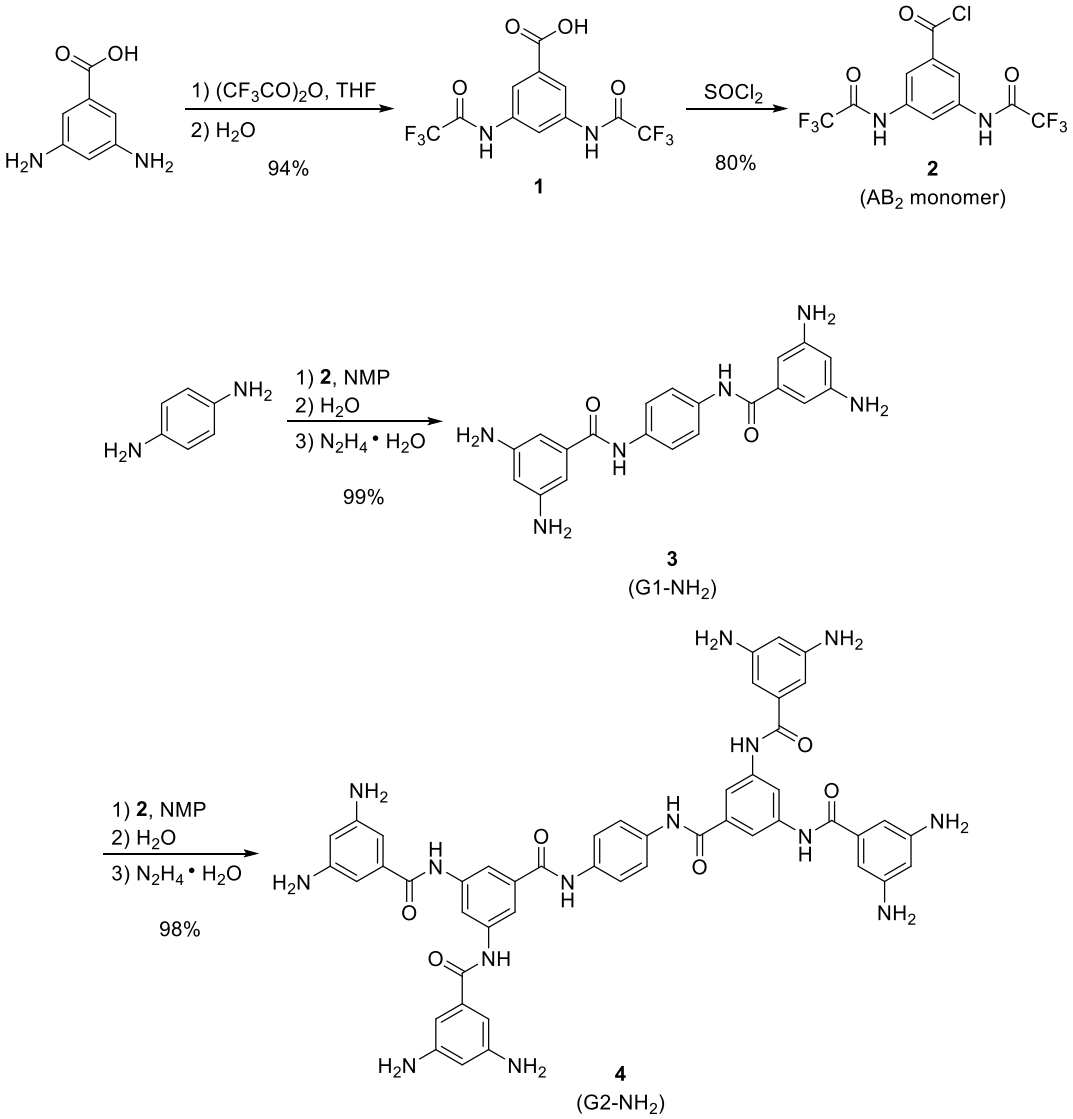

Scheme 4.1: Synthesis of the AB_2 monomer and G1-NH_2, and G2-NH_2 dendrimers.

4.3.1: Optimization of Large-Scale Synthesis and Iodinated Dendrimer Synthesis

One of our first objectives was to demonstrate that the synthesis of the dendrimer could be performed on a large scale. The main problem encountered with the large-scale synthesis was the purification of **2**, which was previously purified by recrystallization from chloroform. When attempting to purify on a 10 gram scale or greater, we observed that the majority of the compound decomposed before the bulk sample had fully dissolved, resulting in difficult recovery

and low yield of the product (24%). Further investigation of this problem on a small scale showed that the decomposition occurs when the solid dissolved too slowly. Thus, rather than removing the thionyl chloride completely until the residue solidified during the reaction workup, the reaction mixture was concentrated to approximately 10% of the original volume such that the products remained dissolved. Approximately 2 mL of hot chloroform per millimole of starting material was then added and followed by recrystallization to afford the desired product. This purification step resulted in a significant increase in the product yield (80%). Upon optimizing the monomer synthesis, scaling up the remaining synthetic steps proceeded smoothly, with **3** and **4** both synthesized on the gram scale.

Iodine-labelled compounds are useful for characterization by RBS because the iodine peak is separated from the backscattering energies for other lighter atoms, allowing for quantification and determination of the number of amines on each dendrimer attached to the membrane. The iodinated dendrimers had been reported previously using the same conditions for the growth of non-iodinated dendrimers.[3] However, the procedure was not reproducible since characterization of the product showed that only one monomer unit had been attached to the core. Careful analysis of the results determined that the amine between the two iodine atoms did not react, likely due to the increased steric hindrance. To address this issue, the reaction between the iodinated core and **2** (AB_2 monomer) was increased from room temperature to 50 °C (Scheme 4.2), resulting in the successful synthesis of G1(I_2)-NH_2 in 99% yield.

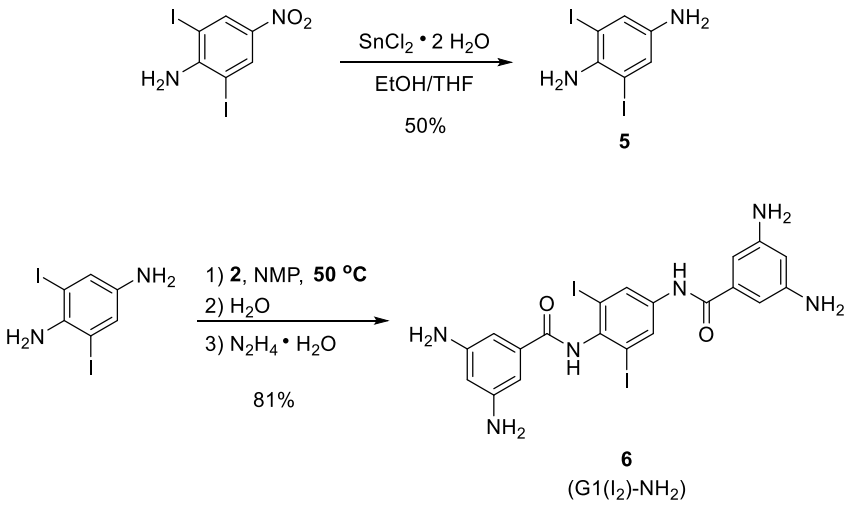

Scheme 4.2: Synthesis of the iodine-labelled dendrimer.

4.3.2: Synthesis and Attachment of Amine-Terminated Solubilizing Chains

Water and methanol are the only solvents compatible with the membranes, although there is a slight tolerance for small amounts of co-solvents that can be used to help solubilize the dendrimers. While **3** shows sufficient solubility in water with a small amount of acetonitrile, a co-solvent to help solubilize **4** enough in water could not be identified. While we did consider the growth of hyperbranched polymers from the surface of the membrane, thereby avoiding the need for solubilizing chains, we decided to stay with the discreet monomers to better understand the structure-function relationship between our modifications and the filtration properties of the membrane. Thus, we synthesized solubilizing chains similar to the triethylene glycol substituents used in previous studies that bore a terminal amine functional group for attachment to the membrane (Figure 4.2).

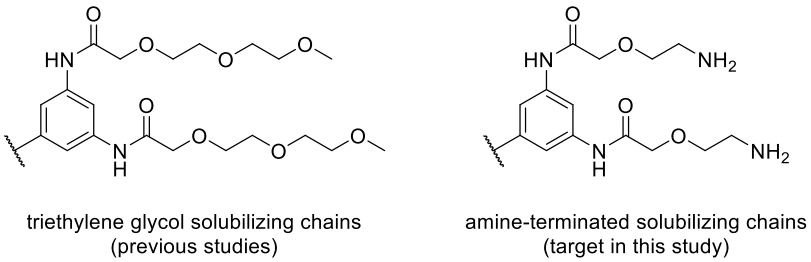

Figure 4.2: Design of amine-terminated solubilizing chains.

The synthesis of the solubilizing chain was envisioned along the same strategy as the AB_2 monomer by using the acyl chloride of the *N*-protected chain, and oxidation of protected 2-(2-aminoethoxy)ethanol was accomplished using a TEMPO/$NaClO_2$ oxidation. Various protecting groups were then investigated for their compatibility with both the oxidation reaction and attachment to the dendrimer (Figure 4.3).

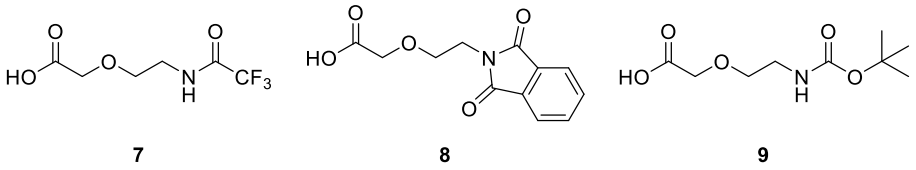

Figure 4.3: The solubilizing chains tested for how compatible the protecting group was with the oxidation and attachment to the G2-NH_2 dendrimer.

The trifluoroacetamide protecting group was first investigated since it is the protecting group used in the dendrimer synthesis, but the high solubility of the product in water prevented isolation of the carboxylic acid. Therefore, the phthalimide protecting group was successfully synthesized. During attachment of the acyl chloride of **8** to the G2 dendrimer, an insoluble

precipitate formed, and the solid was determined to be the dendrimer with approximately 2-3 solubilizing chains attached based on analysis of the remaining compounds in the reaction mixture and the mass of the precipitate. No conditions were found to prevent precipitation in order for the reaction to proceed.

We decided to revisit the trifluoroacetamide group again by decreasing the amount of water in the oxidation reaction because it should have much less of a negative effect on solubility of the dendrimer during the attachment reaction. Optimization of the oxidation reaction led to the successful synthesis and isolation of **7**, which was then tested for attachment to G2-NH_2. Attaching **7** to G2-NH_2 with simultaneous removal of the protecting group in one pot was never successful and the starting material was recovered each time. Separating the condensation and protecting group cleavage steps into two was partially successful. Removing the trifluoroactyl groups on both the dendrimer and small molecular model compounds with hydrazine showed that hydrazine cleaved the aryl-aliphatic amide between the dendrimer and the solubilizing chain even though it had no effect on the aryl-aryl amide bonds within the dendrimer.[7]

With the synthetic challenges encountered using trifluoroacetamide and phthalimide protecting groups, we next investigated the *tert*-butyloxycarbonyl (Boc) protecting group. The two-step synthesis of the carboxylic acid proceeded smoothly in high yields (98% and quantitative yields), but there were problems with solubility during the attachment reaction once again. Attempting to attach the Boc-protected solubilizing chains to **3** using *N*-(3-dimethylaminopropyl)-*N*'-ethylcarbodiimide (EDC) in DMF showed promise because no precipitate formed during the reaction, but the fully functionalized dendrimer was never obtained. Reactions for deprotection of the dendrimer modified with solubilizing chains were investigated using the partially functionalized compound, but no successful conditions have been found to date. These results suggest that the attachment is more successful in DMF than in the original NMP, though optimization of both the attachment and deprotection reactions is needed.

4.4: Covalent Modification of Polyaramide Membranes with Dendrimers

Reacting the G1-NH_2 dendrimer with EDC and sulfo-*N*-hydroxysuccinimide (s-NHS) or 2-chloro-*N*-methylpyridinium iodide (CMPI) as the carboxylate-activating agent allows for the formation of amide bonds between the dendrimers and the active layer of the membrane (see Experimental Section for details). The concentrations of free carboxylate and free amine groups

before and after the coupling reaction were measured using RBS upon labelling with heavy ion probes (Y^{3+} and WO_4^{2-}, respectively).[8-10] It was determined that the free amine concentration in the membrane increased after the coupling reaction and that the free carboxylate concentration decreased (Figure 4.4). The decrease in carboxylate concentration of 0.10 M from EDC/s-NHS coupling and 0.28 M from CMPI coupling suggests the amide bond formation with the dendrimers. This decrease may not directly reflect the concentration of attached dendrimers because the dendrimers may attach to the membrane via more than one amide bond. Based on a previous report, unattached dendrimers could limit the accessibility of the carboxylates to the heavy ion probe,[2] which could be partially responsible for the observed decrease in carboxylate concentration.

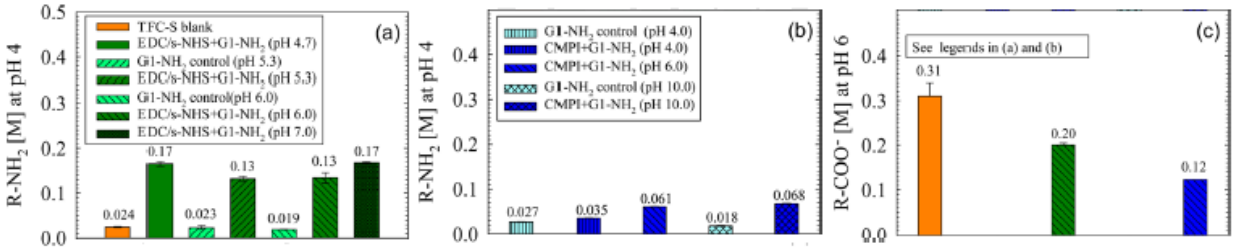

Figure 4.4: The changes in concentration of free amine functional groups from modification with (a) EDC and (b) CMPI as well as (c) the change in concentration of free carboxylate groups.

The concentration of free amines was found to increase from 0.024 M to 0.13-0.17 M and 0.061-0.068 M for coupling with EDC and CMPI, respectively. Control samples exposed to G1-NH_2 without any coupling reagents or exposed to EDC or CMPI without the dendrimer did not show any significant increase in the amine concentration. These results suggest that the surface modification was successful since attachment of a dendrimer molecule should increase the amine concentration, assuming that less than three of the amines per molecule are coupled to the membrane. It was noted that while there was not a significant dependence on the pH of the EDC/s-NHS reaction, the CMPI reaction did display sensitivity to pH. At a pH of 4, which is below the two carboxylate pKa values of 5.4 and 8.4-8.7 measured in the membrane,[2,9] little to no increase in the amine concentration after modification was observed. When the pH of the reaction was increased to 6 and 10, an increase in amine concentration was observed, suggesting successful attachment. This result suggests that the CMPI reaction is dependent on the concentration of deprotonated carboxylate groups, whereas the EDC/s-NHS reaction is not as sensitive.

The increase in free amine groups via CMPI coupling only accounted for 18% of the decrease in free carboxylate groups from the same reaction. It was also interesting that the carboxylate concentration decreased more from the CMPI reaction than from the EDC/s-NHS coupling, though the inverse was true for the free amine concentration. We hypothesized that the two reactions led to a difference in the number of amines per dendrimer attached to the membrane. Using the iodinated dendrimer **6**, we were able to quantify the amount of dendrimers covalently bonded to the membrane by RBS. Analysis of these data combined with the measured amine concentration showed that the dendrimers attach to the membrane through two to three amine groups per dendrimer (64%) in the CMPI reaction, while they attach through only one amine (28%) in the EDC/s-NHS coupling. This result agrees with the trend observed in the concentration of functional groups as well as the filtration properties of each membrane discussed in detail below.

4.5: Filtration Properties of the Modified Membranes

The water flux of the modified membranes decreased 16-19% for the EDC/s-NHS samples and 17-33% with CMPI one, both of which are acceptably small drops in performance. These values cannot be compared to the unattached dendrimers because the G1-PEG dendrimer broke through the membrane during percolation, and reliable performance data could not be obtained.

Permeation experiments show that the rejection of an organic solute (rhodamine-WT) and an inorganic solute ($BaCl_2$) increased for the modified membranes from both coupling reactions relative to the unmodified membrane (Figure 4.5). The permeability of the neutral, relatively large organic surrogate was significantly decreased for membranes prepared from both ECD/s-NHS (82%) and CMPI (64%) reactions.

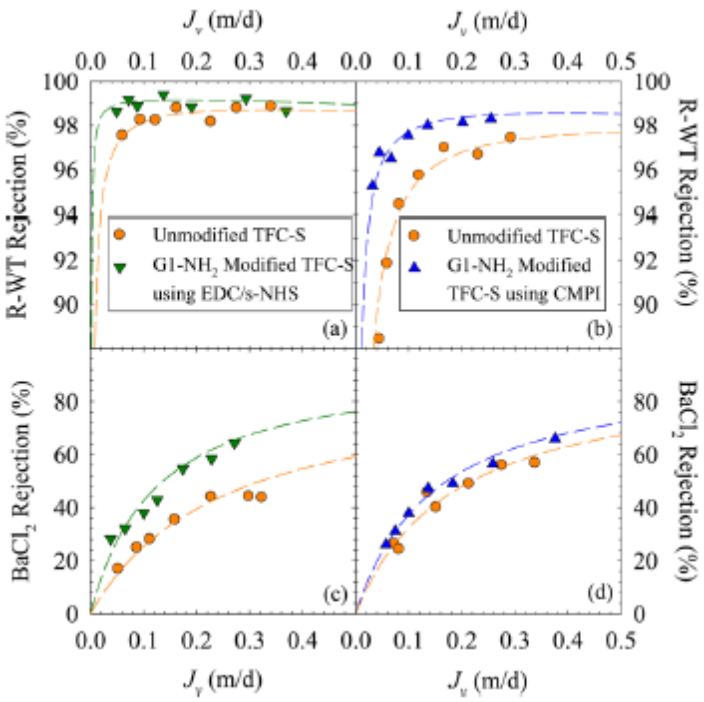

Figure 4.5: Solute rejection data for the organic surrogate rhodamine-WT (a,b) and the inorganic solute BaCl2 (c,d) for membranes with G1-NH2 attached via EDC/s-NHS coupling (a,c) or CMPI (b,d).

With the inorganic surrogate, the permeability of the solute decreased significantly more for membranes modified with EDC/s-NHS (54%) than for those prepared with CMPI (20%), corresponding to the decrease in water permeability of those membranes. As noted above, the membrane modified under CMPI conditions exhibit a lower concentration of free carboxylates because each dendrimer is attached at more points relative to the EDC/s-NHS reaction. Therefore, there is a lower ion concentration in the membrane leading to a weaker Donnan exclusion effect. This result is supported by the pronounced difference between the membranes for the rejection of ions without a corresponding difference in the rejection of the neutral organic compound. The lower concentration of carboxylate ions in the CMPI modified membrane is also in agreement with the poorer water flux compared to the EDC/s-NHS membrane because the active layer is less hydrophilic.

According to the water permeability data, modification of the membrane with EDC/s-NHS is more beneficial to the improvement of its water filtration properties than attachment via CMPI. The EDC/s-NHS conditions led to membranes that exhibit a greater increase in rejection of both the organic and inorganic surrogates while displaying a smaller negative effect on the water flux. Because of the fewer dendrimer attachment points, the EDC/s-NHS reaction affords a

membrane with better physiochemical and result in a higher number of ions left in the membrane while retaining the overall permeation benefits of adding the dendrimers. The residual carboxylate groups could also allow for additional dendrimers to be bonded to the membrane, thereby increasing the obstruction of the pores and the rejection of solutes.

4.6: Stability of the Attached Dendrimers

Our main objective for investigating the attachment of the dendrimers to the membrane was to overcome the instability of an unattached dendrimer coating. When the G1-PEG dendrimers were simply layered onto the surface of the membrane, the enhancement in rejection of rhodamine-WT sharply decreased with increasing pressure (Figure 4.6). This result was attributed to a loss of the dendrimer layer into the solution to be filtered or the breaking of the dendrimers through the active layer, subsequently being washed away with the filtrate. In contrast, when the dendrimers were attached to the membrane, the enhancement of its rejection of rhodamine-WT was stable with increasing pressure. Thus, modification via covalent functionalization enhances membrane stability compared to simple coating of the membrane.

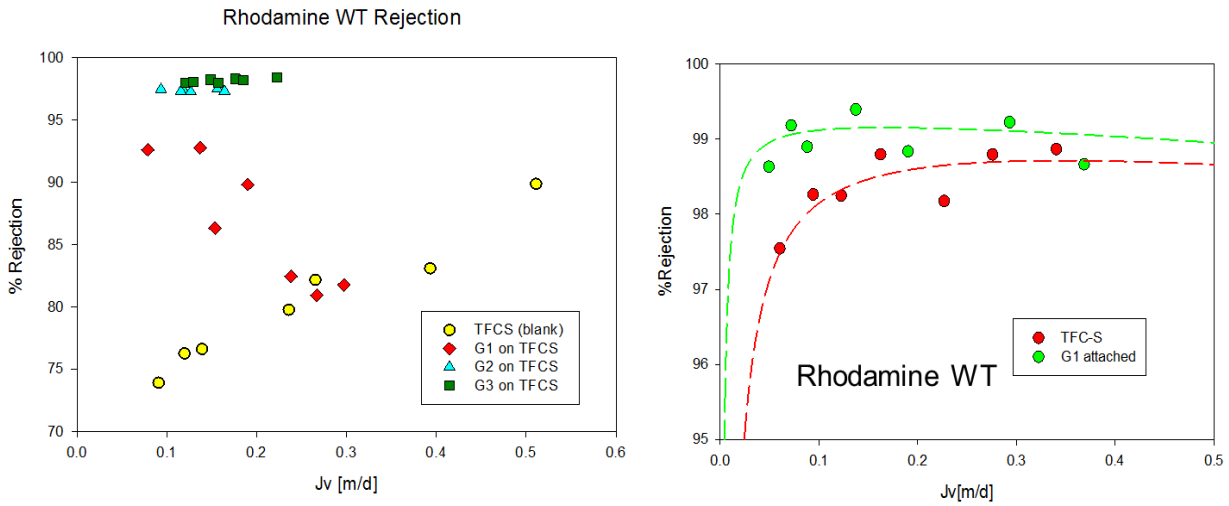

Figure 4.6: Difference in the stability of the dendrimer modification through (a) layering of the dendrimer or (b) covalent attachment of the dendrimer as observed through the rejection of rhodamine-WT with increasing pressure.

4.7: Conclusions

Covalent modification of polyaramide membranes with a polyaramide dendrimer (G1-NH_2) was demonstrated to improve the rejection of both an organic and inorganic surrogates with only a small decrease in the water flux of the membrane, much like previous studies

showing a similar improvement with coatings of polyaramide dendrimers. In contrast to the coatings, the attached dendrimers were stable on the membrane and were able to tolerate higher pressure than the analogous coatings with G1-NH_2 and did not slowly leach off of the membrane. Progress was also made toward adapting the larger and less soluble G2-NH_2 dendrimer with amine-terminated solubilizing chains was also demonstrated.

Two different coupling reagents (EDC/s-NHS and CMPI) were investigated and, while both were successful, the resulting membranes displayed remarkably different physiochemical properties. Characterization of the modified membranes with RBS using heavy ion probes to measure the carboxylate and amine concentrations, as well as iodine-labelled dendrimers, suggested that the dendrimers were coupled to the membrane through multiple amide bonds when CMPI was used and only one amide bond with EDC/s-NHS conditions. These differences in attachment lead to different ion concentrations in the membranes, and subsequently the permeation of water and charged solutes.

4.8: Experimental Section

All air- or moisture-sensitive manipulations were performed under an atmosphere of nitrogen using standard Schlenk techniques. Analytical thin-layer chromatography (TLC) was performed on Kieselgel F-254 precoated silica gel plates. Visualization was performed with UV light (254 nm). Flash chromatography was performed using 60 Å silica gel from Silicycle, Inc. All glassware was oven-dried before use.

Unless otherwise stated, all starting materials and reagents were purchased from Sigma-Aldrich, were reagent grade or better, and were used without further purification. EDC (TCI America), s-NHS (Thermo Scientific), 2-(N-morpolino)ethanesulfonic acid (MES) buffer (Acros Organics), TFC-S NF membrane (Koch Membrane Systems Inc.), rhodamine-WT (35% w/v aqueous solution; Turner Designs).

^{1}H and ^{13}C NMR spectra were obtained on Varian Unity 500 and VXR 500 spectrometers. Chemical shifts are reported in δ (ppm) relative to the residual solvent protons ($CDCl_3$: 7.26 for ^{1}H, 77.0 for ^{13}C; DMSO-d_6: 2.50 for ^{1}H, 39.52 for ^{13}C). Coupling constants (*J*) are expressed in hertz (Hz). Splitting patterns are designated as s (singlet); d (doublet); t (triplet); dd (doublet of doublets); td (triplet of doublets); m (multiplet). Melting points were measured on a Electrothermal Mel-Temp 1001 apparatus. Low resolution ESI mass spectra (ES^{+}/ES^{-}) were

recorded on a Waters Quattro II spectrometer. High resolution ESI mass spectra were recorded on a Micromass Q-Tof Ultima spectrometer.

Permeation experiments with target solutes were performed in a dead-end filtration reactor (model 8050, Millipore Co.). Permeate flow rates were monitored gravimetrically. Experiments were performed at room temperature (20-22 °C) under magnetic stirring. Experiments were performed at hydraulic pressures between 0.07 and 0.41 MPa. Aqueous solutions containing a single solute (2.5 mg/L rhodamine-WT; 400 mg/L $BaCl_2$) were fed into the reactor with stirring and the pH was adjusted to 6.75 ± 0.25. Each sample was tested prior to any modifications. After testing, the sample was flushed repeatedly with nanopure water to remove residual solute and to clean the membrane. After the attachment reaction, permeation testing was performed again.

The concentrations of free carboxylates and amines in the membranes were quantified by Rutherford backscattering spectrometry.[ref] Carboxylate groups were measured at a pH of 6 using yttrium cation (Y^{3+}) as a heavy atom ion probe, while amine groups were measured at a pH of 4 using tungstate (WO_4^{2-}). Ion probe solutions were prepared at concentrations of 10^{-3} and 10^{-6} M for tungstate and 10^{-6} M for yttrium in nanopure water from sodium tungstate dihydrate and yttrium chloride, respectively. To avoid precipitation of yttrium carbonate, the nanopure water was sparged with nitrogen prior to preparation of the solution and during the experiment. The pH of the solutions was adjusted with nitric acid and sodium hydroxide.

4.8.1: Synthesis of Dendrimers and Solubilizing Chains

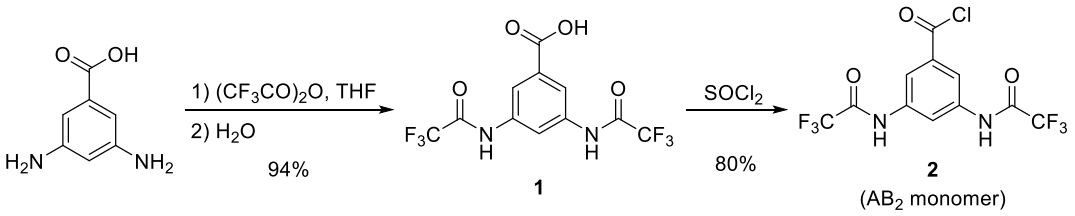

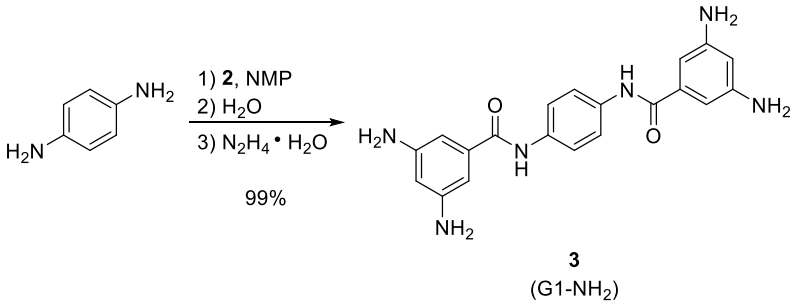

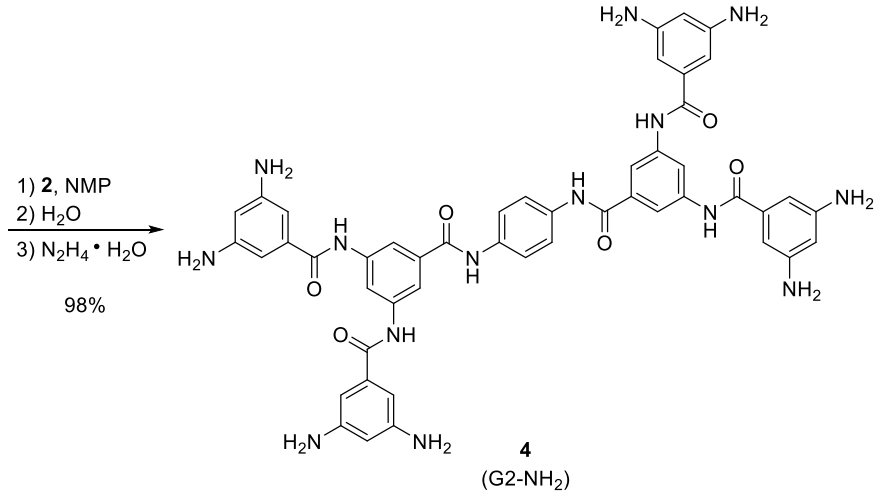

3,5-Bis(2,2,2-trifluoroacetamido)benzoic Acid (1)[7]**:** Trifluoroacetic anhydride (33.5 mL; 0.24 mol) was slowly added to a 0 °C mixture of 3,5-diaminobenzoic acid (11.25 g; 73.9 mmol) in THF (93 mL) under nitrogen. The reaction mixture was then allowed to warm to room temperature and was stirred for 3 hours. Water (93 mL) was added to the reaction mixture and it was stirred for another 6 hours. The reaction mixture was extracted with ether (200 mL; 2 × 50 mL), the combined organic layers were dried (MgSO4), and the solvent was removed in vaccuo. The product was purified by recrystallization from acetonitrile to yield a purple solid (23.92 g; 94%). ^{1}H NMR (DMSO-d_6, 500 MHz) δ: 11.56 (s, 2H), 8.43 (t, 1H, J = 2.0 Hz), 8.15 (d, 2H, J =

2.0 Hz), 3.37 (s, 1H); ^{13}C NMR (DMSO-d_6, 125 MHz) δ: 166.3, 154.9 (q, J = 37 Hz), 137.2, 132.2, 118.6,117.0, 115.7 (q, J = 287 Hz); LRMS (ES^-): m/z = 456.9 (30%), 343.0 (100%).

3,5-Bis(2,2,2-trifluoroacetamido)benzoyl Chloride (2)[7]: 3,5-Bis(2,2,2-trifluoroacetamido)benzoic acid (17.20 g; 50.0 mmol) was suspended in thionyl chloride (150 mL) under nitrogen. The mixture was then refluxed for 6 hours. The reaction mixture was concentrated to approximately 20 mL by vacuum distillation before it was poured into boiling chloroform (100 mL), with additional hot chloroform added until the tan solid dissolved. The supernatant was decanted off of the remaining solid and cooled to yield the product as a tan solid (14.54 g; 80%). ^{1}H NMR ($CDCl_3$, 500 MHz) δ: 8.44 (t, 1H, J = 2.0 Hz), 8.20 (d, 2H, J = 2.0 Hz), 8.16 (s, 2H); LRMS (ES^+): m/z = 390.9 (25%), 375.9 (100%).

G1-NH_2 Dendrimer (3)[7]: 3,5-Bis(2,2,2-trifluoroacetamido)benzoyl chloride (5.60 g; 15.4 mmol) was added to a 0 °C solution of 1,4-diaminobenzene (0.757 g; 7.00 mmol) in NMP (14 mL) under nitrogen. The reaction mixture was allowed to warm to room temperature, stirred for one hour, and then heated to 50 °C. Water (0.08 mL; 4.4 mmol) was added and the reaction mixture was stirred for an hour. Hydrazine monohydrate (4.1 mL; 84.5 mmol) was then added and the reaction mixture was stirred for another 1.5 hours. The reaction mixture was cooled to room temperature and poured into a $NaHCO_3$ solution (~2% wt.; 150 mL). The resulting mixture was filtered and the filter cake was washed with water and dried at 120 °C under vacuum for 16 hours to yield a tan solid (2.60 g; 99%). ^{1}H NMR (DMSO-d_6, 500 MHz) δ: 9.87 (s, 2H), 7.66 (s, 4H), 6.29 (d, 4H, J = 2.0 Hz), 5.98 (t, 2H, J = 2.0 Hz), 4.93 (s, 8H); ^{13}C NMR (DMSO-d_6, 125 MHz) δ:167.0, 149.1, 136.9, 135.0, 121.0, 120.1, 102.1; LRMS (ES^+): m/z = 377.3 (100%); Anal. Calc'd for $C_{20}H_{20}N_6O_2$: C 63.82, H 5.36, N 22.33; Found: C 62.02, H 5.11, N 21.20.

G2-NH_2 Dendrimer (4)[7]: 3,5-Bis(2,2,2-trifluoroacetamido)benzoyl chloride(2.70 g; 7.45 mmol) was added to a 0 °C solution of G1-NH_2 dendrimer (0.635 g; 1.69 mmol) in NMP (6.5 mL) under nitrogen. The reaction mixture was allowed to warm to room temperature, stirred for one hour, and heated to 50 °C. Water (0.04 mL; 2.2 mmol) was added and the reaction mixture was stirred for another hour. Hydrazine monohydrate (3.9 mL; 80.4 mmol) was added and the reaction mixture was stirred for another 1.5 hours. The reaction mixture was cooled to room

temperature and poured into a $NaHCO_3$ solution (~2% wt.; 75 mL). The resulting mixture was filtered and the filter cake was washed with water and dried at 120 °C under vacuum for 16 hours to yield a tan solid (1.51 g; 98%). ^{1}H NMR (DMSO-d_6, 500 MHz) δ: 10.29 (s, 2H), 10.13 (s, 4H), 8.38 (t, 2H, J = 2.0 Hz), 7.92 (d, 4H, J = 2.0 Hz), 7.74 (s, 4H), 6.35 (d, 8H, J = 2.0 Hz), 6.01 (t, 4H, J = 2.0 Hz), 4.95 (s, 16H); ^{13}C NMR (DMSO-d_6, 125 MHz) δ: 167.3, 165.9, 149.1, 139.6, 136.6, 136.1, 135.0, 120.9, 120.4, 114.8, 102.4; LRMS (ES^+): m/z = 913.0 (20%), 550.4 (85%), 522.5 (100%), 494.4 (45%), 455.1 (20%), 334.9 (40%); Anal. Calc'd for $C_{48}H_{44}N_{14}O_6$: C 63.15, H 4.86, N 21.48; Found: C 56.51, H 4.53, N 18.87.

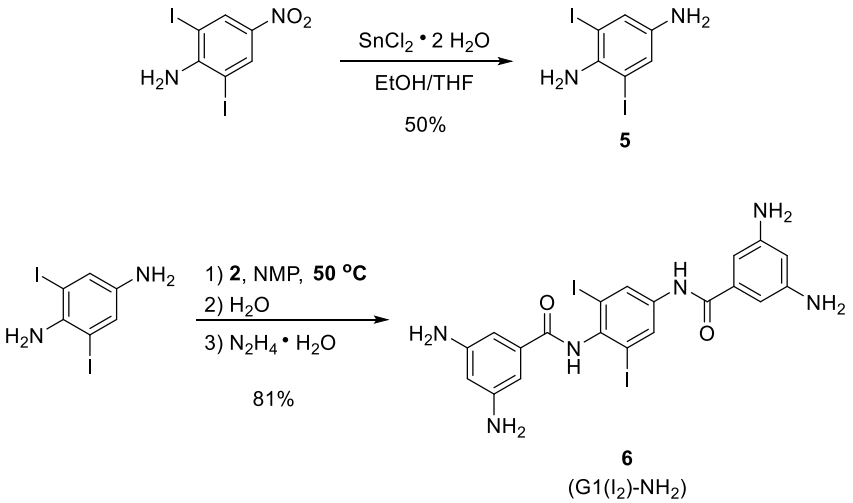

1,4-Diamino-2,6-diiodobenzene (5)[11]**:** 2,6-Diiodo-4-nitroaniline (9.75 g; 25.0 mmol) was added to a suspension of tin(II) chloride dihydrate (16.9 g; 74.9 mmol) in ethanol (100 mL) and THF (50 mL). The reaction mixture was stirred at 55 °C for 16 hours. The reaction mixture was cooled to room temperature and the solvent was removed in *vacuo*. The residue was suspended in ethyl acetate (300 mL) and mixed with saturated Na_2CO_3 solution (100 mL). The mixture was filtered and the organic layer was separated and washed with more saturated Na_2CO_3 solution (2 × 100 mL) and water (3 × 100 mL). The organic layer was dried ($MgSO_4$) and the solvent was removed in *vacuo*. The product was purified by recrystallization from methanol/water to give an orange solid (4.46 g; 50%). ^{1}H NMR (DMSO-d_6, 500 MHz) δ: 7.00 (s, 2H), 4.66 (s, 2H), 4.26 (s, 2H); LRMS (ES^+): m/z = 392.8 (10%), 360.8 (100%).

.

G1(I_2)-NH_2 Dendrimer (6): 3,5-Bis(2,2,2-trifluoroacetamido)benzoyl chloride (3.59 g; 10.0 mmol) was added to a 0 °C solution of 1,4-diamino-2,6-diiodobenzene (1.64 g; 4.54 mmol) in

NMP (13.4 mL) under nitrogen. The reaction mixture was warmed to 50 °C and stirred for 1.5 hours. Water (0.08 mL; 4.4 mmol) was added and the reaction mixture was stirred for another hour before hydrazine monohydrate (4.1 mL; 84.5 mmol) was added and the reaction mixture was stirred for another 2 hours. The reaction mixture was cooled to room temperature and poured into a $NaHCO_3$ solution (~2% wt.; 150 mL). The resulting mixture was filtered and the filter cake was washed with water and freeze-dried for 16 hours to yield a yellow solid (2.82 g; 99%). ^{1}H NMR (DMSO-d_6, 500 MHz) δ: 10.09 (s, 1H), 9.82 (s, 1H), 8.36 (s, 2H), 6.40 (d, 2H, J = 5.0 Hz), 6.29 (d, 2H, J = 5.0 Hz), 6.01 (m, 2H), 4.98 (s, 4H), 4.92 (s, 4H); LRMS (ES^+): m/z = 629.4 (20%), 403.2 (85%), 181.0 (95%); Anal. Calc'd for $C_{20}H_{18}I_2N_6O_2$: C 38.24, H 2.89, N 13.38; Found: C 37.23, H 2.76, N 12.06.

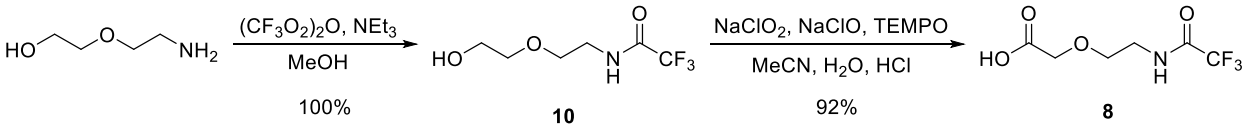

2-(2-(2,2,2-Trifluoroacetamido)ethoxy)ethanol (10)[12]**:** Trifluoroacetic anhydride (7.0 mL; 50.4 mmol) was slowly added to a 0 °C solution of 2-(2-aminoethoxy)ethanol (3.6 mL; 35.9 mmol) and triethylamine (13.0 mL; 93.3 mmol) in methanol (36 mL) under nitrogen. The reaction mixture was allowed to warm to room temperature and stirred for 16 hours. The solvent was removed in *vacuo* and the product was purified by column chromatography (silica gel; 1:1 to 3:2 ethyl acetate:hexane) to yield a pale yellow oil (7.22 g; 100%). ^{1}H NMR ($CDCl_3$, 500 MHz) δ: 8.05 (s, 1H), 3.72 (t, 1H, J = 5.0 Hz), 3.64 (m, 2H), 3.53 (m, 2H), 3.48 (m, 2H), 3.45 (m, 2H); ^{13}C NMR ($CDCl_3$, 125 MHz) δ: 171.4, 115.9 (q, J = 286 Hz), 72.2, 68.8, 61.5, 39.7; LRMS (ES^+): m/z = 425.0 (15%), 275.0 (100%), 247.0 (10%), 234.0 (50%), 219.0 (75%), 202.0 (30%).

2-(2-(2,2,2-Trifluoroacetamido)ethoxy)acetic Acid (7)[13]**:** A solution of sodium chlorite (6.26 g; 69.2 mmol) in water (35 mL) was added to a 35 °C solution of 2-(2-(2,2,2-trifluoroacetamido)ethoxy)ethanol (6.96 g; 34.6 mmol) and TEMPO (0.38 g; 2.43 mmol) in acetonitrile (173 mL). Fresh bleach (1.0 mL; 15 mmol) diluted with water (17 mL) was then added, followed by concentrated HCl (7 drops), and the reaction mixture was stirred at 35 °C for 16 hours. The reaction mixture was cooled to room temperature and extracted with ethyl acetate (3 × 100 mL). The combined organic layers were dried ($MgSO_4$) and the solvent was removed in

vacuo to yield a yellow oil (6.88 g; 92%). ^{1}H NMR ($CDCl_3$, 500 MHz) δ: 10.49 (s, 1H), 7.89 (s, 1H), 4.15 (s, 2H), 3.70 (t, 2H, *J* = 5.0 Hz) , 3.54 (q, 2H, *J* = 5.0 Hz); ^{13}C NMR ($CDCl_3$, 125 MHz) δ: 175.6, 157.4, 113.3 (q, *J* = 286 Hz), 69.4, 67.4, 39.9; LRMS (EI^+): *m/z* = 216.1 (10%), 140.0 (65%), 127.0 (100%), 102.0 (65%), 83.0 (60%). 69.0 (55%), 61.1 (55%); Anal. Calc'd for $C_6H_8F_3NO_4$: C 33.50, H 3.75, N 6.51; Found: C 34.41, H 4.14, N 6.09.

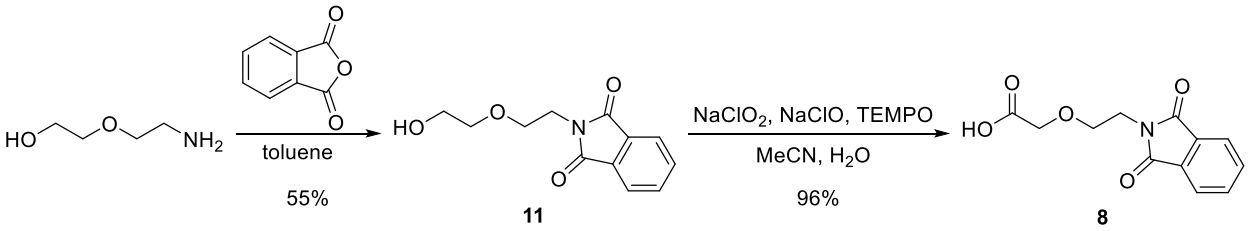

2-(2-(Phthalimido)ethoxy)ethanol (11)[14]**:** A mixture of phthalic anhydride (14.8 g; 0.10 mol) and 2-(2-aminoethoxy)ethanol (12.0 mL; 0.12 mol) in toluene (250 mL) was refluxed under nitrogen for 6 hours. The solvent was removed in *vacuo* and the product was purified by recrystallization from chloroform/petroleum ether. The product was purified further by column chromatography (silica gel; 85:15 dichloromethane:ethyl acetate) to yield a pale yellow solid (12.89 g; 55%). ^{1}H NMR ($CDCl_3$, 500 MHz) δ: 7.81 (m, 2H), 7.69 (m, 2H), 3.88 (t, 2H, *J* = 5.5 Hz), 3.72 (t, 2H, *J* = 5.5 Hz), 3.65 (m, 2H), 3.57 (m, 2H), 2.48 (s, 1H); ^{13}C NMR ($CDCl_3$, 125 MHz) δ:168.3, 133.9, 132.0, 123.2, 72.2, 68.3, 61.6, 37.5.

2-(2-(Phthalimido)ethoxy)acetic Acid (8)[13]**:** A solution of sodium chlorite (1.81 g; 20.0 mmol) in water (10 mL) was added to a 35 °C solution of 2-(2-(phthalimido)ethoxy)ethanol (2.36 g; 10.0 mmol) and TEMPO (0.11 g; 0.70 mmol) in acetonitrile. Fresh bleach (0.30 mL; 4.5 mmol) diluted with water (5 mL) was added and the reaction mixture was stirred at 35 °C for 16 hours. The reaction mixture was cooled to room temperature, poured into water (75 mL), and the pH of the resulting solution was adjusted to approximately 3 with 6 M HCl. It was then extracted with ethyl acetate (3 × 75 mL) and the combined organic layers were dried ($MgSO_4$). The solvent was removed in vaccuo and the product was purified by recrystallization from chloroform/petroleum ether to yield a white solid (2.38 g; 96%). ^{1}H NMR ($CDCl_3$, 500 MHz) δ: 7.86 (m, 2H), 7.73 (m, 2H), 4.12 (s, 2H), 3.95 (t, 2H, *J* = 5.5 Hz), 3.82 (t, 2H, *J* = 5.5 Hz); ^{13}C NMR ($CDCl_3$, 125 MHz) δ:172.8, 168.4, 134.1, 132.0, 123.4, 68.9, 67.6, 37.4; m.p. = 60-62 °C.

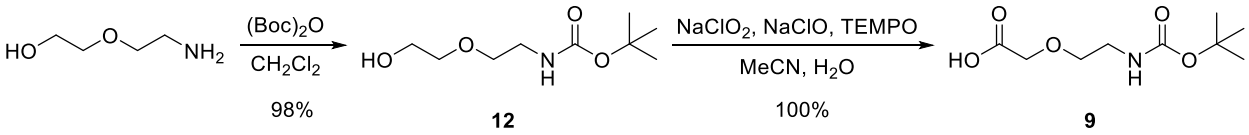

2-(2-(*tert*-Butoxycarbonylamino)ethoxy)ethanol (12)[15]**:** A solution of di-*tert*-butyl dicarbonate (7.20 g; 33.0 mmol) in dichloromethane (10 mL) was slowly added to a solution of 2-(2-aminoethoxy)ethanol (3.0 mL; 29.9 mL) in dichloromethane (40 mL) under nitrogen. The reaction mixture was stirred at room temperature for 16 hours. The reaction solution was washed with saturated $NaHCO_3$ solution (3 × 50 mL) and the organic layer was dried ($MgSO_4$) and the solvent was removed in *vacuo* to yield a clear oil (6.04 g; 98%). ^{1}H NMR ($CDCl_3$, 500 MHz) δ: 5.02 (s, 1H), 3.73 (t, 2H, *J* = 4.5 Hz), 3.55 (m, 4H), 3.33 (q, 2H, *J* = 5.5 Hz), 1.43 (s, 9H).

2-(2-(*tert*-Butoxycarbonylamino)ethoxy)acetic Acid (9)[13]**:** A solution of sodium chlorite (1.81 g; 20.0 mmol) in water (10 mL) was added to a 35 °C solution of 2-(2-(*tert*-butoxycarbonylamino)ethoxy)ethanol (2.05 g; 9.99 mmol) and TEMPO (0.11 g; 0.70 mmol) in acetonitrile (50 mL). Fresh bleach (0.30 mL; 4.5 mmol) diluted with water (5 mL) was then added and the reaction mixture was stirred at 35 °C for 16 hours. The reaction mixture was cooled to room temperature, poured into water (75 mL), and the pH of the resulting solution was adjusted to approximately 3 with 6 M HCl. It was then extracted with ethyl acetate (75 mL; 2 × 50 mL) and the combined organic layers were dried ($MgSO_4$). The solvent was removed in *vacuo* to yield a pale yellow oil (2.18 g; 100%). ^{1}H NMR ($CDCl_3$, 500 MHz) δ: 5.13 (s, 1H), 4.13, (s, 2H), 3.62 (t, 2H, *J* = 5.0 Hz), 3.36 (m, 2H), 1.44 (s, 9H); Anal. Calc'd for $C_9H_{17}NO_5$: C 49.31, H 7.82, N 6.39; Found: C 47.35, H 7.97, N 7.22.

4.8.2: Dendrimer Attachment to the Membranes

EDC/s-NHS Coupling Reaction: A 14 cm^2 coupon of the TFC-S membrane was immersed in the reaction solution containing EDC (26 µM), s-NHS (23 µM), and G1-NH_2 dendrimer (13 µM) in MES buffer solution (1 mM; 100 mL) with a pH between 4.7 and 7.0 (adjusted with NaOH and HNO_3). The sample was left immersed in the reaction solution at 37 °C for 8 hours. The sample was then removed from the reaction solution and immersed in a

sodium chloride solution (400 mg/L) and sonicated at a pH of 4 for 2 hours and a pH of 10 for 2 hours. Samples used for RBS characterization were then immersed in acetonitrile for 2 hours to remove any unreacted dendrimers. Permeation experiment samples were not immersed in acetonitrile, because the solvent decreases the water flux of the membrane by 40% when it is immersed for two hours.

CMPI Coupling Reaction: A similar procedure for EDC coupling was utilized for CMPI, though without s-NHS to stabilize the coupling reagent. The membrane sample was immersed in the reaction solution containing CMPI (23 μM) and G1-NH_2 (13 μM) in MES buffer solution (1 mM; 100 mL) at a pH between 4 and 10, and the reaction was allowed to proceed for 8 hours at 37 °C. The same rinsing protocol was used to clean the membrane samples for testing.

4.9: References and Notes

1) Part of this work has been previously published: Reprinted with permission from Saenz de Jubera, A.M.; Herbison, J.H.; Komaki, Y.; Plewa, M.J.; Moore, J.S.; Cahill, D.G.; Mariñas, B.J. *Environ. Sci. Technol.* **2013**, *47*, 8642-8649. Copyright 2013 American Chemical Society.

2) Saenz de Jubera, A.M.; Gao, Y.; Moore, J.S.; Cahill, D.G.; Mariñas, B.J. *Environ. Sci. Technol.* **2012**, *46*, 9592-9599.

3) Gao, Y.; Saenz de Jubera, A.M.; Mariñas, B.J.; Moore, J.S. *Adv. Funct. Mater.* **2013**, *23*, 598-607.

4) Kang, G.; Liu, M.; Lin, B.; Cao, Y.; Yuan, Q. *Polymer* **2007**, *48*, 1165-1170.

5) Van Wagner, E.M.; Sagle, A.C.; Sharma, M.M.; La, Y.H.; Freeman, B.D. *J. Membr. Sci.* **2011**, *367*, 273-287.

6) Wei, X.; Wang, Z.; Chen, J.; Wang, J.; Wang, S. *J. Membr. Sci.* **2010**, *346*, 152-162.

7) Washio, I.; Shibasaki, Y.; Ueda, M. *Org. Lett.* **2007**, *9*, 1363-1366.

8) Coronell, O.; Mariñas, B.J.; Zhang, X.; Cahill, D.G. *Environ. Sci. Technol.* **2008**, *42*, 5260-5266.

9) Coronell, O.; González, M.I.; Mariñas, B.J.; Cahill, D.G. *Environ. Sci. Technol.* **2010**, *44*, 6808-6814.

10) Mi, B.; Coronell, O.; Mariñas, B.J.; Watanabe, F.; Cahill, D.G. *J. Membr. Sci.* **2006**, *282*, 71-81.

11) Lee, G.W.; Kim, N.K.; Jeong, K.S. *Org. Lett.* **2010**, *12*, 2634-2637.

12) Dykhuizen, E.C.; Kiessling, L.L. *Org. Lett.* **2009**, *11*, 193-196.

13) Zhao, M.; Li, J.; Mano, E.; Song, Z.; Tschaen, D.M.; Grabowski, E.J.J.; Reider, P.J. *J. Org. Chem.* **1999**, *64*, 2564-2566.

14) Lown, J.W.; Koganty, R.R.; Joshua, A.V. *J. Org. Chem.* **1982**, *47*, 2027-2033.

15) Becht, J.M.; Meyer, O.; Helmchen, G. *Synthesis* **2003**, *18*, 2805-2810.